The Pennsylvania State University

The Graduate School

College of Engineering

DEVELOPMENT OF NOVEL CATHODE MATERIALS AND OPTIMIZATION OF ELECTRODE PERFORMANCE TOWARDS SCALING-UP APPLICATIONS OF MICROBIAL FUEL CELLS

A Dissertation in

Environmental Engineering

by

Fang Zhang

Submitted in Partial Fulfillment
of the Requirements
for the Degree of

Doctor of Philosophy

August 2012

The dissertation of Fang Zhang was reviewed and approved* by the following:

Bruce E. Logan
Evan Pugh and Kappe Professor of Environmental Engineering
Dissertation Advisor
Chair of Committee

John M. Regan
Associate Professor of Environmental Engineering

Michael A. Hickner
Assistant Professor of Materials Science and Engineering

Michael J. Janik
Assistant Professor of Chemical Engineering

Peggy Johnson
Professor of Civil Engineering
Head of the Department of Civil and Environmental Engineering

*Signatures are on file in the Graduate School

ABSTRACT

Microbial fuel cells (MFCs) represent an emerging approach for bio-electricity production. Mesh current collectors made of stainless steel (SS) can be integrated into MFC cathode structure with a Pt catalyst and a poly(dimethylsiloxane) (PDMS) diffusion layer (DL). It is shown here that the mesh properties of these cathodes can significantly affect performance. Cathodes made from the coarsest mesh (30-mesh) achieved the highest maximum power of 1616±25 mW m^{-2} (normalized to cathode projected surface area; 47.1±0.7 W m^{-3} based on liquid volume), while the finest mesh (120-mesh) had the lowest power density (599±57 mW m^{-2}). Electrochemical impedance spectroscopy showed that charge transfer and diffusion resistances decreased with increasing mesh opening size. Oxygen permeability increased with mesh opening size, accounting for the decreased diffusion resistance. At higher current densities, diffusion became a limiting factor, especially for fine mesh with low oxygen transfer coefficients. These results demonstrate the critical nature of the mesh size used for constructing MFC cathodes.

PDMS was further investigated as an alternative to Nafion as an air cathode catalyst binder. Cathodes were constructed around either SS mesh or copper mesh using PDMS as both catalyst binder and diffusion layer, and compared to cathodes of the same structure having a Nafion binder. With PDMS binder, copper mesh cathodes produced a maximum power of 1710±1 mW m^{-2}, while SS mesh had a slightly lower power of 1680±12 mW m^{-2}, with both values comparable to those obtained with the Nafion binder. Cathodes with PDMS binder had stable power production of 1510±22 mW m^{-2} (copper) and 1480±56 mW m^{-2} (SS) over 15 days at cycle 15, compared to 40% decrease in power with the Nafion binder. Cathodes with PDMS binder had lower total cathode impedance than Nafion. This is due to a large decrease in diffusion resistance, because hydrophobic PDMS effectively prevented catalyst sites from filling up with water, improving oxygen mass transfer. The cost of PDMS is only 0.23% of that of Nafion. These

results showed that PDMS is a very effective and low-cost alternative to Nafion binder that will be useful for large scale construction of these cathodes for MFC applications.

Activated carbon (AC) air-cathodes are inexpensive and useful alternatives to Pt-catalyzed electrodes in MFCs, but information is needed on their long-term stability for oxygen reduction. AC cathodes were constructed with DLs with two different porosities (30% and 70%) to evaluate the effects of increased oxygen transfer on power. The 70% DL cathode initially produced a maximum power density of 1214±123 mW m^{-2} (cathode projected surface area; 35±4 W m^{-3} based on liquid volume), but it decreased by 40% after one year to 734±18 mW m^{-2}. The 30% DL cathode initially produced less power than the 70% DL cathode, but it only decreased by 22% after one year (from 1014±2 mW m^{-2} to 789±68 mW m^{-2}). Electrochemical tests were used to examine the reasons for the degraded performance. Diffusion resistance in the cathode was found to be the primary component of the internal resistance, and it increased over time. Replacing the cathode after one year completely restored the original power densities. These results suggest that the degradation in cathode performance was due to clogging of the AC micropores. These findings show that AC is a cost-effective material for oxygen reduction that can still produce ~750 mW m^{-2} after one year.

In a separator electrode assembly MFC, oxygen crossover from the cathode raises the anode potential and inhibits current generation by exoelectrogenic bacteria, resulting in difficulties in reactor startup. In order to improve startup performance, MFCs with flat carbon mesh anodes were acclimated at set potentials (–0.2 V or +0.2 V versus standard hydrogen electrode), compared with no set potential control. Performance of these reactors inoculated with wastewater was also compared to those inoculated with cell suspensions from existing MFCs under the same conditions. Anodes inoculated with wastewater and acclimated to –0.2 V produced the highest power (1330±60 mW m^{-2}) but they had the longest startup time (20 days). With inoculation using transferred cell suspensions, consistent and reproducible results in terms

of faster startup (10 days) and high power production were obtained. Additional electrochemical analyses confirmed that inoculation with a transferred culture consistently improved anode performance, with the best activity obtained for anodes acclimated at –0.2 V. These results imply that rapid startup of larger-scale reactors will require inoculation with pre-acclimated cultures, and that acclimation at –0.2 V could improve power production compared to a more positive potential (+0.2 V) or a lack of set potential.

TABLE OF CONTENTS

LIST OF FIGURES

LIST OF TABLES

ACKNOWLEDGEMENTS

First, I would like to express my deep and sincere gratitude to my advisor, Dr. Bruce E. Logan, the Evan Pugh and Kappe professor of Environmental Engineering at Penn State University. He gives me constant support, advice and encouragement throughout my graduate study, not only in academic field, but also for my personal life and development. I really appreciate his patience, willingness to help us and great sense of humor, which make my research life here really enjoyable. From critical thinking, writing to communication skills, he encourages and guides me to be confident and become a qualified researcher. His passion, scientific attitude and great achievements in the area of environmental science and engineering have greatly inspired my growth as a student and a researcher in this field.

I would also like to thank Dr. John Regan, Dr. Michael Hickner, Dr. Michael Janik and Dr. Peggy Johnson for their support and serving as my committee members. Specially, I wish to acknowledge Dr. Michael Hickner for his advice on my research related to materials science.

I want to express my deep appreciation to all my labmates for their help, support and valuable suggestions. I really enjoy the atmosphere in the group that we are truly a family. I would also like to thank Dr. Deepak Pant from VITO, Belgium for his support. I also gratefully thank KAUST which funds me and supports my research during my graduate study.

Finally, I truly appreciate my parents, for their constant love, support, understanding and encouragement. I could never achieve this honorable milestone in my life without their love. Also, I would like to give my special thanks to all my friends in Penn State whose company makes my life here more colorful, and makes me stronger when I face the difficulties and troubles.

Fang Zhang

August, 2012

Chapter 1

Introduction

1.1 Energy crisis and the challenge of global climate change

The energy crisis and global climate change are among the most important challenges and the greatest threats facing the world. Fossil fuels such as oil, coal and natural gas are the primary energy sources for the world, accounting for more than 85% of the world energy consumption *(1)*. However, fossil fuels are non-renewable resources which take millions of years to form from the plant and animal biomass, and the reserves are being depleted much faster than the formation rate. Global annual energy consumption growth rate has been >2% for years, and in the year 2010, consumption growth reached 5.6%, which is the highest rate since 1973 *(1)*. Energy consumption has grown even more rapidly than the economy, indicating the low efficiency of energy utilization. Although energy efficiencies are improving globally and primary energy consumption growth is expected to decrease in the future *(2)*, fossil fuels cannot indefinitely sustain a global economy, especially with a growing population. Renewable energy sources with much higher energy utilization efficiencies are needed for the sustainable development.

Global carbon dioxide (CO_2) emissions have strongly grown with fossil fuel consumption. The global atmospheric concentrations of CO_2 are 36% higher than that before the industrial revolution *(3)*, mainly due to the human activities such as the burning of fossil fuels and deforestation *(4)*. The release of large amounts of bound carbon as CO_2 and other greenhouse gases into the atmosphere is causing changes in our climate that are altering global weather patterns, increasing sea levels, and decreasing biodiversity. The 4^{th} Intergovernmental Panel on Climate Change (IPCC) assessment suggested that greenhouse gas forcing is the dominant cause

of the observed averaged temperature increases in the last 50 years *(4)*. Climate models suggest during the next century global average surface temperature could increase by 2–6 °C, with sea level increases of 0.5–1.5 m *(5)*. Economic growth alone cannot counter threats from climate change, particularly if it remains carbon-intensive, as this will only accelerate global climate change. Therefore low-carbon growth paths that rely on clean renewable energy should be encouraged and supported for the sustainable development *(6)*.

1.2 Energy consumption and energy potential in wastewater treatment

Traditional wastewater treatment is energy intensive, and it accounts for about 3% of the U.S. electrical energy load *(7)*. The energy needed for a typical domestic wastewater treatment plant with both aerobic activated sludge treatment and anaerobic sludge digestion is 0.6 kWh per m^3 of treated wastewater, about half of which is for electrical energy to supply air for the aeration basins *(8)*. More strict water quality requirements usually increase the energy needed for treatment *(9)*.

In order to address water and energy crisis facing the world today, wastewater is being looked at more as a resource than as a waste. Wastewater is a source for water extraction and reuse for other applications, for energy stored as chemical energy in organic contaminants, and as a source of nutrients such as nitrogen (N) and phosphorus (P) for agriculture. Domestic, animal, and food processing wastewaters are estimated to contain a total of 17 GW *(10)*. Even using conventional wastewater treatment, the energy stored in the organics in the wastewater was estimated to be 9.3 times that needed to treat the wastewater *(11)*. Wastewater can also be used as a source of plant fertilizers, which could save energy used to make N and P fertilizers *(8)*.

Anaerobic digestion (AD) has been used to recover the energy from activated sludge biomass as methane gas, which is a useful biofuel. This captured energy could offset between a

quarter and a half of the energy consumed for a wastewater treatment plant *(12)*. However, a larger fraction of energy stored in the dissolved organic contaminants in wastewater is not captured in conventional AD, as it is typically removed by an energy consuming process like aerobic activated sludge treatment. If more of the energy potential in wastewater could be captured for use, and less was expended for treatment, then wastewater treatment plants could become net energy producers. Therefore, the challenge is to achieve energy sustainability with improved energy efficiency for wastewater treatment processes, and carbon neutral methods to capture energy and make wastewater a resource.

1.3 Bio-energy production from waste and wastewater

Different microbial systems and reactors have been applied to convert biomass and other biodegradable organic matter into energy. AD is a relatively mature technology for methane production from wastewater sludges. Complete anaerobic treatment of domestic wastewater has been proposed to achieve net energy production due to the reduced energy consumption and greater fraction of energy recovered in the process *(8)*. However, special attention is needed to ensure appropriate environmental conditions for the growth of methanogenic bacteria, such as elevated temperatures, neutral pH, and higher substrate concentrations than those of typical domestic wastewaters *(13, 14)*. As the soluble organic matter cannot be easily concentrated, and heating large amounts of water is impractical as it would consume a lot of energy, it is difficult to envision how AD alone could be used for the treatment of domestic wastewater with an ambient temperatures and relatively low organic matter concentrations. Methane is also a more powerful greenhouse gas than CO_2 *(15)*, and therefore it cannot be allowed to escape to the atmosphere. Cost-effective and energy-efficient methods for complete methane capture are needed.

Hydrogen is a clean energy carrier, which can be generated from water, biomass, natural gas, or coal. Production of hydrogen from fossil fuels is not sustainable, and more energy is required for the desirable sequestration of CO_2 *(16)*. The dark fermentative production of hydrogen has drawn much research attention as a strategy of sustainable hydrogen production from renewable biomass. However, hydrogen production using this approach is thermodynamically and metabolically limited to a maximum of 4 moles of H_2 per mole of glucose, compared to a stoichiometric value of 12, due to an incomplete oxidation process during the dark fermentation *(17)*. The COD of wastewater using such a process would remain unchanged, as organic matter is incompletely oxidized to intermediate compounds such as acetic acid or lactate. Thus dark fermentative hydrogen production requires a subsequent process to extract hydrogen from the remaining organic matter, and to recover the energy in the intermediate organic matter. This subsequent process can be methane fermentation, photofermentation or microbial electrolysis cells (MECs) for biohydrogen production *(18)*.

Microbial fuel cells (MFCs) represent an emerging approach for bio-electricity generation from wastewater *(19)*. MFCs can be used to recover energy from the soluble COD in the wastewater at ambient temperature, and at the same time reduce the energy consumption, as MFCs avoid the need for aeration, and reduce the amount of solids handling due to less sludge produced than aerobic processes *(19)*. One of the greatest challenges for practical applications of MFCs is to make this technology economically viable.

1.4 Microbial fuel cells for bio-energy production and recovery

In an MFC system, exoelectrogenic bacteria oxidize organic or inorganic matter, and donate electrons to the anode, while releasing protons into the solution *(19-22)*. The released electrons flow through the circuit to the cathode, and are then accepted by a terminal electron acceptor (e.g.

oxygen or ferricyanide). Various substrates have been used for MFCs, including specific chemicals such as volatile acids, carbohydrates, and alcohols, and complex substrates such as various types of wastewaters *(23)*. Different oxidants have been used as electron acceptors for the cathode, such as oxygen, nitrate, ferricyanide, permanganate, ferric iron, and CO_2 *(24-29)*. For practical applications such as wastewater treatment, oxygen is the most promising electron acceptor as it is sustainable and renewable.

Bioelectrochemical systems (BESs) such as MFCs can have other applications besides electricity generation with wastewater as the fuel, including desalination *(24, 30)*, recovery of nutrients in wastewater *(31)*, recovery of low-grade thermal energy *(32)*, and production of valuable products such as hydrogen gas *(33)* and other biofuels *(34)*, and chemicals *(35, 36)*. These added values make BESs more attractive for simultaneous electric power generation, wastewater treatment, co-product recovery, and CO_2 sequestration *(37)*, but it is critical that the costs of BESs be reduced so that these systems can be economical and implemented in large scale wastewater treatment plants *(38, 39)*.

1.5 Objectives

My PhD dissertation focuses on the development of novel low-cost cathode materials, understanding of the factors affecting power production, and the optimization of the electrode performance for scaling up BESs. There are four objectives:

Objective 1: Optimize the mesh opening size for the cathodes containing stainless steel mesh current collectors.

Objective 2: Develop an inexpensive alternative binder to Nafion using the hydrophobic poly(dimethylsiloxane) (PDMS).

Objective 3: Examine the long-term performance of activated carbon air cathodes with different diffusion layer porosities.

Objective 4: Improve the startup performance of carbon mesh anodes with minimized electrode spacing in the separator electrode assembly MFCs.

1.6 Organization of this dissertation

This dissertation is organized into six chapters following this introduction chapter, consisting of a literature review of the materials used in MFCs (chapter 2), four chapters that address the stated objectives, and a final chapter on future work.

In chapter 3, I optimized the mesh opening size for the cathodes that were built around stainless steel (SS) mesh current collectors. The use of SS mesh to replace expensive carbon cloth can greatly reduce the cost of a cathode, and the same power densities can be achieved with either material *(40)*. Cathodes were constructed with SS mesh having five different opening sizes. The mesh size was found to affect the oxygen mass transfer, which greatly affected the power production. Coarser mesh produced higher power due to less hindrance to oxygen transfer, while fine mesh produced much less power. The results of this work was summarized in a paper by Zhang, F.; Merrill, M. D.; Tokash, J. C.; Saito, T.; Cheng, S.; Hickner, M. A.; Logan, B. E., titled "Mesh optimization for microbial fuel cell cathodes constructed around stainless steel mesh current collectors", and it was published in *Journal of Power Sources.* Dr. Matt Merrill and Dr. Justin Tokash gave suggestions on the electrochemical analysis, Dr. Tomonori Saito and Dr. Mike Hickner helped with polymer preparation, and Dr. Shaoan Cheng gave me some useful suggestions for the experiments. I did all the experiments, including cathode preparation and MFC tests, and prepared the first draft of the manuscript. All the co-authors contributed to the revision and final writing of the paper.

In Chapter 4, I proposed the use of PDMS as a low-cost anti-flooding catalyst binder, as a replacement for the very expensive Nafion binder typically used to make MFC cathodes. PDMS was not only used as a diffusion layer polymer as previously described *(40)*, but also as a catalyst binder in this study. MFCs with the cathodes made using the PDMS binder showed comparable power production and improved stability compared to those with cathodes made using the Nafion binder, while the cost for PDMS was only 0.23% of that of Nafion. The hydrophobicity of PDMS prevents the catalyst from being completely flooded by water, which improves oxygen transfer to the catalyst sites and thus achieves improved performance. This anti-flooding effect was confirmed by the decreased diffusion resistance in electrochemical tests. The results of this work was summarized in a paper by Zhang, F.; Chen, G.; Hickner, M. A.; Logan, B. E., titled "Novel anti-flooding poly(dimethylsiloxane) (PDMS) catalyst binder for microbial fuel cell cathodes", and it was accepted by *Journal of Power Sources*. Dr. Guang Chen and Dr. Mike Hickner provided useful suggestions for experiments. I did all the experiments, including the cathode preparation and all the MFC tests, and prepared the draft manuscript. All the co-authors contributed to the revision and final writing of the paper.

In Chapter 5, I examined the long-term performance of the activated carbon air cathodes with different diffusion layer porosities in MFCs. The cathodes were continuously tested in MFC reactors for over one year, and the decrease in power production was found to be a result of degradation in cathode performance. Removal of the cathode biofilm only partially recovered power production, while using a new cathode and the existing anode completely restored power production. Based on measured decreased oxygen permeabilities and increased diffusion resistances of the cathodes, it was concluded that pore clogging was likely to be the reason for performance degradation, as this would have hindered oxygen transfer. The results were summarized in a paper by Zhang, F.; Pant, D.; Logan, B. E., titled "Long-term performance of activated carbon air cathodes with different diffusion layer porosities in microbial fuel cells", and

published in *Biosensors & Bioelectronics*. I did all the tests with the cathodes prepared by Dr. Deepak Pant. I also prepared the original manuscript and all the co-authors contributed to the revision and final writing.

In Chapter 6, I investigated the possibility of improving startup performance with carbon mesh anodes in separator electrode assembly (SEA) MFCs by using set anode potentials. The anodes were acclimated to different set potentials with a wastewater inoculum, and compared to the performance of the reactors inoculated with a pre-acclimated cell suspension under the same conditions. Inoculation with the pre-acclimated culture was found to be necessary for consistent results in terms of faster startup and improved power production. An MFC with a more negative set potential (–0.2 V) with preacclimated cells produced more power than that obtained with MFCs acclimated at a more positive set potential (+0.2 V) or with no potential control. The results were summarized in a paper by Zhang, F.; Xia, X.; Luo, Y.; Sun, D.; Call, D.; Logan, B. E., titled "Improving startup performance with carbon mesh anodes in separator electrode assembly microbial fuel cells", and submitted to *Journal of Power Sources*. I started up the reactors and did all the tests. Xue Xia, Yong Luo and Dan Sun helped to maintain reactors, and gave me some useful suggestions. Dr. Douglas Call helped me with the implementation of differential pulse voltammetry. I also prepared the original manuscript and all the co-authors contributed to the revision and final writing.

1.7 Literature cited

1. *BP Statistical Review of World Energy*; 2011.
2. *BP Energy Outlook 2030*; 2012.
3. Trends in atmospheric carbon dioxide. http://www.esrl.noaa.gov/gmd/ccgg/trends/index.html#global (5/1/2012).
4. *IPCC Fourth Assessment Report: Climate Change 2007*.
5. Schneider, S. H., The greenhouse effect: science and policy. *Science* **1989,** *243*, (4892), 771-781.
6. *World Development Report 2010: Development and Climate Change*.
7. Logan, B. E., Microbial electrochemical technologies for energy sustainability of the water infrastructure. In *Water-Energy Interactions in Water Reuse*, Valentina Lazarova; Kwang-Ho Choo; Cornel, P., Eds. IWA Publishing: 2012.
8. McCarty, P. L.; Bae, J.; Kim, J., Domestic wastewater treatment as a net energy producer–can this be achieved? *Environ. Sci. Technol.* **2011,** *45*, (17), 7100-7106.
9. Meeting the challenges of the water-energy nexus: the role of reuse and wastewater treatment. *Water21* April, 2012, pp 12-17.
10. Logan, B. E., Extracting hydrogen and electricity from renewable resources. *Environ. Sci. Technol.* **2004,** *38*, (9), 160A-167A.
11. Shizas, I.; Bagley, D. M., Experimental determination of energy content of unknown organics in municipal wastewater streams. *J. Energ. Eng.* **2004,** *130*, (2), 45-53.
12. *Wastewater Management Fact Sheet, Energy Conservation*; EPA 832-F-06-024; U.S. Environmental Protection Agency: Washington DC, 2006.

13. Griffin, M. E.; McMahon, K. D.; Mackie, R. I.; Raskin, L., Methanogenic population dynamics during start-up of anaerobic digesters treating municipal solid waste and biosolids. *Biotechnol. Bioeng.* **1998,** *57*, (3), 342-355.

14. Mata-Alvarez, J.; Macé, S.; Llabrés, P., Anaerobic digestion of organic solid wastes. An overview of research achievements and perspectives. *Bioresour. Technol.* **2000,** *74*, (1), 3-16.

15. Lashof, D. A.; Ahuja, D. R., Relative contributions of greenhouse gas emissions to global warming. *Nature* **1990,** *344*, (6266), 529-531.

16. Turner, J. A., Sustainable hydrogen production. *Science* **2004,** *305*, (5686), 972-974.

17. Hallenbeck, P. C., Fermentative hydrogen production: Principles, progress, and prognosis. *Int. J. Hydrogen Energy* **2009,** *34*, (17), 7379-7389.

18. Reith, J. H.; Wijffels, R. H.; Barten, H., *Bio-methane and Bio-hydrogen: Status and Perspectives of Biological Methane and Hydrogen Production*. Dutch Biological Hydrogen Foundation: 2003.

19. Logan, B. E., *Microbial Fuel Cells*. John Wiley & Sons, Inc.: Hoboken, NJ, 2008.

20. Logan, B. E., Exoelectrogenic bacteria that power microbial fuel cells. *Nat. Rev. Microbiol.* **2009,** *7*, (5), 375-381.

21. Lovley, D. R., Bug juice: harvesting electricity with microorganisms. *Nat. Rev. Microbiol.* **2006,** *4*, 497-508.

22. Lovley, D. R., The microbe electric: conversion of organic matter to electricity. *Curr. Opin. Biotechnol.* **2008,** *19*, (6), 564-571.

23. Pant, D.; Van Bogaert, G.; Diels, L.; Vanbroekhoven, K., A review of the substrates used in microbial fuel cells (MFCs) for sustainable energy production. *Bioresour. Technol.* **2010,** *101*, (6), 1533-1543.

24. Cao, X.; Huang, X.; Liang, P.; Xiao, K.; Zhou, Y.; Zhang, X.; Logan, B. E., A new method for water desalination using microbial desalination cells. *Environ. Sci. Technol.* **2009,** *43*, (18), 7148–7152.

25. Clauwaert, P.; Rabaey, K.; Aelterman, P.; De Schamphelaire, L.; Pham, T. H.; Boeckx, P.; Boon, N.; Verstraete, W., Biological denitrification in microbial fuel cells. *Environ. Sci. Technol.* **2007,** *41*, (9), 3354-3360.

26. Zhao, H.; Zhang, Y.; Zhao, B.; Chang, Y.; Li, Z., Electrochemical reduction of carbon dioxide in an MFC–MEC system with a layer-by-layer self-assembly carbon nanotube/cobalt phthalocyanine modified electrode. *Environ. Sci. Technol.* **2012,** *46*, (9), 5198-5204.

27. Liu, H.; Logan, B. E., Electricity generation using an air-cathode single chamber microbial fuel cell in the presence and absence of a proton exchange membrane. *Environ. Sci. Technol.* **2004,** *38*, (14), 4040-4046.

28. ter Heijne, A.; Hamelers, H. V. M.; de Wilde, V.; Rozendal, R. R.; Buisman, C. J. N., Ferric iron reduction as an alternative for platinum-based cathodes in microbial fuel cells. *Environ. Sci. Technol.* **2006,** *40*, 5200-5205.

29. You, S.; Zhao, Q.; Zhang, J.; Jiang, J.; Zhao, S., A microbial fuel cell using permanganate as the cathodic electron acceptor. *J. Power Sources* **2006,** *162*, 1409-1415.

30. Mehanna, M.; Saito, T.; Yan, J.; Hickner, M.; Cao, X.; Huang, X.; Logan, B. E., Using microbial desalination cells to reduce water salinity prior to reverse osmosis. *Energy Environ. Sci.* **2010,** *3*, (8), 1114-1120.

31. Cusick, R. D.; Logan, B. E., Phosphate recovery as struvite within a single chamber microbial electrolysis cell. *Bioresour. Technol.* **2012,** *107*, (0), 110-115.

32. Cusick, R. D.; Kim, Y.; Logan, B. E., Energy capture from thermolytic solutions in microbial reverse-electrodialysis cells. *Science* **2012,** *335*, (6075), 1474-1477.

33. Call, D.; Logan, B. E., Hydrogen production in a single chamber microbial electrolysis cell (MEC) lacking a membrane. *Environ. Sci. Technol.* **2008,** *42*, (9), 3401-3406.

34. Rabaey, K.; Girguis, P.; Nielsen, L. K., Metabolic and practical considerations on microbial electrosynthesis. *Curr. Opin. Biotechnol.* **2011,** *22*, (3), 371-377.

35. Rozendal, R. A.; Leone, E.; Keller, J.; Rabaey, K., Efficient hydrogen peroxide generation from organic matter in a bioelectrochemical system. *Electrochem. Commun.* **2009,** *11*, (9), 1752-1755.

36. Chen, S.; Liu, G.; Zhang, R.; Qin, B.; Luo, Y., Development of the microbial electrolysis desalination and chemical-production cell for desalination as well as acid and alkali productions. *Environ. Sci. Technol.* **2012,** *46*, (4), 2467-2472.

37. Hamelers, H.; Ter Heijne, A.; Sleutels, T.; Jeremiasse, A.; Strik, D.; Buisman, C., New applications and performance of bioelectrochemical systems. *Appl. Microbiol. Biotechnol.* **2010,** *85*, (6), 1673-1685.

38. Rozendal, R. A.; Hamelers, H. V. M.; Rabaey, K.; Keller, J.; Buisman, C. J. N., Towards practical implementation of bioelectrochemical wastewater treatment. *Trends Biotechnol.* **2008,** *26*, (8), 450-459.

39. Pant, D.; Singh, A.; Van Bogaert, G.; Gallego, Y. A.; Diels, L.; Vanbroekhoven, K., An introduction to the life cycle assessment (LCA) of bioelectrochemical systems (BES) for sustainable energy and product generation: Relevance and key aspects. *Renew. Sust. Energ. Rev.* **2011,** *15*, (2), 1305-1313.

40. Zhang, F.; Saito, T.; Cheng, S.; Hickner, M. A.; Logan, B. E., Microbial fuel cell cathodes with poly(dimethylsiloxane) diffusion layers constructed around stainless steel mesh current collectors. *Environ. Sci. Technol.* **2010,** *44*, (4), 1490-1495.

Chapter 2

Literature review

Bioelectrochemical systems (BESs) such as microbial fuel cells (MFCs) represent an emerging approach for bioenergy production *(1-4)*. In an MFC, bacteria grow on the anode and oxidize organic matter or inorganic matter, releasing electrons to the anode and protons into the solution (Figure 2-1). One of the most promising applications of MFCs is wastewater treatment, as organic matter can be removed while at the same time producing power. Oxygen is the most sustainable and cost-effective electron acceptor at the cathode, because oxygen in the air is readily available and free of charge, and air cathode MFCs avoid the need for water aeration. Scale-up is an important issue for the practical application of MFCs, as the cost of the materials must be minimized and inherently scalable architectures need to be used. The high cost for materials used in MFCs remains one of the greatest challenges that need to be addressed to make the large scale systems economically viable. A lot of progress has been made on the development of cost-effective materials for MFCs, some of which have achieved improved power production and better operational stability. This chapter is a review of MFCs with an emphasis on the materials used in these systems. Some related factors that affect power production are also discussed.

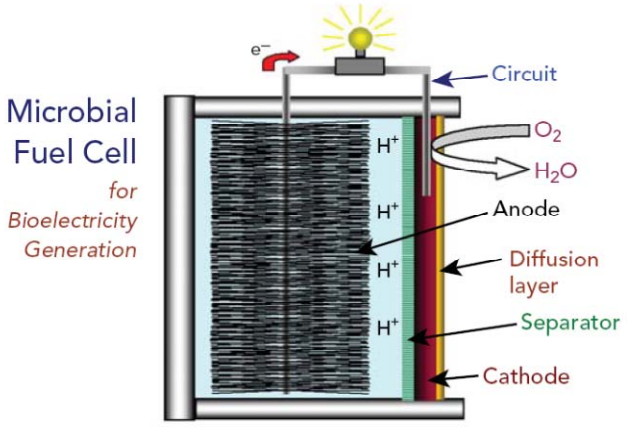

Figure 2-1. Example of an MFC with a graphite brush anode, an air cathode and a separator *(5)*.

2.1 Anode materials

2.1.1 Conventional carbon materials

Carbon materials are the most commonly used anode materials as they are electrochemically and biologically stable, they can provide high specific surface area for biofilm growth, and they have good electrical conductivity *(1, 6)*. Various carbon materials have been examined and compared in MFCs. It has been found that increasing the accessible surface area to bacteria increased the current density *(7)*, but the performance of different anode materials also depended on various other factors, such as reactor configuration, electrode spacing, substrate type and solution conductivity *(8, 9)*.

2.1.1.1 Flat structure

Flat anodes are preferred in order to have compact electrode designs and to minimize electrode spacing. Carbon cloth, carbon paper, and graphite plates are the commonly used flat carbonaceous anode materials. A carbon paper anode modified by mesoporous carbon using layer-by-layer self-assembly method showed increased activated surface area and enhanced electron transfer rate compared to the bare carbon paper anode, resulting in 81% higher power and 68% reduced startup time *(10)*. Carbon cloth is preferred over carbon paper, as carbon cloth is more flexible and appears to have greater porosity than the carbon paper which is slightly brittle and stiff *(6)*. Decreasing the electrode spacing from 4 cm to 2 cm increased power production from 720 to 1210 mW m^{-2} (18 to 60 W m^{-3}) with a carbon cloth anode and a carbon cloth air cathode, due to the decrease of internal resistance *(9)*. Carbon felt is another material that is often used in MFCs *(11, 12)*. Although carbon cloth and carbon felt have achieved good power production in MFCs, the high cost of these materials inhibits their use in large scale applications.

A low-cost carbon mesh anode was investigated as an alternative to carbon cloth with different pre-treatment methods *(13)*. Heating at 450°C was found to be a simpler and less energy-intensive way than ammonia gas treatment at 700°C. The heating process was thought to remove the contaminants interfering with charge transfer processes. Carbon mesh with only heat treatment produced maximum power of 922 mW m^{-2} (46 W m^{-3}), which was only 7% less than the ammonia gas treated carbon cloth (988 mW m^{-2}, 49 W m^{-3}) *(13)*. The disadvantage of carbon mesh is that the weave is very loose.

Flat anodes can be adversely affected by oxygen intrusion from the cathode when it is placed too closely to an air cathode *(14, 15)*. With a carbon cloth anode, power production decreased by 48% when the electrode spacing was reduced from 2 cm to 1 cm *(15)*. An MFC with a carbon mesh anode did not start up and produce power when the anode was placed in a separator electrode assembly (SEA) setup, where the anode and the cathode were pressed together with a separator in the middle *(14)*. However, anodes were acclimated well when the electrodes were well separated *(13, 14)*. After startup, power production with carbon mesh anodes could not be maintained in the SEA setup with the MFCs fed domestic wastewater. Power decreased from 230 to 45 mW m^{-2} during 4 months of operation, compared to the stable power production of 230 mW m^{-2} using a brush anode with a more complex structure *(14)*. This large decrease with carbon mesh anode was most likely due to the oxygen contamination to the anode biofilm. This indicated that better methods to prevent oxygen crossover were needed for stable anode operation with a flat anode, when the electrodes are placed close to each other.

2.1.1.2 Brush structure

A graphite brush that uses small diameter graphite fibers twisted into a titanium core (or other non-corrosive metal) as a current collector, can provide a large surface area for bacteria growth and it has produced relatively high power densities in MFCs. In a single chamber air cathode MFC, an ammonia gas treated graphite brush anode produced 2400 mW m^{-2} (73 W m^{-3}) in a 200 mM phosphate buffer *(16)*. A brush anode has a much higher surface area compared to that of the cathode, and therefore the size of the brush is usually overdesigned (i.e. larger than it needs to be to produce maximum power densities). With the current design, up to 65% of the brush material was removed without appreciably decreasing the maximum power production after acclimation with full brush *(17)*. However, reactors took longer to startup when they initially had 75% less graphite fibers, as oxygen diffusion through the cathode could not be effectively scavenged by the sufficient amount of bacteria on the brush. Because a brush has a complex geometry that likely can protect part of the anode biofilm from oxygen contamination, the brush anode also has shown better anode stability and higher power production that the carbon mesh in SEA configurations. The brush anode produced 240 mW m^{-2} with domestic wastewater, and 1300 mW m^{-2} with 1 g/L sodium acetate in 50 mM phosphate buffer, which were higher than those obtained with flat carbon mesh anodes in the same configuration (230 mW m^{-2} with wastewater, and 960 mW m^{-2} with acetate medium). The reactors with brush anodes also showed better long-term stability, with only slightly decreased power of 230 mW m^{-2} after 4 months of operation, compared to only 45 mW m^{-2} with a carbon mesh anode *(14)*.

Brush anodes are scalable, and therefore can provide sufficient anode surface area for any size of reactor. Brush anodes have been used for biohydrogen production in larger scale microbial electrolysis cells (MECs), which essentially have the same anodes as MFCs, in a 2.5 L bench-sized reactor *(18)* and a pilot-scale MEC with 1000 L volume *(19)*. Recently, multiple graphite

brush anodes were tested in a 0.13 L MFC using SEA setup, and produced a maximum power of 975 mW m^{-2} (based on cathode surface area), had COD removals of >90%, and a maximum coulombic efficiencies (CEs, the ratio of electrons from the substrate oxidation that are recovered as current) of 53% in fed-batch mode (50 Ω external resistance) *(20)*. A single large brush anode was used in each separate module in a pilot scale MFC reactor with a total volume of all modules of approximately 1000 L. However, the results from these tests, conducted by the University of Queensland, were never published *(21)*. Some disadvantages of brush anodes are that the costs could be high, which may prevent their use in large scale applications, the brush structure takes relatively large volumes, and the brush may clog with microbes and materials in wastewaters.

2.1.1.3 Packed structure

Reticulated vitreous carbon (RVC), granular activated carbon (GAC), and graphite granules are commonly used in water and wastewater treatment processes, and they have also been used as anode materials in packed-bed MFCs *(8, 22-25)*. RVC, with a surface area of 51 m^2 per m^3, was tested in a two chamber packed-bed upflow MFC as both anode and cathode, and it produced 170 mW m^{-2} (based on anode surface area; 8.7 W m^{-3} based on anode chamber volume) *(23)*. Replacing the RVC with GAC, and using a U-shaped cathode inside the anode chamber, the upflow MFC produced a maximum volumetric power density of 29.2 W m^{-3} at a volumetric loading rate of 3.40 kg COD/(m^3 day), when fed with sucrose at 35°C. Solution resistance was found to be the most dominant factor that limited power production in this upflow MFC reactor *(24)*. However, hexacyanoferrate catholyte was used in the cathode chambers for these upflow MFCs, which would not be practical for large-scale applications.

In a single chamber MFC that used a platinum-coated carbon cloth air cathode, and GAC for the anode, the power increased from 1 W m^{-3} to 7 W m^{-3} when the electrode spacing was decreased from 7.5 cm to 2 cm. Increasing the amount of GAC from 700 g to 1000 g did not further improve power production due to cathode limitations *(25)*. Graphite granules, with diameters of 1.5-5 mm, specific surface areas of 817-2720 m^2/m^3 and a porosity of 0.53, were used as the anode material in a tubular packed-bed reactor (total anode compartment volume of 0.39 L), producing 48 W m^{-3} with acetate and 38 W m^{-3} with glucose *(8)*. When this material was used for both the anode and cathode, six individual continuous MFC units in a stacked configuration produced a maximum power of 258 W m^{-3} (hourly average) with acetate as the fuel, and a hexacyanoferrate catholyte *(22)*. For the packed-bed reactors, the anode granules need to make good electrical connections to make the complete bed conductive, which is difficult to achieve due to the shape of granules and the bed porosity. These carbon granules are also heavy and could clog due to relatively low porosities.

2.1.2 Nanomaterials

Nanomaterials, such as carbon nanotubes (CNTs) and graphene, have drawn intensive attention in MFC anode studies due to the large surface area provided by these materials, and the improved electron transfer between bacteria and the electrode surface *(26)*. Nanomaterials have been applied as decoration materials for modifying existing anode materials. It has been shown that a glassy carbon electrode modified with CNT promoted direct electron transfer with *Shewanella oneidensis (27)*. CNTs and nanostructured titanium dioxide have been added to polyaniline coated nickel foam anodes to enhance electrical conductivity, and these showed improved performance compared to anodes with only polyaniline *(28, 29)*. However, *Escherichia coli*, a non-exoelectrogen was used as anode inoculum in their studies, and the nickel foam can corrode

under these conditions. Although one study showed that strain evolution eventually resulted in current generation by *E. coli* using a carbon/PTFE composite anode *(30)*, this bacterium failed to generate current in most studies, and it has been used as a negative control for current production *(31)*. Multi-wall CNT modified carbon cloth or carbon paper anodes have shown improved power production compared to a plain anode in single chamber air cathode MFCs *(32, 33)*. Simultaneously adding CNT powders with a *Geobacter sulfurreducens* inoculum into the anode chamber showed improved stability, in terms of voltage production and internal resistance over 40 days, compared to MFCs without CNT addition *(34)*. Therefore, anode modifications with nanomaterials are a feasible method to improve MFC performance.

CNTs have also been directly used as the anode material. CNT coated textiles or sponges, which provide an open three-dimensional macroporous structure, have been examined as anodes in MFCs *(35, 36)*. The sponge is a better substrate for the CNT coating as it lacks junctions, allowing a continuous skin of conductive nanomaterials. MFCs with CNT-coated sponge anodes showed 48% higher current densities than the textiles with otherwise identical conditions, and 1.24 W m^{-2} with domestic wastewater with a relatively small 1 cm^2 anode. Inexpensive graphene could be used as an alternative to CNTs, but this material requires a non-corrosive current collector due to the poorer conductivity with the coated graphene layer compared to the CNT layer *(37)*. Vertically aligned forest type multiwall carbon nanotubes (MWNTs) were grown on a silicon substrate and used as an anode in a 1.25 μL microsized MFC, which is the highest current yet attained among microsized MFCs *(38)*. The high current densities were attributed to the high anode surface-to-volume ratio of MWNTs, improving the charge transfer between bacteria and the anode. Polypyrrole (PPy) coated carbon nanotubes (CNTs) composite were also tested as anodes, but a non-exoelectrogenic bacterium *E. coli* was used as anode bacteria *(39)*.

2.1.3 Metal material

Metal materials are much more conductive than carbon materials, and they have been used as current collectors in several studies *(16, 37)*. In large scale applications, the metal current collectors are likely to be necessary to ensure good conductivity of the large electrodes. The metal materials need to be non-corrosive, and titanium and certain type of stainless steel meet this requirement. It has been shown that stainless steel with 6% of molybdenum (UNS S31254) can be used as an anode even in seawater *(40)*. Thus, this type of stainless steel can be used as an alternative to expensive titanium when anode current collectors are needed *(41)*.

2.1.4 Anode treatment

Anode performance of carbon materials can be enhanced by certain pre-treatment methods. Ammonia gas treatment (700 °C for 60 min) is an effective but energy intensive pre-treatment method that can enhance anode performance, likely due to the increased density of positive charges on the carbon surface *(42)*. Carbon cloth anodes with ammonia gas treatment had a decreased startup time and increased power production (by 48%) compared to plain carbon cloth anodes *(42)*. Heat treatment at a lower temperature of 450°C for 30 min resulted in an only slightly lower power production (7%) compared to the ammonia gas treatment, and it is more cost-effective *(13)*. A combination of soaking the electrode in a solution of ammonium peroxydisulfate (200 g L^{-1}) and concentrated sulfuric acid (100mL L^{-1}) for 15 min, followed by heat treatment, improved power production by 34% compared to that with the plain brush, and by 7% compared to only heat treatment *(43)*. Anodes can also be modified with 4(N,N-dimethylamino)benzenediazonium tetrafluoroborate to increase nitrogen-containing functional

groups, and thus the positive charge on the anode surface, resulting in a comparable power to that obtained with an ammonia gas treated anode *(44)*.

2.2 Cathode materials

In this section, I focus primarily on air-cathode materials because: (1) oxygen in the air is the most sustainable and economical electron acceptor for wastewater treatment applications; (2) this configuration has produced high power densities; and (3) aeration should be avoided in large scale systems as it is an energy intensive process. Cathode performance is usually the limiting factor for power production in most air cathode MFC studies *(45-47)*, due to the poor kinetics of oxygen reduction at neutral pH and ambient temperature, and mass transfer limitations *(48, 49)*. It has been recognized that cathode geometry is not as important as surface area, as power densities are essentially the same with either tubular cathodes or flat cathodes, as long as the same materials and same surface areas are used *(50)*. Cathode surface area and the performance are therefore the most important factors for scaling up MFCs *(51)*.

Air cathodes usually consist of a supporting material, a diffusion layer (facing air) to prevent water leakage and sometimes to control oxygen transfer, and a catalyst layer (facing solution) for catalyzing oxygen reaction. In order for MFCs to be used in practical applications, cathode costs need to be reduced without sacrificing power production. Low-cost alternatives to precious metal catalysts and other components have been studied, and have shown promising results.

2.2.1 Cathode supporting material.

Carbon cloth or carbon paper have been commonly used as MFC cathode supporting materials *(52)*, but fuel cell grade carbon cloth is very expensive ($1000 per m^2). Various materials have been tested as low-cost alternatives, including non-conductive materials coated with a conductive paint *(53-55)*, and different types of metal mesh *(56, 57)*. Membranes including cation and anion exchange membranes (AEM, CEM) and ultrafiltration (UF) membranes were examined as cathode supporting materials for air cathodes *(54, 55)*. A graphite conductive layer was coated outside the membrane to make the surface conductive, but power production was still limited by the poor conductivity of the supporting materials. The highest maximum power of 449 mW m^{-2} was produced by the AEM cathode, due to the lower internal resistance of AEM compared to CEM or UF membranes. Pressing a piece of stainless steel mesh against the AEM membrane increased the power by 28%, with a 38% reduction of internal resistance due to the improved conductivity *(55)*. Canvas cloth was also tested with either nickel or graphite based conductive paint using a non-precious catalyst of MnO_2 in a tubular reactor (170 mL empty volume) *(53)*. More power (86 mW m^{-2}, 10 W m^{-3}) was obtained with nickel paint due to its higher electrical conductivity than the graphite paint. Although this cathode assembly costs only 5% of that of membrane cathodes, its power production was still primarily limited by the conductivity of canvas materials.

Another alternative is to replace the carbon cloth with a current collector that is very conductive, such as stainless steel (SS) or nickel mesh, and to build a catalyst layer (Pt with carbon black, or activated carbon) around the metal mesh. Current collectors are necessary to ensure electrical conductivity for large electrodes. In my previous study, metal mesh was used as the cathode supporting material to replace carbon cloth *(56, 57)*. This approach inherently integrated the current collector into the cathode structure. SS mesh cathodes produced similar

power densities to carbon cloth cathodes, with a poly(dimethylsiloxane) (PDMS)/carbon black diffusion layer *(57)*. SS mesh was also tested with polymethylphenyl siloxane as the diffusion layer *(58)*. Inexpensive carbon mesh, which has been used as a low-cost anode, was also tested as a cathode material. Carbon mesh with a PDMS/carbon black diffusion layer produced the highest power among the carbon mesh cathodes with different diffusion layers, and the power density was close to that of a carbon cloth cathode with a polytetrafluoroethylene (PTFE) diffusion layer *(59)*. Although carbon mesh cathodes need current collectors in large scale applications, less metal is needed with a carbon mesh than an electrode made primarily using only SS mesh, and therefore the reduced cost may justify the use of the carbon mesh.

2.2.2 Catalyst.

2.2.2.1 Platinum (Pt)

Platinum (Pt) is a very effective catalyst for oxygen reduction, and it has been widely used in fuel cell studies, but it is expensive ($140/g) and prone to fouling. Studies have shown that decreasing the Pt amount to as low as 0.1 mg cm^{-2} will not appreciably affect power densities in air cathode MFCs *(60)*. Development of biofilm on the cathode could inhibit proton transfer, causing decreased power production. Removal of biofilm developed on a Pt/C cathode completely restored cathode performance after 42 days of operation *(61)*. However, a longer-term test of one year with Pt/C cathodes showed that there was significant degradation in performance over time. Power was increased up to 26% when the cathode biofilms were removed, and by 118% when new cathodes were used *(62)*. Thus, development of cathode biofilm alone was not the primary reason for the long-term degradation in cathode performance.

Vulcan XC-72 carbon black is the most commonly used support for Pt. Better catalyst supports, such as CNTs *(63, 64)*, or better methods for applying the catalyst, such as electrochemical deposition *(65)* and plasma sputtering *(66)*, have shown improved performance compared to cathodes made using the more typical painting method. In another study, polyamidoamine (PAMAM) dendrimer-encapsulated platinum nanoparticles (Pt-DENs) showed better performance with a lower loading amount than electrodeposited Pt *(67)*. However, the use of Pt catalyst is still not cost-effective due to its extremely high cost. Low-cost alternatives with better long-term stability are needed for practical applications.

2.2.2.2 Non-Pt Catalytic material

Non-precious metal

Non-precious metals such as Fe, Co, Ni, and Mn, have been studied as catalysts, and some of them have achieved equal or better performance than Pt-based cathodes. Metal macrocyclic compounds have shown good catalytic activities for oxygen reduction. Iron(II) phthalocyanine (FePc) and cobalt tetramethoxyphenylporphyrin (CoTMPP) have been tested in several studies *(60, 68, 69)*. In electrochemical tests, FePc and CoTMPP showed comparable or better capabilities than Pt/C cathodes at current densities above 0.2 mA cm^{-2}, and CoTMPP was slightly better than FePc *(69)*. In a highly saline solution using 250 mM NaCl, CoTMPP showed 25% higher power production compared to a Pt/C carbon cloth cathode, and 27% higher power than the activated carbon cathode *(70)*. Iron-chelated complex (iron ethylenediaminetetraacetic acid, Fe-EDTA) was proposed to be used in an air cathode , and it was adsorbed on an activated carbon cloth *(71)*. The absorbed Fe-EDTA air cathode produced 20% more power when PTFE was added to prevent the desorption of iron. Pyrolyzed carbon supported Fe-EDTA (prepared in an argon atmosphere at 800°C) produced a high power of 1122 mW m^{-2}, which was similar to that

obtained with Pt/C (1166 mW m^{-2}) *(72)*. However, desorption of Fe-EDTA occurred in the reactor over time, and the catalyst needed to be replenished.

Catalyst supports also affect the performance of these non-precious metal catalysts. By using a Ketjen black carbon support that had a higher surface area than Vulcan XC-72 carbon black, power production with FePc improved from 530 mW m^{-2} (Vulcan XC-72) to 634 mW m^{-2} (Ketjen carbon). This power was higher than that obtained with Pt (593 mW m^{-2}) *(68)*. Oxygen reduction on FePc supported on Ketjen black carbon is independent of pH over a range of 0-7, and the reaction is mainly controlled by Fe^{II}/Fe^{III} redox couple *(73)*. Amino-functionalized MWNTs where shown to be a better support for FePc than other carbon materials, including carbon black, pristine MWNTs and carboxylic acid functionalized MWNTs *(74)*. Iron tetrasulfophthalocyanine (FeTsPc) had 54% enhanced power production after adsorption onto a graphene surface (817 mW m^{-2}), which was close to that produced with a Pt/C cathode (856 mW m^{-2}) under the same conditions *(75)*. With the same carbon support, incorporation of FePc with metal oxide such as cobalt oxide showed 37% improved power production compared to only FePc *(76)*.

Manganese oxides (MnO_2) have also been used for oxygen reduction. Manganese did not work well with Pc compared to other metals *(68)*, but carbon-supported MnO_2 have shown good catalytic activity in neutral solutions *(77)*. CNTs were shown to be a better catalyst support than carbon black or graphite powder with MnO_2 *(58, 78)*. Increasing the percentage of MnO_2 in the MnO_2/CNT composite from 0% to 68% resulted in an increase in power production from 688 to 2676 mW m^{-2} *(58)*. Catalytic activities of MnO_2 with different crystal structural forms were also examined, and a β-type MnO_2 showed more than 4 times higher power than the α type MnO_2 *(78)*. The Mn^{III}/Mn^{IV} species acted as mediators in the oxygen reduction mechanism, and doping with divalent ions enhanced the oxygen reduction reaction towards the 4-electron pathway rather than peroxide intermediates *(77)*. MnO_2 was used as the catalyst with a canvas cloth cathode, but the

low power was likely due to the poor conductivity of the supporting material *(53)*. Spinel manganese–cobalt oxide was also tested, but power was rather low in this study *(79)*. Other metal oxides, such as lead dioxide, have also been tested as an alternative to Pt, but the potential toxicity effect of lead would restrict its application *(80)*. While these non-precious metal catalysts have shown promising results in short term MFC tests or electrochemical tests, long-term stability evaluations are needed for their future applications.

Carbon material

Carbon materials with extremely large specific surface areas, but no precious metal catalysts, have shown promising results in catalyzing oxygen reduction in MFC cathodes. The large surface areas of many carbon materials can decrease oxygen reduction overpotentials due to the very low current densities. In a two-chamber MFC, with aeration of the catholyte, plain granular graphite cathode produced 50 W m^{-3} (normalized to cathode liquid volume) or 21 W m^{-3} (cathode total volume) in a continuous flow MFC fed acetate *(81)*. An activated carbon felt was used as the cathode in an upflow MFC, which also required aeration in the cathode chamber, producing 315 mW m^{-2} (normalized to the cross-sectional area of the separator). This power production was higher than that with plain carbon paper (67 mW m^{-2}), common carbon felt (77 mW m^{-2}) or even Pt coated carbon paper (124 mW m^{-2} with Pt loading of 0.2 mg cm^{-2}) *(12)*. However, aeration is a very energy intensive process and should be avoided in MFCs. Plain graphite plates were used in an MFC in another study to treat domestic wastewater under acidogenic conditions, producing power of ~150 mW m^{-2}. This cathode was placed at the top of the reactor and exposed to air to avoid the need for water aeration *(82)*.

Different carbon materials have been used for air cathodes, and these have produced promising results as alternatives to Pt/C catalyst. Carbon powder with a pre-treatment (heat treatment and HCl immersion) before the N-doped treatment using HNO_3 showed higher power

production than those without any treatment, or with only N-doped treatment. A larger carbon loading on the cathode improved power production to be similar to that with a Pt/C catalyst *(83)*. Polyaniline nanofiber on carbon black showed 2.7 times higher power than cathodes without carbon black, but the power was 18% lower than that with a Pt/C catalyst *(84)*. A polypyrrole/carbon black (Ppy/C) composite obtained higher power compared to a non-pyrolysed FePc cathode, but the power production with Ppy/C was still lower than that obtained with the Pt/C cathode *(85)*.

Carbon nanomaterials such as CNTs, carbon nanofibers (CNF) and graphene have recently been shown to be effective catalysts for oxygen reduction in polymer electrolyte membrane (PEM) fuel cells *(86, 87)* and MFCs *(88, 89)*. Vertically aligned nitrogen doped CNTs (VA-NCNT) were used as the catalyst in air cathode MFCs, which produced higher power (1600 mW m^{-2}) than the Pt/C catalyst (1393 mW m^{-2}), and had better long-term stability *(89)*. Oxygen reduction on this VA-NCNT cathode occurs via a four-electron pathway that directly produces water in either acidic or neutral phosphate buffer solutions *(86, 89)*. Nitrogen-doped CNFs and graphene are also promising alternatives to Pt/C catalysts as they showed comparable power production *(88, 90)*. CNFs were prepared by simple pyrolysis of pyridine on SS mesh, which also avoided the need of a binder *(88)*. The interaction force between CNFs and SS mesh surface was shown to be strong enough to tolerate flushing with water. Nitrogen-doped graphene was synthesized in gram-scale amounts with a denotation process, and it had good catalytic activity and long-term stability for oxygen reduction via a combination of two-electron and four-electron pathways *(90)*.

An air cathode was easily be made using activated carbon (AC) and tested in MFCs. AC was cold pressed onto a nickel mesh current collector, producing power of 1220 mW m^{-2}, which was higher than that obtained with a Pt/C carbon cloth cathode (1060 mW m^{-2}) *(56)*. This activated carbon air cathode produced 1300 mW m^{-2} with a brush anode in an MFC with a SEA

setup that was fed acetate, and 240 mW m^{-2} in the same reactor with domestic wastewater *(14)*. Addition of Pt to these carbon materials with large surface areas can improve power production, but to a smaller extent (e.g. 24% with activated carbon felt in aqueous catholyte using dissolved oxygen, and 16% with activated carbon air cathode) *(12, 56)*, compared to that with the carbon cloth which has a much smaller surface area (~4 times) *(60)*. Therefore, these carbon materials are very cost-effective and efficient in power production, holding great promise for large scale applications.

2.2.3 Binder

A binder is usually needed when the catalyst is applied to a supporting material. The binder is usually a polymer, and it plays an important role in maintaining a good three-phase interface for oxygen reduction: air (oxygen), water (protons), and solid (electricity) *(21)*. Nafion is the most widely used binder as it has high proton conductivity and strong chemical stability. However, Nafion is quite expensive, as it costs more than $600 per m^2 when used as a binder in an MFC. Inexpensive alternatives to Nafion are therefore needed for the practical applications. Low-cost hydrophobic polytetrafluoroethylene (PTFE) has been tested as the binder in several studies with Pt/C catalyst *(60, 91)*. Adding PTFE with Nafion as a binder adversely affected power production, with power decreasing almost linearly from 1060 mW m^{-2} with only Nafion to 549 mW m^{-2} with only PTFE *(91)*. In another study comparing a PTFE binder with Nafion, although less power production was obtained with PTFE binder, it showed less performance degradation over time than the Nafion binder *(60)*. PTFE binder has been successfully used as the binder in the construction of activated carbon air cathodes *(56, 92)*.

Other low-cost polymers were also synthesized and tested as binders in MFCs, with different ion exchange capacities (IEC) or with different functionalization, allowing the

understanding of the effects of different functional groups or other factors affecting the cathode performance. Cathodes with poly(phenylsulfone) (Radel) sulfonated to various extents to vary the binder IECs were tested as alternatives to Nafion in air cathode MFCs. Hydrophobic non-sulfonated Radel showed better electrochemical performance and the lower charge transfer resistance than the sulfonated Radel. Cathodes made with the non-sulfonated Radel had the most stable performance compared to the sulfonated Radel binder cathodes over more than 20 cycles, and after this time it had comparable performance to cathodes made with the Nafion binder. This suggested that the ionic binder resulted in ionic gradients that impeded proton transfer *(93)*. Non-ionic hydrophilic polymers poly(styrene)-*b*-poly(ethylene oxide) diblock copolymers (PS-*b*-PEO) with different PEO lengths were tested to investigate the effect of the hydrophilicity on cathode performance. It was demonstrated that increasing the hydrophilicity of the neutral catalyst binders enhanced electrochemical and MFC performance, likely due to the increased accessible surface area for oxygen reduction *(94)*. Although cathodes with these alternative binders all initially had a lower power production than those with Nafion, performance of the best materials became nearly equivalent to Nafion in longer term tests *(93, 94)*.

Cationic fluorinated polymer binders, which are quaternary ammonium functionalized fluorinated poly(arylene ether) (Q-FPAE), have also been tested in MFCs, showing similar performance to those made with a Nafion binder *(95)*. Cathodes made with the Q-FPAE binder also showed more stable performance and higher power production than those with anionic (sulfonated) or cationic (quaternary ammonium-functionalized) Radel. More quaternary ammonium groups promoted the absorption of water, which was thought to improve proton transfer. The presence of fluorine in these hydrophilic polymer binders increased the ionic transport and improved resistance to biofouling, resulting in a more stable long-term cathode performance *(95)*. A hydrophilic anion exchange ionomer (AEI), quaternary 1,4-diazabicyclo-[2.2.2]-octane (DABCO) polysulfone (QDPSU) was also proposed as air cathode catalyst binders

(96). Using the FePc catalyst, this binder showed higher cathode potentials in the polarization tests than the Nafion binder, but the reactors were not acclimated well before the polarization test. Both anodes failed to sustain high current densities, and the anode in the reactor with the Nafion binder cathode had higher anode potentials than the one with the QDPSU binder, so there were differences in the reactors other than those due to the cathodes. Despite these differences, it was suggested that the improved oxygen reduction activity from QDPSU was due to the interaction between the ionomer and oxygen, and the improved OH^- transfer *(96)*.

Other polymers have been used as binders for air cathodes. Polyvinylidene fluoride (PVDF) was used as a binder for CNT supported MnO_2 catalysts for oxygen reduction with domestic wastewater, and MFCs with these cathodes produced 98 mW m^{-2} *(78)*. Positively charged diethylamine-functionalized polymer (DEA) was used as a Pt catalyst binder on the cathode to improve the establishment of a nitrifying biofilm and enhance ammonia removal. MFCs with the DEA binder had a higher ammonia removal efficiency of up to 97% than Nafion (91%), but a slightly lower power density of 900 mW m^{-2}, compared to 945 mW m^{-2} with a Nafion binder *(97)*.

2. 3 Membranes, separators and spacers

2.3.1 Membranes

It has been shown that proton exchange membranes (PEMs) are not necessary for power generation in single chamber air cathode MFCs. When a PEM (Nafion) was hot-pressed to a carbon cloth air cathode, the CE increased from 9–12% to 40–50%, but power was reduced from 12.5 to 6.6 W m^{-3} *(98)*. Various types of membranes have been used to separate the anode and the cathode chambers in MFCs, including AEM, CEM, forward osmosis (FO) and bipolar, for

reasons other than just power production. Pairs of AEMs and CEMs have been inserted between the anode and the cathode chambers for simultaneous desalination, electricity generation and wastewater treatment *(99, 100)*. Thinner, laboratory-synthesized membranes produced better salt removal efficiencies than commercial AEMs and CEMs (Membrane International Inc.) *(99)*. Adding a bipolar membrane between anode chamber and AEM allowed for simultaneous production of HCl and NaOH in the cell, in addition to achieving desalination, when additional voltage was added to the cell *(101)*. The combination of a reverse electrodialysis stack (RED), which consists of several AEM and CEM pairs, with an MFC greatly enhanced the MFC performance, resulting in a high power of 4.3 W m^{-2} when acetate was used as the fuel *(102)*. Capture of low-grade thermal energy as electricity can be achieved by using ammonia bicarbonate as a draw solution, while at the same time producing 2.9 W m^{-2} using domestic wastewater *(103)*. Using FO membrane as a separator between the anode and cathode chamber accomplished wastewater treatment, water extraction (from the wastewater), and electricity generation *(104)*.

2.3.2 Separators

In SEA MFCs, membranes can be used as separators to prevent short-circuiting. The use of these membranes in MFCs increases CEs but also increases internal resistance and decreases power production *(8, 54, 55, 61, 105-107)*. With a SS mesh to prevent membrane deformation, AEMs consistently produced better performance than CEMs in MFCs, as the use of CEM resulted in a higher pH gradient across the membrane and larger changes in solution conductivity than those observed with an AEM *(105)*.

An ideal separator material should have a high proton permeability which does not inhibit proton transfer to the cathode, a low oxygen permeability to improve CE, and resistance to

biodegradation. With an SEA setup, volumetric power densities of MFCs can be greatly increased due to the reduced reactor volume *(21, 61, 108)*. A porous material called J-cloth was proposed as a separator material. When electrodes were closely spaced, the use of this material significantly decreased the internal resistance, resulting in a high power of 627 W m^{-3} (1120 mW m^{-2}) in fed-batch mode, and 1010 W m^{-3} in continuous flow mode (double SEAs and an empty bed volume of 2.5 mL) *(108)*. However, this separator material is biodegradable which limits its usefulness for practical applications. Glass fiber is a non-biodegradable material that showed performance comparable to that of J-cloth *(61)*. With glass fiber (thickness of 1.0 mm) and a flat carbon cloth anode, power production was 70 W m^{-3} (1195 mW m^{-2}) with a single SEA, and 150 W m^{-3} with double SEAs (963 mW m^{-2}). Power was further increased to 696 W m^{-3} (895 mW m^{-2}) using a 0.3 cm electrode spacing and double SEAs. The decreased power densities based on surface area were due to the adverse effect of oxygen intrusion on power production with the double SEA configuration and the closer electrode spacing. Glass fiber separators have a disadvantage of unraveling in reactors during operation *(14, 20)*, and anode fibers can easily penetrate this material causing short-circuiting. A textile separator has been used to avoid these drawbacks associated with glass fiber separators *(20)*.

Mesh supporters have been used to avoid water gaps between a separator and the cathode, without adversely affecting the power production *(105, 109)*. Pressing a SS mesh against AEM or CEM membrane separators prevented membrane deformation and thus eliminated the water gaps between the membrane and the cathode *(105)*. With a brush anode and a glass fiber separator, the maximum power density with a plastic mesh supporter and a single cathode was 75 W m^{-3}, which was the same as that produced in the MFC without a supporter (74 W m^{-3}) *(109)*.

CEs are usually inversely correlated with power production, as materials that hinder oxygen transfer usually also impede proton transport *(110, 111)*. Nylon and glass fiber separators with different pore sizes were examined in MFCs, and larger pore sizes were found to be

beneficial for higher power production due to the less proton hindrance, but they produced lower CEs *(111)*. An alternative approach to avoid water accumulation and pH gradients between the separator and the cathode is to coat the water-facing side of the cathodes with a polymer *(110)*. Anion exchange, cation exchange, and neutral polymer coatings of different thicknesses were compared in MFCs, and the performance of cathodes made with these materials also showed the same trade-offs between power production and CEs as cathodes with separators made with different materials. A thin layer of anion exchange polymer coating resulted in the highest power (1167 mW m^{-2}) among different polymer coatings tested, and this was 2.6 times that obtained with a cation exchange coating (439 mW m^{-2}). Thicker coatings reduced oxygen diffusion into the anode chamber and had increased CEs (56–64%) compared to an uncoated cathode (29%), but power values were very low (255–574 mW m^{-2}) *(110)*. Therefore, separator materials that have high proton or water transport properties, but low oxygen permeabilities, are needed for both high power production and high CEs for MFCs that have a SEA configuration.

2.3.3 Spacers

Spacers have been proposed to make more compact MFC electrode stacks without adversely affecting the performance *(112)*, but there is little research reported on their use in MFCs. The use of a spacer between the cathodes can minimize the distance between adjacent cathodes, and thus minimize overall reactor size when stacks of MFCs are used. A single 1.5 mm expanded plastic mesh spacer was used in MFCs to produce a maximum power density (973 mWm^{-2}), which was similar to that of an MFC with the cathode exposed directly to air (no spacer) *(112)*. This suggests that the use of spacers can help reduce reactor volume and therefore cost.

2.4 Outlook

A review of these materials shows great advances are being made that bring MFCs closer to practal large- scale applications. The cost of the materials used in MFCs has been greatly reduced, while even better performance has been obtained with some of the low-cost alternatives. However, more work is still needed to optimize these systems and demonstrate long-term stability for these materials. With a deeper understanding of the factors that limit power generation and long term performance of the system, the development of other novel materials could further enhance the performance and reduce cost. It is hoped that with sustained progress into cost-effective materials and designs, MFCs will be implemented in wastewater treatment plants in the near future.

2.5 Literature cited

1. Logan, B. E., *Microbial Fuel Cells*. John Wiley & Sons, Inc.: Hoboken, NJ, 2008.
2. Logan, B. E., Exoelectrogenic bacteria that power microbial fuel cells. *Nat. Rev. Microbiol.* **2009,** *7*, (5), 375-381.
3. Logan, B. E.; Aelterman, P.; Hamelers, B.; Rozendal, R.; Schröder, U.; Keller, J.; Freguiac, S.; Verstraete, W.; Rabaey, K., Microbial fuel cells: methodology and technology. *Environ. Sci. Technol.* **2006,** *40*, (17), 5181-5192.
4. Lovley, D. R., Bug juice: harvesting electricity with microorganisms. *Nat. Rev. Microbiol.* **2006,** *4*, 497-508.
5. Logan, B. E., Energy sustainability of the water infrastructure using microbial fuel cell technologies. In *Clarke Prize Lecture*, Fountain Valley, CA, 2009.

6. Wei, J.; Liang, P.; Huang, X., Recent progress in electrodes for microbial fuel cells. *Bioresour. Technol.* **2011,** *102*, (20), 9335-9344.
7. Chaudhuri, S. K.; Lovley, D. R., Electricity generation by direct oxidation of glucose in mediatorless microbial fuel cells. *Nat. Biotechnol.* **2003,** *21*, (10), 1229-1232.
8. Rabaey, K.; Clauwaert, P.; Aelterman, P.; Verstraete, W., Tubular microbial fuel cells for efficient electricity generation. *Environ. Sci. Technol.* **2005,** *39*, (20), 8077-8082.
9. Liu, H.; Cheng, S.; Logan, B. E., Power generation in fed-batch microbial fuel cells as a function of ionic strength, temperature, and reactor configuration. *Environ. Sci. Technol.* **2005,** *39*, (14), 5488-5493.
10. Zhang, Y. P.; Sun, J.; Hou, B.; Hu, Y. Y., Performance improvement of air-cathode single-chamber microbial fuel cell using a mesoporous carbon modified anode. *J. Power Sources* **2011,** *196*, (18), 7458-7464.
11. Borole, A. P.; Hamilton, C. Y.; Vishnivetskaya, T. A.; Leak, D.; Andras, C.; Morrell-Falvey, J.; Keller, M.; Davison, B., Integrating engineering design improvements with exoelectrogen enrichment process to increase power output from microbial fuel cells. *J. Power Sources* **2009,** *191*, (2), 520-527.
12. Deng, Q.; Li, X.; Zuo, J.; Ling, A.; Logan, B. E., Power generation using an activated carbon fiber felt cathode in an upflow microbial fuel cell. *J. Power Sources* **2010,** *195*, (4), 1130-1135.
13. Wang, X.; Cheng, S.; Feng, Y.; Merrill, M. D.; Saito, T.; Logan, B. E., The use of carbon mesh anodes and the effect of different pretreatment methods on power production in microbial fuel cells. *Environ. Sci. Technol.* **2009,** *43*, (17), 6870-6874.
14. Hays, S.; Zhang, F.; Logan, B. E., Performance of two different types of anodes in membrane electrode assembly microbial fuel cells for power generation from domestic wastewater. *J. Power Sources* **2011,** *196*, (20), 8293-8300.

15. Cheng, S.; Liu, H.; Logan, B. E., Increased power generation in a continuous flow MFC with advective flow through the porous anode and reduced electrode spacing. *Environ. Sci. Technol.* **2006,** *40*, (7), 2426-2432.

16. Logan, B. E.; Cheng, S.; Watson, V.; Estadt, G., Graphite fiber brush anodes for increased power production in air-cathode microbial fuel cells. *Environ. Sci. Technol.* **2007,** *41*, (9), 3341-3346.

17. Hutchinson, A. J.; Tokash, J. C.; Logan, B. E., Analysis of carbon fiber brush loading in anodes on startup and performance of microbial fuel cells. *J. Power Sources* **2011,** *196*, (22), 9213-9219.

18. Rader, G. K.; Logan, B. E., Multi-electrode continuous flow microbial electrolysis cell for biogas production from acetate. *Int. J. Hydrogen Energy* **2010,** *35*, (17), 8848-8854.

19. Cusick, R.; Bryan, B.; Parker, D.; Merrill, M.; Mehanna, M.; Kiely, P.; Liu, G.; Logan, B., Performance of a pilot-scale continuous flow microbial electrolysis cell fed winery wastewater. *Appl. Microbiol. Biotechnol.* **2011,** *89*, (6), 2053-2063.

20. Ahn, Y.; Logan, B., A multi-electrode continuous flow microbial fuel cell with separator electrode assembly design. *Appl. Microbiol. Biotechnol.* **2012,** *93*, (5), 2241-2248.

21. Logan, B., Scaling up microbial fuel cells and other bioelectrochemical systems. *Appl. Microbiol. Biotechnol.* **2010,** *85*, (6), 1665-1671.

22. Aelterman, P.; Rabaey, K.; Pham, T. H.; Boon, N.; Verstraete, W., Continuous electricity generation at high voltages and currents using stacked microbial fuel cells. *Environ. Sci. Technol.* **2006,** *40*, 3388-3394.

23. He, Z.; Minteer, S. D.; Angenent, L. T., Electricity generation from artificial wastewater using an upflow microbial fuel cell. *Environ. Sci. Technol.* **2005,** *39*, (14), 5262-5267.

24. He, Z.; Wagner, N.; Minteer, S. D.; Angenent, L. T., The upflow microbial fuel cell with an interior cathode: assessment of the internal resistance by impedance spectroscopy. *Environ. Sci. Technol.* **2006,** *40*, (17), 5212-5217.

25. Jiang, D.; Li, B., Granular activated carbon single-chamber microbial fuel cells (GAC-SCMFCs): A design suitable for large-scale wastewater treatment processes. *Biochem. Eng. J.* **2009,** *47*, (1–3), 31-37.

26. Minteer, S. D.; Atanassov, P.; Luckarift, H. R.; Johnson, G. R., New materials for biological fuel cells. *Mater. Today* **2012,** *15*, (4), 166-173.

27. Peng, L.; You, S.-J.; Wang, J.-Y., Carbon nanotubes as electrode modifier promoting direct electron transfer from Shewanella oneidensis. *Biosens. Bioelectron.* **2010,** *25*, (5), 1248-1251.

28. Qiao, Y.; Bao, S.-J.; Li, C. M.; Cui, X.-Q.; Lu, Z.-S.; Guo, J., Nanostructured polyaniline/titanium dioxide composite anode for microbial fuel cells. *ACS Nano* **2007,** *2*, (1), 113-119.

29. Qiao, Y.; Li, C. M.; Bao, S.-J.; Bao, Q.-L., Carbon nanotube/polyaniline composite as anode material for microbial fuel cells. *J. Power Sources* **2007,** *170*, (1), 79-84.

30. Zhang, T.; Cui, C.; Chen, S.; Ai, X.; Yang, H.; Shen, P.; Peng, Z., A novel mediatorless microbial fuel cell based on direct biocatalysis of Escherichia coli. *Chem. Commun.* **2006**, (21), 2257-2259.

31. Qu, Y.; Feng, Y.; Wang, X.; Logan, B. E., Use of a coculture to enable current production by *Geobacter sulfurreducens*. *Appl. Environ. Microbiol.* **2012,** *78*, (9), 3484-3487.

32. Sun, J.-J.; Zhao, H.-Z.; Yang, Q.-Z.; Song, J.; Xue, A., A novel layer-by-layer self-assembled carbon nanotube-based anode: Preparation, characterization, and application in microbial fuel cell. *Electrochim. Acta* **2010,** *55*, (9), 3041-3047.

33. Tsai, H.-Y.; Wu, C.-C.; Lee, C.-Y.; Shih, E. P., Microbial fuel cell performance of multiwall carbon nanotubes on carbon cloth as electrodes. *J. Power Sources* **2009,** *194*, (1), 199-205.

34. Liang, P.; Wang, H.; Xia, X.; Huang, X.; Mo, Y.; Cao, X.; Fan, M., Carbon nanotube powders as electrode modifier to enhance the activity of anodic biofilm in microbial fuel cells. *Biosens. Bioelectron.* **2011,** *26*, (6), 3000-3004.

35. Xie, X.; Hu, L.; Pasta, M.; Wells, G. F.; Kong, D.; Criddle, C. S.; Cui, Y., Three-dimensional carbon nanotube−textile anode for high-performance microbial fuel cells. *Nano Lett.* **2010,** *11*, (1), 291-296.

36. Xie, X.; Ye, M.; Hu, L.; Liu, N.; McDonough, J. R.; Chen, W.; Alshareef, H. N.; Criddle, C. S.; Cui, Y., Carbon nanotube-coated macroporous sponge for microbial fuel cell electrodes. *Energy Environ. Sci.* **2012,** *5*, (1), 5265-5270.

37. Xie, X.; Yu, G.; Liu, N.; Bao, Z.; Criddle, C. S.; Cui, Y., Graphene-sponges as high-performance low-cost anodes for microbial fuel cells. *Energy Environ. Sci.* **2012,** *5*, (5), 6862-6866.

38. Mink, J. E.; Rojas, J. P.; Logan, B. E.; Hussain, M. M., Vertically grown multiwalled carbon nanotube anode and nickel silicide integrated high performance microsized (1.25 μL) microbial fuel cell. *Nano Lett.* **2012,** *12*, (2), 791-795.

39. Zou, Y.; Xiang, C.; Yang, L.; Sun, L.-X.; Xu, F.; Cao, Z., A mediatorless microbial fuel cell using polypyrrole coated carbon nanotubes composite as anode material. *Int. J. Hydrogen Energy* **2008,** *33*, (18), 4856-4862.

40. Dumas, C.; Mollica, A.; Féron, D.; Basséguy, R.; Etcheverry, L.; Bergel, A., Marine microbial fuel cell: Use of stainless steel electrodes as anode and cathode materials. *Electrochim. Acta* **2007,** *53*, (2), 468-473.

41. Logan, B.; Cheng, S.; Watson, V.; Estadt, G., Graphite fiber brush anodes for increased power production in air-cathode microbial fuel cells. *Environ. Sci. Technol.* **2007,** *41*, (9), 3341-3346.

42. Cheng, S.; Logan, B. E., Ammonia treatment of carbon cloth anodes to enhance power generation of microbial fuel cells. *Electrochem. Commun.* **2007,** *9*, (3), 492-496.

43. Feng, Y.; Yang, Q.; Wang, X.; Logan, B. E., Treatment of carbon fiber brush anodes for improving power generation in air–cathode microbial fuel cells. *J. Power Sources* **2010,** *195*, (7), 1841-1844.

44. Saito, T.; Mehanna, M.; Wang, X.; Cusick, R. D.; Feng, Y.; Hickner, M. A.; Logan, B. E., Effect of nitrogen addition on the performance of microbial fuel cell anodes. *Bioresour. Technol.* **2011,** *102*, (1), 395-398.

45. Natarajan, D.; Van Nguyen, T., Three-dimensional effects of liquid water flooding in the cathode of a PEM fuel cell. *J. Power Sources* **2003,** *115*, (1), 66-80.

46. He, Z.; Huang, Y.; Manohar, A. K.; Mansfeld, F., Effect of electrolyte pH on the rate of the anodic and cathodic reactions in an air-cathode microbial fuel cell. *Bioelectrochemistry* **2008,** *74*, (1), 78-82.

47. Zhao, F.; Harnisch, F.; Schröder, U.; Scholz, F.; Bogdanoff, P.; Herrmann, I., Challenges and constraints of using oxygen cathodes in microbial fuel cells. *Environ. Sci. Technol.* **2006,** *40*, (17), 5193-5199.

48. Adler, S. B., Mechanism and kinetics of oxygen reduction on porous La1-xSrxCoO3-[delta] electrodes. *Solid State Ionics* **1998,** *111*, (1-2), 125-134.

49. Holze, R.; Vielstich, W., The kinetics of oxygen reduction at porous teflon-bonded fuel cell electrodes. *J. Electrochem. Soc.* **1984,** *131*, (10), 2298-2303.

50. Zuo, Y.; Logan, B. E., Power generation in MFCs with architectures based on tubular cathodes or fully tubular reactors. *Water Sci. Technol.* **2011,** *64*, (11), 2253-2258.

51. Cheng, S.; Logan, B. E., Increasing power generation for scaling up single-chamber air cathode microbial fuel cells. *Bioresour. Technol.* **2011,** *102*, (6), 4468-4473.

52. Cheng, S.; Liu, H.; Logan, B. E., Increased performance of single-chamber microbial fuel cells using an improved cathode structure. *Electrochem. Commun.* **2006,** *8*, 489-494.

53. Zhuang, L.; Zhou, S.; Wang, Y.; Liu, C.; Geng, S., Membrane-less cloth cathode assembly (CCA) for scalable microbial fuel cells. *Biosens. Bioelectron.* **2009,** *24*, (12), 3652-3656.

54. Zuo, Y.; Cheng, S.; Call, D.; Logan, B. E., Tubular membrane cathodes for scalable power generation in microbial fuel cells. *Environ. Sci. Technol.* **2007,** *41*, (9), 3347-3353.

55. Zuo, Y.; Cheng, S.; Logan, B. E., Ion exchange membrane cathodes for scalable microbial fuel cells. *Environ. Sci. Technol.* **2008,** *42*, (18), 6967-6972.

56. Zhang, F.; Cheng, S.; Pant, D.; Bogaert, G. V.; Logan, B. E., Power generation using an activated carbon and metal mesh cathode in a microbial fuel cell. *Electrochem. Commun.* **2009,** *11*, (11), 2177-2179.

57. Zhang, F.; Saito, T.; Cheng, S.; Hickner, M. A.; Logan, B. E., Microbial fuel cell cathodes with poly(dimethylsiloxane) diffusion layers constructed around stainless steel mesh current collectors. *Environ. Sci. Technol.* **2010,** *44*, (4), 1490-1495.

58. Chen, Y.; Lv, Z.; Xu, J.; Peng, D.; Liu, Y.; Chen, J.; Sun, X.; Feng, C.; Wei, C., Stainless steel mesh coated with MnO2/carbon nanotube and polymethylphenyl siloxane as low-cost and high-performance microbial fuel cell cathode materials. *J. Power Sources* **2012,** *201*, (0), 136-141.

59. Luo, Y.; Zhang, F.; Wei, B.; Liu, G.; Zhang, R.; Logan, B. E., Power generation using carbon mesh cathodes with different diffusion layers in microbial fuel cells. *J. Power Sources* **2011,** *196*, (22), 9317-9321.

60. Cheng, S.; Liu, H.; Logan, B. E., Power densities using different cathode catalysts (Pt and CoTMPP) and polymer binders (Nafion and PTFE) in single chamber microbial fuel cells. *Environ. Sci. Technol.* **2006,** *40*, 364-369.

61. Zhang, X.; Cheng, S.; Wang, X.; Huang, X.; Logan, B. E., Separator characteristics for increasing performance of microbial fuel cells. *Environ. Sci. Technol.* **2009,** *43*, (21), 8456-8461.

62. Kiely, P. D.; Rader, G.; Regan, J. M.; Logan, B. E., Long-term cathode performance and the microbial communities that develop in microbial fuel cells fed different fermentation endproducts. *Bioresour. Technol.* **2011,** *102*, (1), 361-366.

63. Wang, H. M.; Wu, Z. C.; Plaseied, A.; Jenkins, P.; Simpson, L.; Engtrakul, C.; Ren, Z. Y., Carbon nanotube modified air-cathodes for electricity production in microbial fuel cells. *J. Power Sources* **2011,** *196*, (18), 7465-7469.

64. Shao, Y.; Liu, J.; Wang, Y.; Lin, Y., Novel catalyst support materials for PEM fuel cells: current status and future prospects. *J. Mater. Chem.* **2009,** *19*, (1), 46-59.

65. Xie, X.; Pasta, M.; Hu, L.; Yang, Y.; McDonough, J.; Cha, J.; Criddle, C. S.; Cui, Y., Nano-structured textiles as high-performance aqueous cathodes for microbial fuel cells. *Energy Environ. Sci.* **2011,** *4*, (4), 1293-1297.

66. Lefebvre, O.; Tang, Z.; Fung, M. P. H.; Chua, D. H. C.; Chang, I. S.; Ng, H. Y., Electrical performance of low cost cathodes prepared by plasma sputtering deposition in microbial fuel cells. *Biosens. Bioelectron.* **2012,** *31*, (1), 164-169.

67. Yang, X. L.; Lu, J. D.; Zhu, Y. H.; Shen, J. H.; Zhang, Z.; Zhang, J. M.; Chen, C.; Li, C. Z., Microbial fuel cell cathode with dendrimer encapsulated Pt nanoparticles as catalyst. *J. Power Sources* **2011,** *196*, (24), 10611-10615.

68. HaoYu, E.; Cheng, S.; Scott, K.; Logan, B., Microbial fuel cell performance with non-Pt cathode catalysts. *J. Power Sources* **2007,** *171*, (2), 275-281.

69. Zhao, F.; Harnisch, F.; Schröder, U.; Scholz, F.; Bogdanoff, P.; Herrmann, I., Application of pyrolysed iron (II) phthalocyanine and CoTMPP based oxygen reduction catalysts as cathode materials in microbial fuel cells. *Electrochem. Commun.* **2005,** *7*, 1405-1410.

70. Wang, X.; Cheng, S.; Zhang, X.; Li, X.-y.; Logan, B. E., Impact of salinity on cathode catalyst performance in microbial fuel cells (MFCs). *Int. J. Hydrogen Energy* **2011,** *36*, (21), 13900-13906.

71. Aelterman, P.; Versichele, M.; Genettello, E.; Verbeken, K.; Verstraete, W., Microbial fuel cells operated with iron-chelated air cathodes. *Electrochim. Acta* **2009,** *54*, (24), 5754-5760.

72. Wang, L.; Liang, P.; Zhang, J.; Huang, X., Activity and stability of pyrolyzed iron ethylenediaminetetraacetic acid as cathode catalyst in microbial fuel cells. *Bioresour. Technol.* **2011,** *102*, (8), 5093-5097.

73. Yu, E.; Cheng, S.; Logan, B.; Scott, K., Electrochemical reduction of oxygen with iron phthalocyanine in neutral media. *J. Appl. Electrochem.* **2009,** *39*, (5), 705-711.

74. Yuan, Y.; Zhao, B.; Jeon, Y.; Zhong, S. K.; Zhou, S. G.; Kim, S., Iron phthalocyanine supported on amino-functionalized multi-walled carbon nanotube as an alternative cathodic oxygen catalyst in microbial fuel cells. *Bioresour. Technol.* **2011,** *102*, (10), 5849-5854.

75. Zhang, Y. Z.; Mo, G. Q.; Li, X. W.; Ye, J. S., Iron tetrasulfophthalocyanine functionalized graphene as a platinum-free cathodic catalyst for efficient oxygen reduction in microbial fuel cells. *J. Power Sources* **2012,** *197*, 93-96.

76. Ahmed, J.; Yuan, Y.; Zhou, L. H.; Kim, S., Carbon supported cobalt oxide nanoparticles-iron phthalocyanine as alternative cathode catalyst for oxygen reduction in microbial fuel cells. *J. Power Sources* **2012,** *208*, 170-175.

77. Roche, I.; Scott, K., Carbon-supported manganese oxide nanoparticles as electrocatalysts for oxygen reduction reaction (orr) in neutral solution. *J. Appl. Electrochem.* **2009,** *39*, (2), 197-204.

78. Lu, M.; Kharkwal, S.; Ng, H. Y.; Li, S. F. Y., Carbon nanotube supported MnO2 catalysts for oxygen reduction reaction and their applications in microbial fuel cells. *Biosens. Bioelectron.* **2011,** *26*, (12), 4728-4732.

79. Mahmoud, M.; Gad-Allah, T. A.; El-Khatib, K. M.; El-Gohary, F., Power generation using spinel manganese–cobalt oxide as a cathode catalyst for microbial fuel cell applications. *Bioresour. Technol.* **2011,** *102*, (22), 10459-10464.

80. Morris, J. M.; Jin, S.; Wang, J.; Zhu, C.; Urynowicz, M. A., Lead dioxide as an alternative catalyst to platinum in microbial fuel cells. *Electrochem. Commun.* **2007,** *9*, (7), 1730-1734.

81. Freguia, S.; Rabaey, K.; Yuan, Z.; Keller, J., Non-catalyzed cathodic oxygen reduction at graphite granules in microbial fuel cells. *Electrochim. Acta* **2007,** *53*, (2), 598-603.

82. Mohan, S. V.; Srikanth, S.; Sarma, P. N., Non-catalyzed microbial fuel cell (MFC) with open air cathode for bioelectricity generation during acidogenic wastewater treatment. *Bioelectrochemistry* **2009,** *75*, (2), 130-135.

83. Shi, X.; Feng, Y.; Wang, X.; Lee, H.; Liu, J.; Qu, Y.; He, W.; Kumar, S. M. S.; Ren, N., Application of nitrogen-doped carbon powders as low-cost and durable cathodic catalyst to air–cathode microbial fuel cells. *Bioresour. Technol.* **2012,** *108*, (0), 89-93.

84. Ahmed, J., Polyaniline nanofiber/carbon black composite as oxygen reduction catalyst for air cathode microbial fuel cells. *J. Electrochem. Soc.* **2012,** *159*, (5), B497.

85. Yuan, Y.; Zhou, S. G.; Zhuang, L., Polypyrrole/carbon black composite as a novel oxygen reduction catalyst for microbial fuel cells. *J. Power Sources* **2010,** *195*, (11), 3490-3493.

86. Gong, K.; Du, F.; Xia, Z.; Durstock, M.; Dai, L., Nitrogen-doped carbon nanotube arrays with high electrocatalytic activity for oxygen reduction. *Science* **2009,** *323*, (5915), 760-764.

87. Maldonado, S.; Stevenson, K. J., Direct preparation of carbon nanofiber electrodes via pyrolysis of iron(II) phthalocyanine: electrocatalytic aspects for oxygen reduction. *J. Phys. Chem. B* **2004,** *108*, (31), 11375-11383.

88. Chen, S.; Chen, Y.; He, G.; He, S.; Schröder, U.; Hou, H., Stainless steel mesh supported nitrogen-doped carbon nanofibers for binder-free cathode in microbial fuel cells. *Biosens. Bioelectron.* **2012,** *34*, (1), 282-285.

89. Feng, L.; Yan, Y.; Chen, Y.; Wang, L., Nitrogen-doped carbon nanotubes as efficient and durable metal-free cathodic catalysts for oxygen reduction in microbial fuel cells. *Energy Environ. Sci.* **2011,** *4*, (5), 1892-1899.

90. Feng, L. Y.; Chen, Y. G.; Chen, L., Easy-to-operate and low-temperature synthesis of gram-scale nitrogen-doped graphene and its application as cathode catalyst in microbial fuel cells. *ACS Nano* **2011,** *5*, (12), 9611-9618.

91. Wang, X.; Feng, Y.; Liu, J.; Shi, X.; Lee, H.; Li, N.; Ren, N., Power generation using adjustable Nafion/PTFE mixed binders in air-cathode microbial fuel cells. *Biosens. Bioelectron.* **2010,** *26*, (2), 946-948.

92. Pant, D.; Van Bogaert, G.; De Smet, M.; Diels, L.; Vanbroekhoven, K., Use of novel permeable membrane and air cathodes in acetate microbial fuel cells. *Electrochim. Acta* **2010,** *55*, (26), 7710-7716.

93. Saito, T.; Merrill, M. D.; Watson, V. J.; Logan, B. E.; Hickner, M. A., Investigation of ionic polymer cathode binders for microbial fuel cells. *Electrochim. Acta* **2010,** *55*, (9), 3398-3403.

94. Saito, T.; Roberts, T. H.; Long, T. E.; Logan, B. E.; Hickner, M. A., Neutral hydrophilic cathode catalyst binders for microbial fuel cells. *Energy Environ. Sci.* **2011,** *4*, (3), 928-934.

95. Chen, G.; Wei, B.; Logan, B. E.; Hickner, M. A., Cationic fluorinated polymer binders for microbial fuel cell cathodes. *RSC Advances* **2012**.

96. Yu, E. H.; Burkitt, R.; Wang, X.; Scott, K., Application of anion exchange ionomer for oxygen reduction catalysts in microbial fuel cells. *Electrochem. Commun. in press*.

97. Yan, H.; Saito, T.; Regan, J. M., Nitrogen removal in a single-chamber microbial fuel cell with nitrifying biofilm enriched at the air cathode. *Water Res.* **2012,** *46*, (7), 2215-2224.

98. Liu, H.; Logan, B. E., Electricity generation using an air-cathode single chamber microbial fuel cell in the presence and absence of a proton exchange membrane. *Environ. Sci. Technol.* **2004,** *38*, (14), 4040-4046.

99. Mehanna, M.; Saito, T.; Yan, J.; Hickner, M.; Cao, X.; Huang, X.; Logan, B. E., Using microbial desalination cells to reduce water salinity prior to reverse osmosis. *Energy Environ. Sci.* **2010,** *3*, (8), 1114-1120.

100. Kim, Y.; Logan, B. E., Series assembly of microbial desalination cells containing stacked electrodialysis cells for partial or complete seawater desalination. *Environ. Sci. Technol.* **2011,** *45*, (13), 5840-5845.

101. Chen, S.; Liu, G.; Zhang, R.; Qin, B.; Luo, Y., Development of the microbial electrolysis desalination and chemical-production cell for desalination as well as acid and alkali productions. *Environ. Sci. Technol.* **2012,** *46*, (4), 2467-2472.

102. Kim, Y.; Logan, B. E., Microbial reverse electrodialysis cells for synergistically enhanced power production. *Environ. Sci. Technol.* **2011,** *45*, (13), 5834-5839.

103. Cusick, R. D.; Kim, Y.; Logan, B. E., Energy capture from thermolytic solutions in microbial reverse-electrodialysis cells. *Science* **2012,** *335*, (6075), 1474-1477.

104. Zhang, F.; Brastad, K. S.; He, Z., Integrating forward osmosis into microbial fuel cells for wastewater treatment, water extraction and bioelectricity generation. *Environ. Sci. Technol.* **2011,** *45*, (15), 6690-6696.

105. Zhang, X.; Cheng, S.; Huang, X.; Logan, B. E., Improved performance of single-chamber microbial fuel cells through control of membrane deformation. *Biosens. Bioelectron.* **2010,** *25*, (7), 1825-1828.

106. Liang, P.; Huang, X.; Fan, M.-Z.; Cao, X.-X.; Wang, C., Composition and distribution of internal resistance in three types of microbial fuel cells. *Appl. Microbiol. Biotechnol.* **2007,** *77*, 551-558.

107. Kim, J. R.; Cheng, S.; Oh, S.-E.; Logan, B. E., Power generation using different cation, anion and ultrafiltration membranes in microbial fuel cells. *Environ. Sci. Technol.* **2007,** *41*, (3), 1004-1009.

108. Fan, Y.; Hu, H.; Liu, H., Enhanced coulombic efficiency and power density of air-cathode microbial fuel cells with an improved cell configuration. *J. Power Sources* **2007,** *171*, (2), 348-354.

109. Zhang, X.; Cheng, S.; Liang, P.; Huang, X.; Logan, B. E., Scalable air cathode microbial fuel cells using glass fiber separators, plastic mesh supporters, and graphite fiber brush anodes. *Bioresour. Technol.* **2011,** *102*, (1), 372-375.

110. Watson, V. J.; Saito, T.; Hickner, M. A.; Logan, B. E., Polymer coatings as separator layers for microbial fuel cell cathodes. *J. Power Sources* **2011,** *196*, (6), 3009-3014.

111. Zhang, X.; Cheng, S.; Huang, X.; Logan, B. E., The use of nylon and glass fiber filter separators with different pore sizes in air-cathode single-chamber microbial fuel cells. *Energy Environ. Sci.* **2010,** *3*, (5), 659-664.

112. Yang, Q.; Feng, Y.; Logan, B. E., Using cathode spacers to minimize reactor size in air cathode microbial fuel cells. *Bioresour. Technol.* **2012,** *110*, (0), 273-277.

Chapter 3

Mesh optimization for microbial fuel cell cathodes constructed around stainless steel mesh current collectors [1]

Abstract

Mesh current collectors made of stainless steel (SS) can be integrated into microbial fuel cell (MFC) cathodes constructed of a reactive carbon black and Pt catalyst mixture and a poly(dimethylsiloxane) (PDMS) diffusion layer. It is shown here that the mesh properties of these cathodes can significantly affect performance. Cathodes made from the coarsest mesh (30-mesh) achieved the highest maximum power of 1616±25 mW m^{-2} (normalized to cathode projected surface area; 47.1±0.7 W m^{-3} based on liquid volume), while the finest mesh (120-mesh) had the lowest power density (599±57 mW m^{-2}). Electrochemical impedance spectroscopy showed that charge transfer and diffusion resistances decreased with increasing mesh opening size. Oxygen permeability increased with mesh opening size, accounting for the decreased diffusion resistance. At higher current densities, diffusion became a limiting factor, especially for fine mesh with low oxygen transfer coefficients. These results demonstrate the critical nature of the mesh size used for constructing MFC cathodes.

---

[1] Materials presented in this chapter was published in the following paper: Zhang, F.; Merrill, M. D.; Tokash, J. C.; Saito, T.; Cheng, S.; Hickner, M. A.; Logan, B. E., Mesh optimization for microbial fuel cell cathodes constructed around stainless steel mesh current collectors. *Journal of Power Sources* **2011,** *196*, (3), 1097-1102.

3.1 Introduction

Microbial fuel cells (MFCs) are devices that use bacteria as catalysts to oxidize organic or inorganic matter and generate current *(1-5)*. One promising application for MFCs is wastewater treatment, where energy is recovered from organic matter while at the same time the wastewater is treated. Many chemicals have been used as electron acceptors in MFCs, but oxygen is the most cost-effective, sustainable and environmental friendly electron acceptor for wastewater treatment applications. Air cathodes, which have one side exposed to air and the other exposed to wastewater, provide an efficient method for transferring oxygen to the cathode catalytic sites. Oxygen used at the cathode is readily replenished directly from air without the need for wastewater aeration *(6)*.

The power densities produced by MFCs are mainly limited by the cathode performance and high ohmic resistance of these systems *(7, 8)*. Cathode design is challenging due to the relative poor kinetics of oxygen reduction reaction under neutral pH conditions in MFCs, compared to hydrogen fuel cells where cathodes work at much lower pH *(9)*. Improving cathode performance is therefore critical for increasing power production in MFCs by changes in system architecture that reduce internal resistance, such as by reducing electrode spacing and increasing solution conductivity *(10, 11)*. However, the most critical factor in the development of new cathodes for MFCs is to use inexpensive materials that lack precious metals.

Metal current collectors are usually needed for fuel cell electrodes especially for large scale systems to avoid large in-plane resistances across the electrode area, and therefore MFC electrodes are being constructed around inexpensive current collectors. For example, graphite fiber brush electrodes have a twisted metal core to facilitate electron transfer from the bacteria to the circuit. Using this type of anode a maximum power density of 2400 mW m^{-2} was produced in a small laboratory-scale reactor *(12)*. Stainless steel (SS) mesh has been used as a cathode current

collector *(13, 14)*. By adding a SS mesh to the surface of an anion exchange membrane coated with a conductive graphite paint, power was increased from 450 mW m^{-2} to 575 mW m^{-2} *(14)*. It was recently shown that the current collector could be directly integrated into the cathode structure by constructing the cathode around the current collector. Inexpensive activated carbon (AC) and a polytetrafluoroethylene (PTFE) binder were pressed onto a Ni mesh, with an additional PTFE layer serving as a diffusion layer. This AC cathode produced a maximum of 1220 mW m^{-2}, despite the lack of a metal catalyst *(15)*. A different type of mesh cathode was constructed using SS mesh by coating one side of the mesh with a poly(dimethylsiloxane) (PDMS) and carbon black diffusion layer (air side) and the other side with a Pt/C catalyst layer *(13)*. Power densities were optimized by limiting oxygen diffusion by varying the number of PDMS/carbon black diffusion layers. The optimum condition was two diffusion layers, which produced power densities of 1610 mW m^{-2} *(13)*. In both of these studies the effect of the mesh size on the electrode was not considered. However, the opening size and amount of metal used in the mesh could affect oxygen transfer, proton transfer, electrical conductivity, and relative contact between the coatings and metal surfaces, all of which can affect cathode performance.

In this study, we examined the effect of mesh size on cathode performance for SS mesh having five different sizes, with all mesh containing the same PDMS/carbon black diffusion layers and Pt/C catalyst. The different mesh cathodes were analyzed for power production, resistances due to cathode charge transfer and diffusion, electrode capacitance, and oxygen transfer.

3.2 Materials and methods

3.2.1 Cathodes

Cathodes were constructed from stainless steel mesh, Pt, and PDMS as previously described *(13)*. SS woven wire (plain weave) sizes, characterized by the number of openings per linear inch (from coarse to fine) were: 30×30, 50×50, 70×70, 90×90 and 120×120 (Table 3-1, type 304 SS, McMaster-Carr, OH). Mesh characteristics of openings per linear inch, wire diameter, opening size and fractional open area were specified by the manufacturers. Specific surface area (surface area per unit volume ratio) and porosity of the mesh (void fraction) were calculated based on the assumption that the mesh thickness was twice that of the individual wire diameters, and that the wires were uniformly cylindrical and in point-to-point contact. Two layers of PDMS/carbon black were applied to the air side as diffusion layer *(13)*. After applying the diffusion layer, the Pt catalyst layer with a nominal loading of 0.5 mg per cm^2 of cathode projected area (5 mg cm^{-2} 10% Pt on Vulcan XC-72 with 33.3 μL cm^{-2} of 5 wt% Nafion solution as binder) was applied to the SS mesh on the side facing the solution *(8)*.

3.2.2 MFC construction and operation

MFCs were single-chamber cubic-shaped reactors constructed as previously described *(16)*, with an anode chamber 4 cm long and 3 cm in diameter. The anode was a single ammonia gas treated graphite fiber brush (25 mm diameter × 25 mm length; fiber type PANEX 33 160K, ZOLTEK) *(12, 17)*. All reactors were inoculated using the effluent from an MFC operated for over two years. The medium contained sodium acetate as the fuel (1.0 g L^{-1}), and a phosphate buffer nutrient solution (PBS; conductivity of 6.82 mS cm^{-1}) containing: Na_2HPO_4, 4.58 g L^{-1}; $NaH_2PHO_4 \cdot H_2O$ 2.45 g L^{-1}; NH_4Cl 0.31 g L^{-1}; KCl 0.13 g L^{-1}; trace minerals (12.5 mL L^{-1}) and

vitamins (5 mL L^{-1}) *(18)*. Reactors were all operated in fed-batch mode at 30 °C and were refilled each time when the voltage decreased to less than 20 mV forming one complete cycle of operation.

Table 3-1. R_{ct}, R_d and capacitance at OCP, 0.1 V and 0 V with cathode made from mesh of different size.

Mesh size / N inch^{-1}		30	50	70	90	120
Opening size / mm		0.53	0.28	0.20	0.15	0.12
Wire diameter / mm		0.30	0.23	0.17	0.14	0.09
Fractional open area / %		40.8	30.3	29.8	25.4	30.5
Porosity		0.70	0.61	0.61	0.57	0.62
Specific surface area / mm^{-1}		3.9	6.8	9.5	12.4	16.2
R_{ct} / Ω cm^2	**OCP**	4.9	3.7	5.1	5.4	6.6
	0.1 V	1.6	1.7	3.1	3.6	5.1
	0 V	0.04	0.03	0.02	0.74	1.3
R_d / Ω cm^2	**OCP**	6.6	8.7	12.4	10.8	12.2
	0.1 V	0.6	1.0	0.6	1.2	1.4
	0 V	1.0	1.1	0.8	12.2	12.6
C / Ω^{-1} s^n cm^{-2}	**OCP**	1.42	1.06	0.95	0.81	0.50
	0.1 V	2.12	1.20	1.30	0.98	0.74
	0 V	1.05	0.81	0.87	0.97	0.65
n	**OCP**	0.79	0.82	0.89	0.90	0.86
	0.1 V	0.70	0.72	0.73	0.75	0.71
	0 V	0.36	0.42	0.49	0.81	0.81

3.2.3 Calculations and measurements

Voltage (E) across the external resistor (1 kΩ, except as noted) in the MFC circuit was measured at 20 min intervals using a data acquisition system (2700, Keithley Instrument, OH) connected to a personal computer. Current ($I = E/R$) and power ($P = IE$) were calculated as previously described *(3)*, with the current density and power density normalized by the projected surface area of the cathode. To obtain the polarization and power density curves as a function of current, external circuit resistances were varied from 1000 to 20 Ω in decreasing order every 20 min.

Physical characteristics of woven wire mesh can affect reactor performance, as shown in other engineered systems such as catalytic reactors and filters *(19-21)*. The wire diameter and the fractional opening (porosity) of a typical screen are the most significant factors. Under static flow conditions (no advective transport though the mesh), transport by diffusion can be modeled using $D_{Cj,p} = D_{Cj}\,(\theta/\tau_f)$ (macroporous matrix diffusion model), where $D_{Cj,p}$ is the diffusion constant for chemical *C* in the porous matrix filled with phase *j*, D_{Cj} the diffusion constant for chemical *C* in phase *j*, θ the porosity of the porous medium, and τ_f the tortuosity factor *(22)*. For plain weaves the fluid path length and the screen thickness are essentially equal and $\tau_f = 1$ *(19)*. In order to assess how mesh porosity affected mesh mass transfer properties, oxygen permeability was measured in terms of oxygen transfer coefficient as previously described using the same 4-cm reactor examined in MFC tests *(23)*. Dissolved oxygen concentrations were measured using a non-consumptive oxygen probe (NeoFox, Ocean Optics, Inc., Dunedin, FL).

The mesh characteristics can also be expected to affect charge transfer and current distribution in cathodes. Electrochemical impedance spectroscopy (EIS) can be used to characterize electrode properties and measure the MFC internal resistance R_{int} *(24-26)*. Electrochemical properties including three sources of resistance: charge transfer resistance (R_{ct}), diffusion resistance (R_d), solution resistance (R_s), and capacitance of the catalyst double layer are determined by fitting the measured impedance data to an equivalent circuit.

Linear sweep voltammetry (LSV) and EIS were used to electrochemically characterize the cathodes using a potentiostat (PC4/750, Gamry Instruments). Cathodes were placed in an electrochemical cell consisting of a working electrode (cathode with 7 cm^2 projected surface area), an Ag/AgCl reference electrode (RE-5B; BASi, West Lafayette, IN) and a Pt counter electrode *(13)*. For LSV tests, the cathode was equilibrated to +0.5 V for one hour and then scanned at –1 mV s^{-1} to 0 V (vs. standard hydrogen electrode, SHE) with current interrupt IR compensation to dynamically correct uncompensated resistance errors. Impedance measurements

were conducted at open circuit and polarized conditions which were 0.1 V and 0 V versus SHE (–0.1 V and –0.2 V vs. Ag/AgCl) over a frequency range of 100 kHz to 1 mHz with a sinusoidal perturbation of 10 mV amplitude. Resistances and capacitances were normalized to cathode projected surface area.

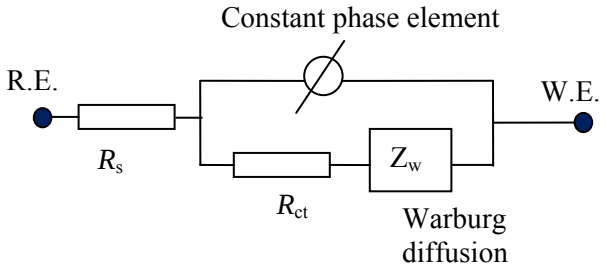

Figure 3-1. Equivalent circuit of the electrochemical cell for EIS.

EIS spectra were fitted into an equivalent circuit using Gamry Echem Analyst software (provided by the potentiostat manufacturer). The equivalent circuit used here assumes that the cathode reaction is affected by both reaction kinetics and diffusion (Figure 3-1), with the symbol R_s for solution resistance and R_{ct} for charge transfer resistance. A constant phase element (CPE) was used instead of a capacitor in order to model double layer capacitance when surface roughness or a distribution of reactions across the surface can affect overall kinetics. The CPE has two parameters: C and n. C indicates the capacitance, and it is the value of the admittance at ω = 1 rad s^{-1} (~0.16 Hz). The phase angle depression factor, n, has a value between 0 and 1 and it describes the level of ideality for the CPE circuit element (n = 1 is perfectly ideal capacitive behavior). A porous bounded Warburg element was used to evaluate diffusion resistance in terms of two parameters: Y_0 and B. Y_0 is the magnitude of the admittance at ω = 1 rad s^{-1}, while B characterizes the time it takes for a reactant to diffuse through a thin film, which in our case is the thin film of electrolyte between the electrode and the permeable PDMS membrane. The ratio B/Y_0 indicates the magnitude of diffusion resistance R_d.

3.3 Results

3.3.1 Performance of SS mesh cathodes in MFCs with different mesh sizes

Large differences in power production by cathodes with different mesh size were observed based on polarization data. MFCs with 30-mesh cathodes achieved the highest power density of 1616±25 mW m^{-2} (± S.D., duplicate reactors), which was similar to that produced with 50-mesh of 1563±128 mW m^{-2} (Figure 3-2A). Cathodes made from 70-mesh achieved a slightly lower power density of 1415±125 mW m^{-2}. Power production was much lower when smaller mesh opening sizes were used, with 982±62 mW m^{-2} for the 90-mesh and 599±57 mW m^{-2} for the 120-mesh (Figure 3-2A). Cathode potentials followed the same trend as the power production, and anode potentials were all similar, providing evidence that the cathode performance was the reason for the differences in power generation among these reactors (Figure 3-2B).

3.3.2 LSV tests

SS mesh cathodes with different mesh size were examined using LSV to evaluate the effect of SS mesh size on electrochemical performance in the absence of bacteria. Current densities of cathodes increased in magnitude with increasing mesh opening sizes and with increasing overpotentials (Figure 3-3). Cathodes made from 30- and 50-mesh had similar current densities across the higher scanned potentials, while 50-mesh performed slightly better at low potentials. Current densities of the SS mesh cathodes with smaller mesh openings had reduced activities compared to the coarser meshes, and the cathode made from the finest mesh (120-mesh) had the lowest current response at any given scanned potential (Figure 3-3). These scans demonstrate inherent differences in electrochemical properties of cathodes based on their mesh (opening) sizes.

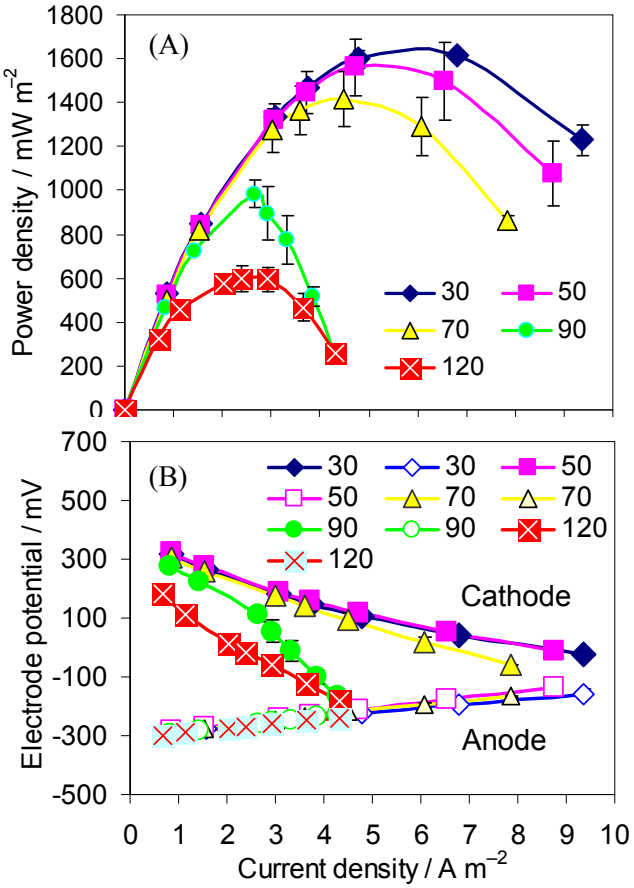

Figure 3-2. (A) Power densities and (B) Electrode potentials of SS mesh cathodes with different mesh size as a function of current density (normalized to cathode projected surface area) obtained by varying the external circuit resistance (1000 - 20 Ω). (Error bars ± SD based on measurement of two duplicate reactors.)

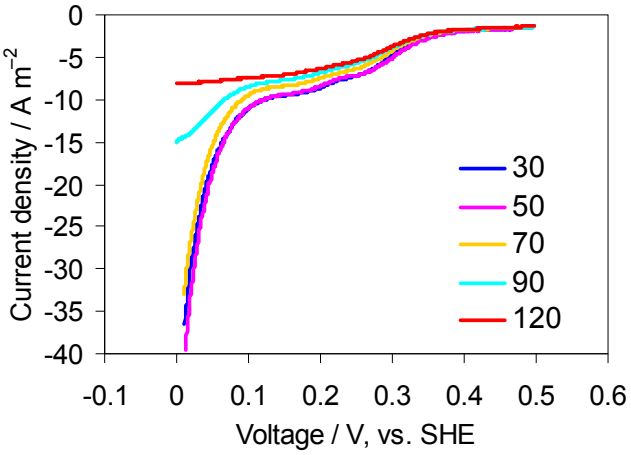

Figure 3-3. LSV of SS mesh cathodes with different mesh size.

3.3.3 Impedance of the cathodes

EIS was performed at open circuit and polarized conditions of 0.1 V and 0 V. Open circuit cathode potential ranged between 0.354-0.385 V (vs. SHE) from fine to coarse mesh. Internal resistance decreased with an increase in mesh opening size (from fine to coarse mesh, Figure 3-4 and Figure 3-5), which is due to differences in current density at the various fixed potentials under consideration. This behavior is shown by a decrease in the size of the semi-circle produced in Nyquist plots (Figure 3-4). As expected, solution resistances (R_s) were all similar for the cathodes at different polarized conditions due to the use of the same cell configuration and solution in EIS tests (Figure 3-5). However, other electrochemical properties (R_{ct}, R_d and double layer capacitance) were altered by the use of cathodes with different sized mesh. R_{ct} generally decreased with increasing mesh opening size, and decreased with increasing oxygen reduction overpotential (OCP → 0.1 V → 0 V; Figure 3-5). At 0.1 V, the cathode made from 30-mesh had the smallest R_{ct} of 1.6 Ω cm^2 while 120-mesh had the largest of R_{ct} = 5.1 Ω cm^2. These values

decreased to R_{ct} = 0.04 Ω cm^2 (30 mesh) and 1.3 Ω cm^2 (120 mesh) at the higher overpotential (0 V).

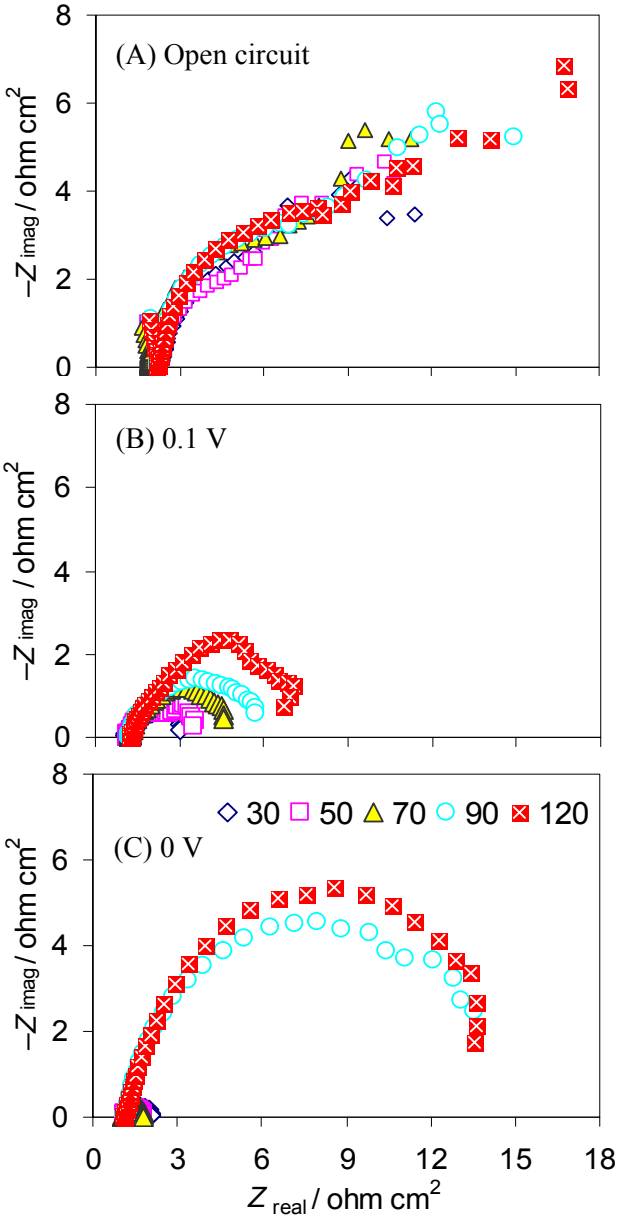

Figure 3-4. Nyquist plots of EIS spectra by SS mesh cathodes with different mesh size at (A) open circuit, (B) 0.1 V, (C) 0 V. (Resistances normalized to cathode projected surface area.)

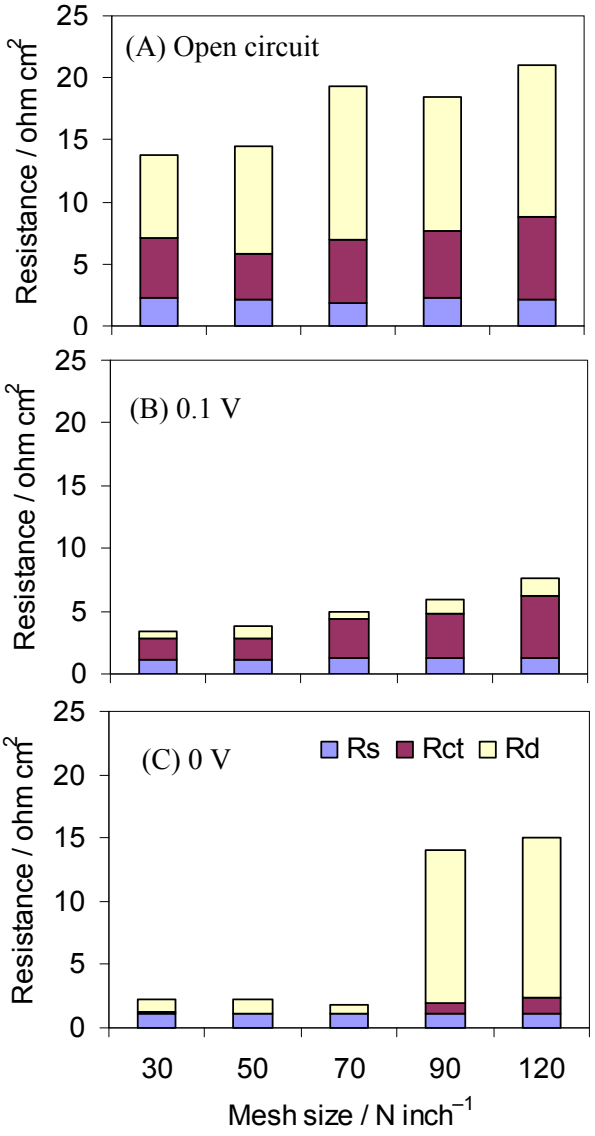

Figure 3-5. Component analysis of internal resistance at different EIS operation conditions for cathodes with different sized mesh: (A) open circuit, (B) 0.1 V, (C) 0 V. (Resistances normalized to cathode projected surface area.)

Diffusion resistances also decreased from fine to coarse mesh at open circuit and polarized conditions. R_d decreased from 1.4 Ω cm^2 to 0.6 Ω cm^2 as mesh size decreased from 120- to 30-mesh (0.1 V). At the higher overpotential (0 V), R_d had larger variations with mesh size, with R_d = 12.2 Ω cm^2 for 90-mesh, and R_d = 12.6 Ω cm^2 for 120-mesh. These values are an order

of magnitude larger than those of other coarser mesh cathodes (all <1.2 Ω cm^2) (Table 3-1, Figure 3-5C). Thus, the increase in the diameter of the semi-circle in Nyquist plots when EIS was performed at 0 V compared to 0.1 V, was mainly due to the increase of R_d (Figure 3-4 B and C).

Double layer capacitance increased from fine to coarse mesh at both open circuit and polarized conditions (Table 3-1). This increase was due to more charge buildup at the interface between electrode and electrolyte because of higher current densities achieved by coarser mesh cathodes. It was also likely that coarser mesh cathodes produced more interface between electrode and electrolyte.

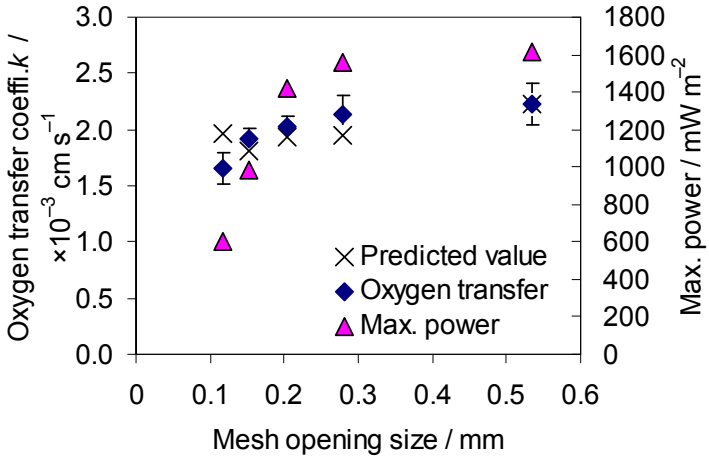

Figure 3-6. Experimental and predicted oxygen transfer coefficient (based on the macroporous matrix diffusion model) of SS mesh cathodes with different sized mesh, and maximum power densities achieved by these cathodes, against mesh opening size.

3.3.4 Oxygen permeability

Cathodes with different mesh size had different oxygen permeabilities, likely due to hindered diffusion by the mesh. Oxygen transfer coefficients increased with increasing opening size of mesh. Cathodes made from 30-mesh had the highest oxygen transfer coefficient of 2.2±0.2 $\times 10^{-3}$

cm s^{-1} and finer mesh had lower values from 2.1±0.2 $\times 10^{-3}$ cm s^{-1} (50-mesh) to 1.7±0.1 $\times 10^{-3}$ cm s^{-1} (120-mesh) (Figure 3-6). It was expected from the macroporous matrix diffusion model that the oxygen transfer coefficient would have a linear relationship against mesh porosity, and this was shown by general good agreement between predicted (based on the initial experimental value for the 30-mesh sample) and experimental oxygen transfer coefficients. However, maximum power production increased much more rapidly than the oxygen transfer coefficients with the increasing mesh opening size from 0.1 mm to 0.3 mm (Figure 3-6), suggesting that other characteristics of the system such as wire diameter and contact between metal and catalyst, affected overall power production. Additional comparisons of oxygen transfer to porosity and fractional open area did not explain the observed increases in power (see Appendix A).

3.4 Discussion

Reactor performance generally increased with increasing mesh opening size from fine to coarse mesh. The best performance was obtained with SS mesh cathodes made using 30-mesh, resulting in a maximum power density of 1616±25 mW m^{-2} (47.1±0.7 W m^{-3}). Cathodes made from 50-mesh had similar performance to those made with 30-mesh, but the use of finer mesh resulted in less power production and lower cathode potentials. Cathode made from 90-mesh produced 982 ± 62 mW m^{-2}, which was lower than that obtained in previous tests (1610±56 mW m^{-2}) *(13)*, primarily due to differences in solution conductivity (8.2 mS cm^{-1} compared to 6.8 mS cm^{-1} here), but also perhaps the use of different inocula and variations in materials (different batches of stainless steel mesh).

Both electrochemical studies and MFC tests show that mesh properties can appreciably affect MFC performance. Coarser mesh cathodes exhibited higher current densities in LSV voltammograms and produced higher power in MFCs, due to lower values of both R_{ct} and R_d. R_s

were all similar among all the cathodes, and this solution resistance can be reduced by minimizing the space between anode and cathode using a separator *(27, 28)*. When EIS was conducted at a fixed cathode potential of 0.1 V, close to the point of maximum power production for most cathodes in MFC tests (Figure 3-2B), R_{ct} was the largest contributor to resistance, indicating that the cathode reaction was primarily kinetically limited under our operating conditions. Kinetic limitations suggest that improving oxygen reduction kinetics is important for improving MFC performance. Comparing R_{ct} at different potentials, a higher oxygen reduction overpotential resulted in a lower R_{ct} because of the larger driving force for electron transfer. At a given potential, coarser mesh cathodes had lower R_{ct} values than the finer mesh. There are two possible reasons for this difference. One is that coarser mesh with larger wire diameter had more mesh/catalyst contacts which would lower the resistance for electrons going across metal surface and distributing among catalyst sites. The other possible reason is that catalysts could be more effective in oxygen reduction on coarser mesh cathodes, as inferred from the variation in double layer capacitance of the cathodes as discussed below.

Double layer capacitance can be related to the electrode-electrolyte networks in the catalytic layer because capacitance is induced by the buildup of charge at the electrode-electrolyte interface. Measurement of the double layer capacitance can be used as an *in situ* assessment of the wetted surface area, i.e. the electroactive surface area *(29, 30)*. In this study, double layer capacitance increased from 120-mesh to 30-mesh, suggesting that the coarser mesh had larger active surface area and thus a higher catalyst utilization. It is possible that a coarse mesh allows more catalyst/mesh contacts as the catalyst layer "sinks" into the openings of the mesh, while the catalyst layer sits on top of the fine mesh. In that case, the catalyst layer on coarse mesh coats more of the wires and produces more catalyst/mesh contacts, so that the coarse mesh can produce more interface between the metal surface, catalyst layer, and the electrolyte. Larger currents

achieved by coarser mesh also contributed to more surface charge buildup, resulting in a higher capacitance for the coarser mesh cathodes.

Oxygen transfer through cathodes was hindered by the impermeable SS mesh, with measured mass transfer coefficients in general agreement with diffusion calculations. The lack of agreement with the model for this oxygen transfer coefficient was possibly a result of the impact of overall diffusion rates in the microporous PDMS and carbon black layer rather than mass transfer controlled by overall porosity of the SS mesh openings. The variations in cathode oxygen permeabilities resulted in different R_d values, with coarser mesh having higher oxygen transfer coefficients and lower R_d values. When EIS was conducted at 0 V, the R_d was much larger than R_{ct} (Figure 3-5C), and diffusion limitations became the dominant factor affecting cathode performance. We observed that the R_d values for the 90-mesh and 120-mesh cathodes substantially increased at 0 V, most likely due to oxygen depletion at the high current densities. Therefore, 30, 50, 70-mesh cathodes with much less R_d exhibited much higher current densities at 0 V in LSV tests (due to a lack of oxygen diffusion limitations in these mesh cathodes) compared to finer mesh cathodes (90, 120-mesh).

3.5 Conclusions

These experiments have shown that SS mesh can appreciably affect the cathode performance. By selecting commercially available SS mesh with different mesh size numbers, mesh properties such as opening size, wire diameter, surface area all varied. These changes in properties affected oxygen transfer and the efficiency of catalyst, as indicated by a change in the double layer capacitance, charge transfer resistance, and diffusion resistance of the cathodes. MFC performance was primarily kinetics limited for our operating conditions, and this was the main reason for the variations in MFC performance with the different SS mesh cathodes. Oxygen

transfer hindrance through the mesh was more related to opening size of the SS mesh, and this hindrance further affected the diffusion resistance of the cathodes. Cathode oxygen reduction rates were limited by diffusion at higher current densities, however, especially for the fine mesh. Coarse mesh provided the best performance, and the maximum power production reached a plateau when we increased the mesh opening size (Figure 3-6). Therefore, based on our experiments the 30- or 50-mesh are the most optimal materials for maximizing power production. These coarse meshes also have better mechanical strength because of the larger diameter wires used for fabrication, favoring their use in practical applications as current collectors in MFC cathodes.

3.6 Acknowledgments

The authors thank David Jones and Ellen Bingham for help with the analytical measurements. This research was supported by Award KUS-I1-003-13 from the King Abdullah University of Science and Technology (KAUST).

3.7 Literature cited

1. Logan, B. E., *Microbial Fuel Cells*. John Wiley & Sons, Inc.: Hoboken, NJ, 2008.
2. Logan, B. E., Exoelectrogenic bacteria that power microbial fuel cells. *Nat. Rev. Microbiol.* **2009,** *7*, (5), 375-381.
3. Logan, B. E.; Aelterman, P.; Hamelers, B.; Rozendal, R.; Schröder, U.; Keller, J.; Freguiac, S.; Verstraete, W.; Rabaey, K., Microbial fuel cells: methodology and technology. *Environ. Sci. Technol.* **2006,** *40*, (17), 5181-5192.

4. Lovley, D. R., Bug juice: harvesting electricity with microorganisms. *Nat. Rev. Microbiol.* **2006,** *4*, 497-508.

5. Rabaey, K.; Verstraete, W., Microbial fuel cells: novel biotechnology for energy generation. *Trends Biotechnol.* **2005,** *23*, (6), 291-298.

6. Liu, H.; Ramnarayanan, R.; Logan, B. E., Production of electricity during wastewater treatment using a single chamber microbial fuel cell. *Environ. Sci. Technol.* **2004,** *38*, (7), 2281-2285.

7. Kim, B.; Chang, I.; Gadd, G., Challenges in microbial fuel cell development and operation. *Appl. Microbiol. Biotechnol.* **2007,** *76*, (3), 485-494.

8. Cheng, S.; Liu, H.; Logan, B. E., Power densities using different cathode catalysts (Pt and CoTMPP) and polymer binders (Nafion and PTFE) in single chamber microbial fuel cells. *Environ. Sci. Technol.* **2006,** *40*, 364-369.

9. Gil, G. C.; Chang, I. S.; Kim, B. H.; Kim, M.; Jang, J. K.; Park, H. S.; Kim, H. J., Operational parameters affecting the performance of a mediator-less microbial fuel cell. *Biosens. Bioelectron.* **2003,** *18*, (4), 327-334.

10. Liu, H.; Cheng, S.; Logan, B. E., Power generation in fed-batch microbial fuel cells as a function of ionic strength, temperature, and reactor configuration. *Environ. Sci. Technol.* **2005,** *39*, (14), 5488-5493.

11. Cheng, S.; Liu, H.; Logan, B. E., Increased power generation in a continuous flow MFC with advective flow through the porous anode and reduced electrode spacing. *Environ. Sci. Technol.* **2006,** *40*, 2426-2432.

12. Logan, B. E.; Cheng, S.; Watson, V.; Estadt, G., Graphite fiber brush anodes for increased power production in air-cathode microbial fuel cells. *Environ. Sci. Technol.* **2007,** *41*, (9), 3341-3346.

13. Zhang, F.; Saito, T.; Cheng, S.; Hickner, M. A.; Logan, B. E., Microbial fuel cell cathodes with poly(dimethylsiloxane) diffusion layers constructed around stainless steel mesh current collectors. *Environ. Sci. Technol.* **2010,** *44*, (4), 1490-1495.

14. Zuo, Y.; Cheng, S.; Logan, B. E., Ion exchange membrane cathodes for scalable microbial fuel cells. *Environ. Sci. Technol.* **2008,** *42*, (18), 6967-6972.

15. Zhang, F.; Cheng, S.; Pant, D.; Bogaert, G. V.; Logan, B. E., Power generation using an activated carbon and metal mesh cathode in a microbial fuel cell. *Electrochem. Commun.* **2009,** *11*, (11), 2177-2179.

16. Liu, H.; Logan, B. E., Electricity generation using an air-cathode single chamber microbial fuel cell in the presence and absence of a proton exchange membrane. *Environ. Sci. Technol.* **2004,** *38*, (14), 4040-4046.

17. Cheng, S.; Logan, B. E., Ammonia treatment of carbon cloth anodes to enhance power generation of microbial fuel cells. *Electrochem. Commun.* **2007,** *9*, (3), 492-496.

18. Cheng, S.; Xing, D.; Call, D. F.; Logan, B. E., Direct biological conversion of electrical current into methane by electromethanogenesis. *Environ. Sci. Technol.* **2009,** *43*, (10), 3953-3958.

19. Armour, J. C.; Cannon, J. N., Fluid flow through woven screens. *AlChE J.* **1968,** *14*, (3), 415-420.

20. Satterfield, C. N.; Cortez, D. H., Mass transfer characteristics of woven-wire screen catalysts. *Ind. Eng. Chem. Fundam.* **1970,** *9*, (4), 613-620.

21. Kolodziej, A.; Lojewska, J., Experimental and modelling study on flow resistance of wire gauzes. *Chem. Eng. Process.* **2009,** *48*, (3), 816-822.

22. Logan, B. E., *Environmental Transport Processes*. Wiley: New York, 1999.

23. Cheng, S.; Liu, H.; Logan, B. E., Increased performance of single-chamber microbial fuel cells using an improved cathode structure. *Electrochem. Commun.* **2006,** *8*, 489-494.

24. He, Z.; Mansfeld, F., Exploring the use of electrochemical impedance spectroscopy (EIS) in microbial fuel cell studies. *Energy Environ. Sci.* **2009,** *2*, (2), 215-219.

25. Manohar, A. K.; Bretschger, O.; Nealson, K. H.; Mansfeld, F., The use of electrochemical impedance spectroscopy (EIS) in the evaluation of the electrochemical properties of a microbial fuel cell. *Bioelectrochemistry* **2008,** *72*, (2), 149-154.

26. Manohar, A. K.; Mansfeld, F., The internal resistance of a microbial fuel cell and its dependence on cell design and operating conditions. *Electrochim. Acta* **2009,** *54*, (6), 1664-1670.

27. Fan, Y.; Hu, H.; Liu, H., Enhanced coulombic efficiency and power density of air-cathode microbial fuel cells with an improved cell configuration. *J. Power Sources* **2007,** *171*, (2), 348-354.

28. Zhang, X.; Cheng, S.; Wang, X.; Huang, X.; Logan, B. E., Separator characteristics for increasing performance of microbial fuel cells. *Environ. Sci. Technol.* **2009,** *43*, (21), 8456-8461.

29. Eaton, A. D.; Clesceri, L. S.; Greenberg, A. E., *Standard Methods for the Examination of Water and Wastewater*. 19 ed.; APHA, AWWA, WEF: Washington DC, 1995.

30. Jarek, S.; Thonstad, J., Double-layer capacitance and polarization potential of baked carbon anodes in cryolite-alumina melts. *J. Appl. Electrochem.* **1987,** *17*, (6), 1203-1212.

Chapter 4

Novel anti-flooding poly(dimethylsiloxane) (PDMS) catalyst binder for microbial fuel cell cathodes [2]

Abstract

Poly(dimethylsiloxane) (PDMS) was investigated as an alternative to Nafion as an air cathode catalyst binder in microbial fuel cells (MFCs). Cathodes were constructed around either stainless steel (SS) mesh or copper mesh using PDMS as both catalyst binder and diffusion layer, and compared to cathodes of the same structure having a Nafion binder. With PDMS binder, copper mesh cathodes produced a maximum power of 1710±1 mW m^{-2}, while SS mesh had a slightly lower power of 1680±12 mW m^{-2}, with both values comparable to those obtained with Nafion binder. Cathodes with PDMS binder had stable power production of 1510±22 mW m^{-2} (copper) and 1480±56 mW m^{-2} (SS) over 15 days at cycle 15, compared to 40% decrease in power with the Nafion binder. Cathodes with PDMS binder had lower total cathode impedance than Nafion. This is due to a large decrease in diffusion resistance, because hydrophobic PDMS effectively prevented catalyst sites from filling up with water, improving oxygen mass transfer. The cost of PDMS is only 0.23% of that of Nafion. These results showed that PDMS is a very effective and low-cost alternative to Nafion binder that will be useful for large scale construction of these cathodes for MFC applications.

---

[2] Materials presented in this chapter was summarized in the following paper: Zhang, F.; Chen, G.; Hickner, M. A.; Logan, B. E., Novel anti-flooding poly(dimethylsiloxane) (PDMS) catalyst binder for microbial fuel cell cathodes. *Journal of Power Sources* **2012** in press.

4.1 Introduction

Microbial fuel cell (MFC) based technologies have attracted considerable attention as a method to extract bioelectricity from biomass, especially from organic matter and pollutants in wastewater *(1-5)*. In an MFC bacteria oxidize organic or inorganic matter and donate electrons to the anode to generate current *(3, 4)*. Air cathode MFCs are the most promising configuration for applications involving wastewater treatment, due to the electrical power output, simple structure of the reactors, and the lack of a need for aerating the wastewater. However, oxygen reduction at the cathode is limited by poor kinetics under MFC typical operating conditions (ambient temperature and neutral pH), and mass transport limitations due to diffusion of oxygen through the cathode porous structure, the low solubility and diffusivity of oxygen in water, and accumulation of inert gas in the pores *(6, 7)*. As a result, the cathode is usually the limiting factor in power production in most MFCs *(8-10)*. Cathode performance and its limited surface area have therefore been found to be two of the main challenges for scaling up MFCs for wastewater treatment applications *(11)*.

Nafion has been used as a standard catalyst binder polymer for MFCs, due to its high proton conductivity. Efforts have been made to find alternatives to Nafion, because it is a very expensive polymer which costs $667 per m^2. Low-cost hydrophobic polytetrafluoroethylene (PTFE) has been tested as the binder in several studies *(12, 13)*. Replacing Nafion with PTFE in an MFC decreased power generation from 480±20 mW m^{-2} to 360±10 mW m^{-2}, although the PTFE binder showed less degradation in performance over time *(12)*. Mixtures of PTFE and Nafion have been examined, and power decreased inversely with the amount of PTFE in the binder. With only the PTFE binder, the maximum power was 549 mW m^{-2}, compared to 1060 mW m^{-2} obtained using only Nafion *(13)*. Comparison of sulfonated and non-sulfonated poly(sulfone) showed that the non-ionic binder had better electrochemical performance and the

lowest charge transfer resistance, suggesting that the ionic binder resulted in ionic gradients that impeded proton transfer *(14)*. The ionic binder had the highest initial power of 1660 mW m^{-2} in the 2nd cycle, but the non-sulfonated poly(sulfone) (Radel) produced the most power (1200 mW m^{-2}, with 100 mM phosphate buffer) after 22 cycles, and it was the best in terms of long-term stability. Further tests with hydrophilic polymers have shown that non-ionic polymers, with greater water uptake, increased the accessible surface area for oxygen reduction and thus increased the performance *(15)*. Although these alternative binders all initially had a lower power production than Nafion, performance of the best materials became nearly equivalent to Nafion in longer term tests *(14, 15)*.

Water flooding is a significant negative factor for cathode performance in fuel cell studies as it reduces oxygen transfer to the reaction sites in the cathode. Water flooding within the catalyst, or in the diffusion layer, can result in a non-uniform distribution of reactant over the active catalyst area *(16)*. Flooding reduces cathode performance in two separate ways: by covering electrochemically active sites with liquid water, and by hindering oxygen transport to the reaction sites *(8)*. In air cathode MFCs, cathodes have one side facing the solution and the other side facing air, with the cathode catalyst directly in contact with liquid water. Compared to polymer electrolyte membrane (PEM) fuel cell operation conditions, MFCs operate at much lower temperatures with passive air flow, and any product water would be more likely to condense to liquid water and thus would not be easily removed by convection on the air side. These disadvantages could result in water flooding problems in MFCs, but this issue has not been well addressed in these systems.

Most strategies for mitigating water flooding in fuel cells are based on introducing hydrophobic materials into the cathode structure, for example by applying a hydrophobic diffusion layer to the air-side of the cathode, or using a micro-porous layer *(17, 18)*. Wet proofing using polytetrafluoroethylene (PTFE) was shown to increase the performance of nickel foam

cathodes in MFCs, likely through the inhibition of nickel corrosion and reduction in cathode flooding *(19)*. An anti-flooding cathode catalyst layer was developed for a PEM fuel cell by adding dimethyl silicone oil into the catalyst layer with a Nafion binder, which increased hydrophobicity and more effectively expelled water out of the voids of the catalyst layer, and increased power *(20)*. These studies showed that creating more hydrophobic conditions can be beneficial for power production by mitigating water flooding at the cathode catalyst layer.

The hydrophobic polymer poly(dimethylsiloxane) (PDMS) was examined here as a novel anti-flooding catalyst binder for MFC cathodes because it is also highly permeable to oxygen. Unlike Nafion, PDMS is not ionically conductive. PDMS is an inexpensive polymer, which has previously only been used to make diffusion layers on the air-side of MFC cathode to prevent water leakage, because it is easy to apply with a low curing temperature *(17, 21)*. In order to examine the usefulness of PDMS as a catalyst binder, cathodes were constructed around stainless (SS) or copper mesh, with a PDMS binder for the catalyst layer on the solution-side, and a PDMS diffusion layer on the air-side to prevent water leakage. Copper mesh was compared to SS mesh due to its high electrical conductivity, which could benefit increased power production. Cathodes were made using 50-mesh materials, which were previously shown to have high power production among a series of different sized mesh *(21)*. These cathodes were compared to cathodes made with the same materials except for the use of a Nafion binder. Cathodes were tested in MFCs for 15 cycles using pre-acclimated anodes to examine the effect of the binder and mesh materials on power production, cathode potentials, and coulombic recoveries. Cathodes were also characterized abiotically using galvanostatic polarization and electrochemical impedance spectroscopy in an electrochemical cell.

4.2 Materials and methods

4.2.1 Cathodes

Cathodes were constructed around 50×50 mesh (mesh opening size of 0.28 mm and wire diameter of 0.23 mm) as previously described *(21)*, except that PDMS was used as the catalyst binder, with either SS (Type 304) or copper mesh (McMaster-Carr, OH). For the catalyst layer, 5 wt% PDMS was used as the binder for 0.5 mg cm^{-2} Pt (treatment), and compared to cathodes made with Nafion binder (33.3 μL cm^{-2} of 5 wt% Nafion solution) (control). PDMS was prepared using a 10:1 mixture of SYLGARD 184 silicone elastomer base and SYLGARD184 silicone elastomer curing agent (Dow Corning, MI), that was further diluted to 5 wt% with toluene *(17)*. To avoid inactivating the Pt catalyst at high temperatures, the PDMS binder was cured at room temperature for at least two days before being used. Two layers of PDMS/carbon black were also on the air-facing side as the diffusion layer to prevent water leakage through the cathode as previously described *(17)*.

4.2.2 MFC construction and operation

MFCs were single-chamber cubic-shaped reactors with an anode chamber 4 cm long and 3 cm in diameter *(22)*. The anodes were graphite fiber brushes that were heat treated at 450 °C for 30 min and inoculated with a pre-acclimated cell suspension from an existing MFC *(23)*. MFCs were fully acclimated and operated in fed-batch mode using carbon cloth cathodes with Pt catalyst at 30 °C before changing to the metal mesh cathodes. The medium contained 1 g L^{-1} sodium acetate dissolved in 50 mM phosphorus buffer (Na_2HPO_4, 4.58 g L^{-1}; $NaH_2PHO_4 \cdot H_2O$ 2.45 g L^{-1}; NH_4Cl 0.31 g L^{-1}; KCl 0.13 g L^{-1}; trace minerals and vitamins; conductivity of 6.95 mS cm^{-1}). The external resistance was set at the resistance which produced the maximum power in polarization

tests at cycle 1 and cycle 6: 50 Ω for cathodes with PDMS binder, and 75 Ω for cathodes with Nafion binder (except during cycles 2 to cycle 5, where cathodes with copper mesh and Nafion binder were set at 50 Ω). All reactors were operated in duplicate at 30 °C.

4.2.3 Calculations and measurements

Voltage (*E*) across the external resistor in the MFC circuit was measured at 20 min intervals using a data acquisition system (2700, Keithley Instrument, OH) connected to a personal computer. Current ($I = E/R$) and power ($P = IE$) were normalized by the projected surface area of the cathode (7 cm^2). Polarization tests were performed using the single-cycle method at the first cycle and cycle 6 by varying the external circuit resistances from 1000 to 20 Ω in decreasing order (20 min per resistance). Coulombic recoveries were calculated as the ratio of recovered coulombs to the theoretical amount of coulombs that can be produced from acetate oxidation *(1)*.

4.2.4 Electrochemical tests

Cathodes were characterized using galvanostatic polarization and electrochemical impedance spectroscopy (EIS) with a potentiostat (PC4/750, Gamry Instruments) in an abiotic electrochemical cell. The electrochemical cell consists of a working electrode (air cathode with 7 cm^2 projected surface area), an Ag/AgCl reference electrode (Bioanalytical Systems, Inc., RE-5B; +0.211 V versus a standard hydrogen electrode, SHE) and a Pt mesh counter electrode *(17)*. The cathode in this electrochemical cell was identical to that in the MFC, with the solution present on the catalyst side of the cathode and air on the other side. Galvanostatic polarization was performed immediately after putting the cathode into the electrochemical cell, and repeated one day later to characterize the change of cathode performance due to water flooding. In

galvanostatic polarization tests a different current was set (0 to –10 mA, in 0.5 mA increments) for 30 min for the first four points, and at 15 minutes intervals thereafter. Current were then normalized by the cathode surface area and current density was plotted as a function of the steady state potential.

EIS tests were performed after the galvanostatic polarization tests. Impedance measurements were conducted at polarized conditions of 0.2 V, 0.1 V and 0 V (vs SHE), which were potentials similar to the MFC cathode operating potentials, over a frequency range of 100 kHz to 1 mHz with a sinusoidal perturbation of 10 mV amplitude. Spectra were fitted to an equivalent circuit as previously described *(21)* to obtain the solution resistance R_s, charge transfer resistance R_{ct}, and diffusion resistance R_d.

4.3 Results and discussion

4.3.1 Power production of cathodes using different binders

Cathodes were examined in MFCs for their power production with pre-acclimated anodes that produced stable power before the mesh cathodes were used. Polarization tests taken at the cycle 1 and 6 showed that the anode performance was identical among reactors with different cathodes and at different cycles (Figure 4-1C and D), and therefore changes in power over time were due to differences in cathode performance. With a PDMS binder, copper and SS mesh cathodes resulted in similar performance. Cathodes with PDMS binder initially had poorer performance, with maximum power production of 1260±51 mW m^{-2} with copper mesh, and similar power of 1210±33 mW m^{-2} with SS mesh (Figure 4-1A and C). This low power production was assumed to be due to inhibition of proton transfer that attributed to a low water content, which would have resulted from using a material like PDMS that had a high hydrophobicity. When the cathodes

became better wetted with water produced from the current over time, the proton transfer to the active sites was improved, cathode potentials increased (Figure 4-1C and D), and power increased to 1710±1 mW m^{-2} (cycle 4) with copper mesh, and to 1680±12 mW m^{-2} with SS mesh (cycle 7). Power production after this time decreased by *ca.* 12% to 1510±22 mW m^{-2} with copper mesh and 1480±56 mW m^{-2} with SS mesh at cycle 15 (Figure 4-2), likely due to the biofouling of the cathode surface.

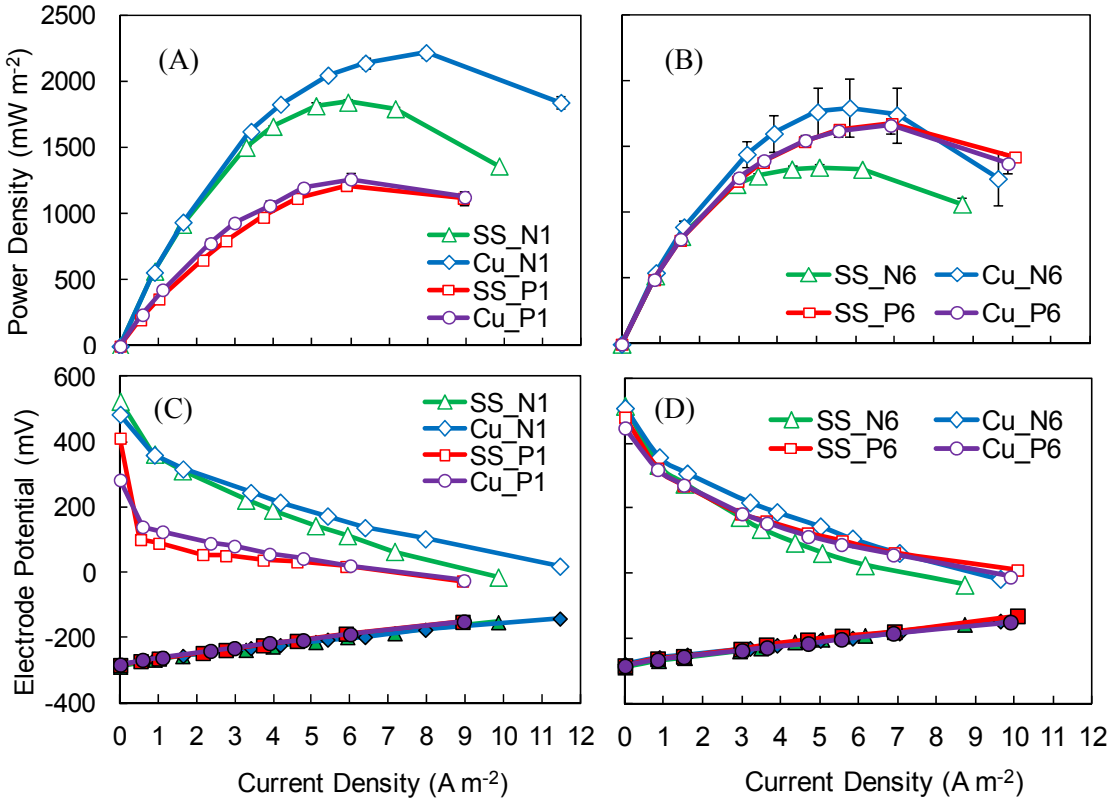

Figure 4-1. Power density curves at (A) the first cycle and (B) cycle 6, and electrode potentials (solid symbols for anode potentials and open symbols for cathode potentials) at (C) the first cycle and (D) cycle 6, with stainless steel (SS) or copper (Cu) mesh cathodes using PDMS binder compared to Nafion binder.

With Nafion binder, high power densities were initially produced, with 2220±34 mW m^{-2} using copper mesh and 1840±17 mW m^{-2} with SS mesh (Figure 4-1A and C). Copper mesh had

better performance than SS mesh when using the Nafion binder, more likely due to a higher electrical conductivity of copper which decreased charge transfer resistance (see below). After several cycles the advantage of Nafion disappeared, which could be a result of several factors, including biofouling. This change in power was reflected by decreased cathode potentials from cycle 1 to 6 (Figure 4-1C and D). The maximum power continuously decreased over time, reaching 1360±3 mW m^{-2} for the copper mesh and 1060±54 mW m^{-2} with the SS mesh at cycle 15 with the Nafion binder. These final values were 28% lower than those produced with the PDMS binder with SS mesh, and 10% lower than those with copper mesh (Figure 4-2). Decreases in cathode performance over time with Nafion have previously been reported in several studies *(12, 14, 15, 24)*. Therefore, while power densities were initially larger with a Nafion binder, the MFCs with the PDMS binder in the cathode produced more stable maximum power than those with Nafion over time, achieving higher power production after several cycles. The reduced performance degradation with PDMS binder might be due in some part to its anti-fouling properties introduced by its hydrophobic surface, making it less prone to performance degradation over time compared to Nafion.

The power achieved here using PDMS binder in the cathodes was the highest among studies investigating alternatives to a Nafion binder. In these previous studies carbon cloth was used as the cathode material, but this material produces power densities similar to those obtained with SS mesh *(17)*. Although a lower buffer concentration of 50 mM was used in this study compared to 100 mM, the maximum power density with the PDMS binder (1710±1 mW m^{-2} with copper mesh) was still higher than the best performance achieved using the neutral hydrophilic binder of 1470 mW m^{-2} *(15)*, and the best result among poly(sulfone) binders of 1660 mW m^{-2} with 100 mM phosphate buffer *(14)*. The cathodes with PDMS binder had more stable power production than those using a Nafion binder, which was consistent with previous results that non-ionic binders showed more stable performance than Nafion binder *(14, 15)*. Power production at

cycle 15 (15 days of operation; average of *ca.* 1500 mW m^{-2} with SS or copper) remained higher than the best result of 1310 mW m^{-2} at cycle 11 (20 days of operation, 100 mM phosphate buffer) using neutral hydrophilic binders *(15)*. Completely replacing the Nafion binder with PTFE has been shown to result in a very low power production of 549 mW m^{-2} *(13)*, which was less than one third of power production that obtained here using the PDMS binder (although a brush anode was used in this study, as opposed to a carbon cloth anode). The use of PDMS binder does not require heating, compared to the PTFE binder that needs to be heated to 370 °C after application for melting PTFE. Thus the use of PDMS binder is both easily applied, and improves for power production over time.

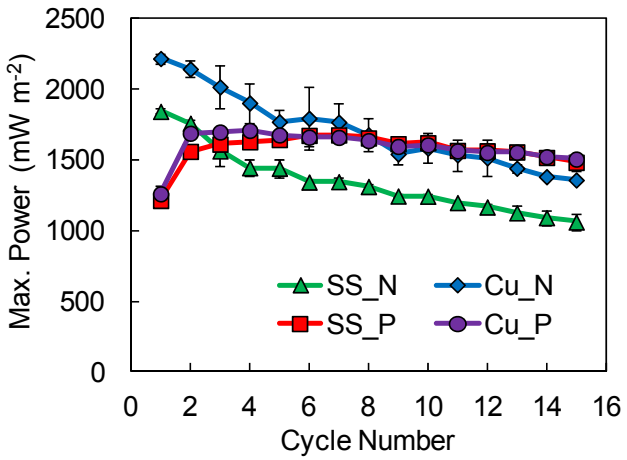

Figure 4-2. Maximum power production over cycles with cathodes built around either stainless steel or copper mesh, with PDMS or Nafion binder. (Data for cycle 1 and 6 obtained from polarization tests, rest data obtained by setting external resistor at the resistance where maximum power was obtained in the polarization tests.)

4.3.2 Coulombic recovery

In general, the different cathodes had similar coulombic recoveries (CRs), which is expected as the cathodes had the same diffusion layers and similar current densities. At cycle 15, copper mesh cathodes with the PDMS binder had only a slightly higher CR of 62±2%, compared to 56±1% for

SS mesh with Nafion binder, 54±2% for copper mesh with Nafion and 53±2% for SS mesh with PDMS binder (Figure 4-3). The small differences in CR might have resulted from variations in the amount of biofilm that developed over time on cathodes. As the external resistors were set to the resistance where maximum power was obtained, these coulombic recoveries were not obtained at exactly the same current densities, but do indicate the CRs when the MFCs produced maximum power.

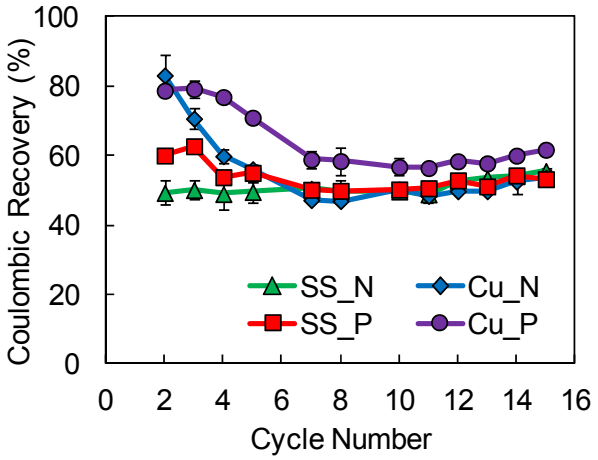

Figure 4-3. Coulombic recoveries over cycles with cathodes built around either stainless steel or copper mesh, with PDMS or Nafion binder.

4.3.3 Cathode galvanostatic polarization

Cathodes were examined under abiotic conditions in an electrochemical cell to compare their performance in the absence of bacteria and a substrate. Cathodes with the PDMS binder initially had higher overpotentials than those with Nafion binder at low current densities, which we attributed to insufficient wetting of the cathode surface. When a larger current density was set, oxygen reduction occurred at a higher rate, which would have formed water faster inside the cathode, thus wetting the cathode surface more rapidly at the catalyst site. This could explain the

similar performance of the PDMS cathodes and those with Nafion binder at higher current densities (Figure 4-4A). When the galvanostatic polarization tests were repeated one day later, which would have allowed more time for wetting of the hydrophobic PDMS binder, all cathodes showed nearly identical performance at all current densities (Figure 4-4B). These results were generally consistent with the MFC tests, where at the first cycle cathodes with Nafion binder showed much higher potentials than PDMS binder, but after six cycles the cathode potentials were very similar to each other.

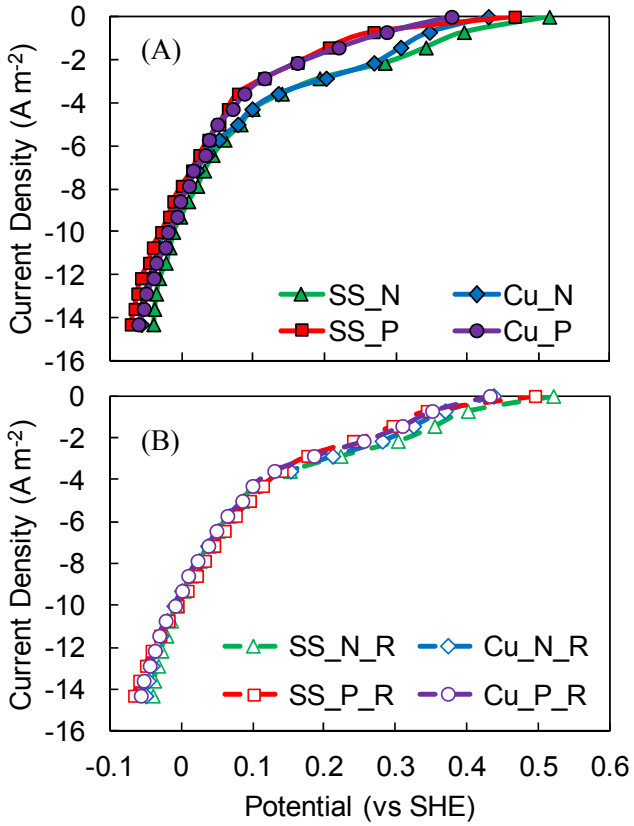

Figure 4-4. Galvanostatic polarization of cathodes built around either stainless steel or copper mesh, with PDMS or Nafion binder: (A) immediately after putting cathodes into the reactor; (B) one day after the pervious polarization test.

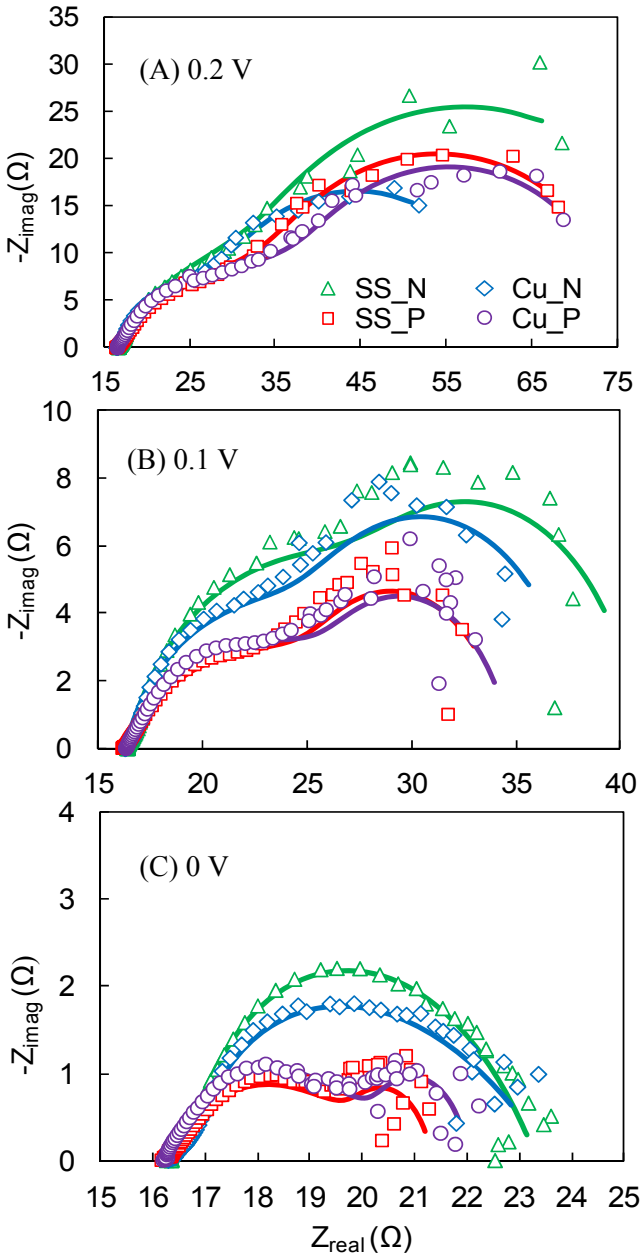

Figure 4-5. Nyquist plots of EIS spectra after at different cathode potentials of (A) 0.2 V, (B) 0.1 V, (C) 0 V. Symbols represent experimental data, and lines represent data fit with the equivalent circuit.

4.3.4 Electrochemical impedance spectroscopy

EIS was performed at different cathode potentials of 0.2 V, 0.1 V and 0 V, which were similar to those of the cathodes in MFC tests. Total impedance decreased with increasing oxygen reduction overpotential (0.2 V → 0.1 V → 0 V), as shown by the decrease in the size of the semi-circle produced in Nyquist plots, due to the increasing kinetic driving force by larger overpotentials (Figure 4-5). At a high potential of 0.2 V (i.e. low overpotential), cathodes with PDMS binder performed similarly to those with Nafion binder. Copper mesh cathodes with Nafion had the smallest total impedance, as shown by the smallest semi-circle in the Nyquist plots. Cathodes with the PDMS binder had a smaller total impedance than the cathode with SS mesh and Nafion binder (Figure 4-5A). At lower potentials of 0.1 V and 0 V, cathodes with the PDMS binder have less impedance than those with Nafion, as shown by smaller semi-circles in the Nyquist plots (Figure 4-5B and C). Copper mesh had similar EIS spectra to those with SS mesh using PDMS binder, and a smaller impedance than SS mesh with Nafion binder (Figure 4-5), consistent with the similar power production with two metal mesh using PDMS binder and higher power production with the copper mesh and Nafion binder.

EIS spectra were fitted to an equivalent circuit to identify the individual components of the cathode internal resistance. Solution resistances (R_s) were similar due to the use of the same cell configurations and solution (Figure 4-6). This part of resistance became dominant at high overpotentials, although this resistance could be reduced by changing the reactor design to have a separator electrode assembly (SEA) setup with closely spaced electrodes *(25)*. Cathodes with PDMS binder generally had higher charge transfer resistances (R_{ct}) than those with Nafion binder, probably due to the lack of proton conductivity with PDMS. With PDMS binder, copper and SS mesh showed similar R_{ct}, which all decreased with increasing overpotential, with average of 18 Ω at 0.2 V, 10 Ω at 0.1 V and 3.8 Ω at 0 V. With Nafion binder, copper mesh showed smaller R_{ct}

than SS mesh at lower overpotentials, due to higher electrical conductivity of copper, resulting in the higher power production with copper than SS. Copper mesh had R_{ct} of 12 Ω compared to 15 Ω with SS mesh at 0.2 V, and 9 Ω compared to 13 Ω with SS at 0.1 V. At the highest overpotential of 0 V, copper and SS mesh had similar and much reduced R_{ct} of 0.4 Ω, which was much smaller than the 3.8 Ω obtained with the PDMS binder (Figure 4-6).

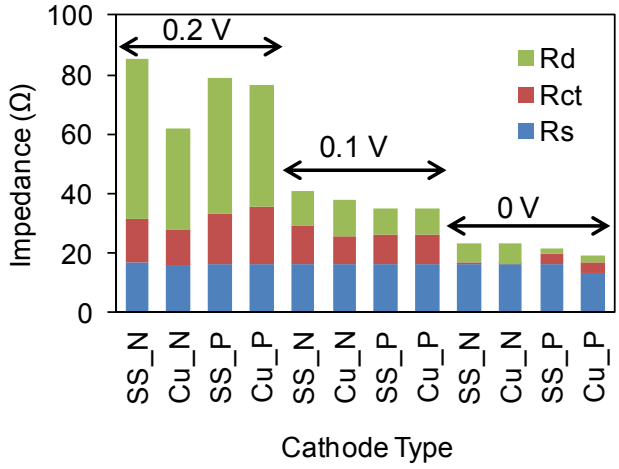

Figure 4-6. Component analysis of EIS spectra at different cathode potentials of 0.2 V, 0.1 V and 0 V, with cathodes built around either stainless steel or copper mesh, with PDMS or Nafion binder.

Cathodes with a PDMS binder had a lower diffusion resistance (R_d) than those with a Nafion binder, which we attribute to the improved anti-flooding properties of the PDMS binder. With the same binder, R_d was similar for the copper and SS mesh, except for cathodes with Nafion binder at 0.2 V. At low overpotentials, where moderate or lower water production would have occurred due to smaller current densities, cathodes with PDMS binder did not have much smaller R_d's (17-33% less than those with Nafion binder, depending on the potential and metal type). At the highest overpotential (0 V) where current was very large, water production would have been much higher. Under this condition, cathodes with the PDMS binder had much smaller

R_d's of 1.5 Ω with SS, and 1.9 Ω with copper, compared to 6.7 Ω with SS and 6.9 Ω with copper and the Nafion binder (Figure 4-6). Therefore, the total cathode impedance decreased with the PDMS binder, as a result of largely decreased R_d and slightly increased R_{ct}. We attribute the decrease in R_d to be a result of the improved anti-flooding properties of PDMS compared to Nafion. The results here are consistent with previous EIS studies that have shown that the cathode diffusion resistance was larger than the charge transfer resistance of MFC air cathodes *(21, 26)*.

4.3.5 Cathode cost

The cost of the PDMS elastomer kit was $50 (500 g), which translates to a cost of $1.5 per m^2 when used as the binder, and is a small cost compared to the other cathode materials. The PDMS cost is also substantially less than that of Nafion ($667 per m^2, based on $200 for 100 mL of 5 wt% solution). Thus the use of PDMS is much more cost-effective than a Nafion binder. The cost of cathode mesh (50×50 SS) was <$40 per m^2, based on our purchase of a small piece of material for this study. The bulk price of stainless steel is $4 per kg, compared to $8 per kg for copper. Although the cost of copper mesh is higher, the use of this material might be justified in large scale applications where good conductivity may be important for very large cathodes. Although a Pt/C catalyst was used in this study, previous work has shown that this material can be replaced by inexpensive activated carbon that produces only slightly less power densities than Pt *(27)*. Based on these results, PDMS appears to be a promising binder for MFCs that can improve long-term cathode performance and reduce capital costs.

4.4 Conclusions

These results have shown that PDMS is a promising low-cost alternative binder to Nafion for MFCs that can achieve comparable power densities and improved stability over time. We attribute these improvements to the anti-flooding and possible anti-fouling effects of PDMS that resulted from its hydrophobicity. Cathodes with PDMS binder had coulombic recoveries similar to those with a Nafion binder. Electrochemical tests showed that cathodes with PDMS binder had better performance based on reduced impedance, due to a decrease in the diffusion resistance, with only a slight increase in charge transfer resistance. This decrease in diffusion resistance was likely a result of the hydrophobic PDMS preventing the catalyst sites from becoming completely filled with water, which would have improved oxygen mass transfer. This open structure could also have reduced proton conductivity, but apparently this was not an issue with this material. The cost of PDMS is quite low, which is about 0.23% of the cost of using a Nafion binder with these cathodes. PDMS is therefore a very promising low-cost alternative to Nafion, which will make it useful for large scale applications of MFCs.

4.5 Acknowledgments

The authors thank D. W. Jones for help with the analytical measurements. This research was supported by Award KUS-I1-003-13 from the King Abdullah University of Science and Technology (KAUST).

4.6 Literature cited

1. Logan, B. E., *Microbial Fuel Cells*. John Wiley & Sons, Inc.: Hoboken, NJ, 2008.
2. Logan, B. E.; Aelterman, P.; Hamelers, B.; Rozendal, R.; Schröder, U.; Keller, J.; Freguiac, S.; Verstraete, W.; Rabaey, K., Microbial fuel cells: methodology and technology. *Environ. Sci. Technol.* **2006,** *40*, (17), 5181-5192.
3. Lovley, D. R., Bug juice: harvesting electricity with microorganisms. *Nat. Rev. Microbiol.* **2006,** *4*, 497-508.
4. Lovley, D. R., The microbe electric: conversion of organic matter to electricity. *Curr. Opin. Biotechnol.* **2008,** *19*, (6), 564-571.
5. Rabaey, K.; Verstraete, W., Microbial fuel cells: novel biotechnology for energy generation. *Trends Biotechnol.* **2005,** *23*, (6), 291-298.
6. Adler, S. B., Mechanism and kinetics of oxygen reduction on porous La1-xSrxCoO3-[delta] electrodes. *Solid State Ionics* **1998,** *111*, (1-2), 125-134.
7. Holze, R.; Vielstich, W., The kinetics of oxygen reduction at porous teflon-bonded fuel cell electrodes. *J. Electrochem. Soc.* **1984,** *131*, (10), 2298-2303.
8. Natarajan, D.; Van Nguyen, T., Three-dimensional effects of liquid water flooding in the cathode of a PEM fuel cell. *J. Power Sources* **2003,** *115*, (1), 66-80.
9. He, Z.; Huang, Y.; Manohar, A. K.; Mansfeld, F., Effect of electrolyte pH on the rate of the anodic and cathodic reactions in an air-cathode microbial fuel cell. *Bioelectrochemistry* **2008,** *74*, (1), 78-82.
10. Zhao, F.; Harnisch, F.; Schröder, U.; Scholz, F.; Bogdanoff, P.; Herrmann, I., Challenges and constraints of using oxygen cathodes in microbial fuel cells. *Environ. Sci. Technol.* **2006,** *40*, (17), 5193-5199.

11. Cheng, S.; Logan, B. E., Increasing power generation for scaling up single-chamber air cathode microbial fuel cells. *Bioresour. Technol.* **2011,** *102*, (6), 4468-4473.

12. Cheng, S.; Liu, H.; Logan, B. E., Power densities using different cathode catalysts (Pt and CoTMPP) and polymer binders (Nafion and PTFE) in single chamber microbial fuel cells. *Environ. Sci. Technol.* **2006,** *40*, 364-369.

13. Wang, X.; Feng, Y.; Liu, J.; Shi, X.; Lee, H.; Li, N.; Ren, N., Power generation using adjustable Nafion/PTFE mixed binders in air-cathode microbial fuel cells. *Biosens. Bioelectron.* **2010,** *26*, (2), 946-948.

14. Saito, T.; Merrill, M. D.; Watson, V. J.; Logan, B. E.; Hickner, M. A., Investigation of ionic polymer cathode binders for microbial fuel cells. *Electrochim. Acta* **2010,** *55*, (9), 3398-3403.

15. Saito, T.; Roberts, T. H.; Long, T. E.; Logan, B. E.; Hickner, M. A., Neutral hydrophilic cathode catalyst binders for microbial fuel cells. *Energy Environ. Sci.* **2011,** *4*, (3), 928-934.

16. Li, H.; Tang, Y.; Wang, Z.; Shi, Z.; Wu, S.; Song, D.; Zhang, J.; Fatih, K.; Zhang, J.; Wang, H.; Liu, Z.; Abouatallah, R.; Mazza, A., A review of water flooding issues in the proton exchange membrane fuel cell. *J. Power Sources* **2008,** *178*, (1), 103-117.

17. Zhang, F.; Saito, T.; Cheng, S.; Hickner, M. A.; Logan, B. E., Microbial fuel cell cathodes with poly(dimethylsiloxane) diffusion layers constructed around stainless steel mesh current collectors. *Environ. Sci. Technol.* **2010,** *44*, (4), 1490-1495.

18. Cheng, S.; Liu, H.; Logan, B. E., Increased performance of single-chamber microbial fuel cells using an improved cathode structure. *Electrochem. Commun.* **2006,** *8*, (3), 489-494.

19. Liu, J.; Feng, Y.; Wang, X.; Yang, Q.; Shi, X.; Qu, Y.; Ren, N., The effect of water proofing on the performance of nickel foam cathode in microbial fuel cells. *J. Power Sources* **2012,** *198*, (0), 100-104.

20. Li, A.; Chan, S. H.; Nguyen, N.-t., Anti-flooding cathode catalyst layer for high performance PEM fuel cell. *Electrochem. Commun.* **2009,** *11*, (4), 897-900.

21. Zhang, F.; Merrill, M. D.; Tokash, J. C.; Saito, T.; Cheng, S.; Hickner, M. A.; Logan, B. E., Mesh optimization for microbial fuel cell cathodes constructed around stainless steel mesh current collectors. *J. Power Sources* **2011,** *196*, (3), 1097-1102.

22. Liu, H.; Logan, B. E., Electricity generation using an air-cathode single chamber microbial fuel cell in the presence and absence of a proton exchange membrane. *Environ. Sci. Technol.* **2004,** *38*, (14), 4040-4046.

23. Logan, B. E.; Cheng, S.; Watson, V.; Estadt, G., Graphite fiber brush anodes for increased power production in air-cathode microbial fuel cells. *Environ. Sci. Technol.* **2007,** *41*, (9), 3341-3346.

24. Kiely, P. D.; Rader, G.; Regan, J. M.; Logan, B. E., Long-term cathode performance and the microbial communities that develop in microbial fuel cells fed different fermentation endproducts. *Bioresour. Technol.* **2011,** *102*, (1), 361-366.

25. Zhang, X.; Cheng, S.; Wang, X.; Huang, X.; Logan, B. E., Separator characteristics for increasing performance of microbial fuel cells. *Environ. Sci. Technol.* **2009,** *43*, (21), 8456-8461.

26. Zhang, F.; Pant, D.; Logan, B. E., Long-term performance of activated carbon air cathodes with different diffusion layer porosities in microbial fuel cells. *Biosens. Bioelectron.* **2011,** *30*, (1), 49-55.

27. Zhang, F.; Cheng, S.; Pant, D.; Bogaert, G. V.; Logan, B. E., Power generation using an activated carbon and metal mesh cathode in a microbial fuel cell. *Electrochem. Commun.* **2009,** *11*, (11), 2177-2179.

Chapter 5

Long-term performance of activated carbon air cathodes with different diffusion layer porosities in microbial fuel cells [3]

Abstract

Activated carbon (AC) air-cathodes are inexpensive and useful alternatives to Pt-catalyzed electrodes in microbial fuel cells (MFCs), but information is needed on their long-term stability for oxygen reduction. AC cathodes were constructed with diffusion layers (DLs) with two different porosities (30% and 70%) to evaluate the effects of increased oxygen transfer on power. The 70% DL cathode initially produced a maximum power density of 1214±123 mW m^{-2} (cathode projected surface area; 35±4 W/m^3 based on liquid volume), but it decreased by 40% after one year to 734±18 mW m^{-2}. The 30% DL cathode initially produced less power than the 70% DL cathode, but it only decreased by 22% after one year (from 1014±2 mW m^{-2} to 789±68 mW m^{-2}). Electrochemical tests were used to examine the reasons for the degraded performance. Diffusion resistance in the cathode was found to be the primary component of the internal resistance, and it increased over time. Replacing the cathode after one year completely restored the original power densities. These results suggest that the degradation in cathode performance was due to clogging of the AC micropores. These findings show that AC is a cost-effective material for oxygen reduction that can still produce ~750 mW m^{-2} after one year.

---

[3] Material presented in this chapter was published in the following paper: Zhang, F.; Pant, D.; Logan, B. E., Long-term performance of activated carbon air cathodes with different diffusion layer porosities in microbial fuel cells. *Biosensors and Bioelectronics* **2011,** *30*, (1), 49-55.

5.1 Introduction

Microbial fuel cells (MFCs) are emerging technologies for extracting bioelectricity from biomass, especially from pollutants in wastewater *(1-4)*. In an MFC bacteria are used as the anode catalysts to oxidize organic or inorganic matter and generate electric current *(3, 5)*. Air cathodes are commonly used, but the cost of traditional air cathodes is high due to the use of expensive platinum (Pt) catalyst, Nafion binder, and high grade carbon cloth *(6)*. Cathodes constructed from metal mesh such as stainless steel or nickel mesh have been used to avoid the need for carbon cloth. These metal mesh electrodes are much cheaper than carbon cloth cathodes, and the metal increases the cathode conductivity allowing for larger scale electrodes *(7-9)*. Inexpensive activated carbon (AC) has been found to be effective for oxygen reduction in MFCs. AC cathodes were made with a polytetrafluoroethylene (PTFE) binder pressed onto a nickel mesh, and an additional porous PTFE layer serving as a diffusion layer (DL) *(10)*. These AC cathodes produced a maximum power of 1220 mW m^{-2} using brush anode with a 4 cm electrode spacing, despite the lack of a precious metal catalyst *(7)*. The high catalytic activity of AC was primarily due to its extremely large surface area (1.2×10^5 m^2 per m^2 of projected surface area), which produced small local current densities but low overpotentials *(11)*. Previously tested AC cathodes had a highly porous DL (70% porosity), which resulted in a 5-10% water loss per day due to evaporation. Reducing the diffusion layer porosity would help to reduce water losses, but the effect of that change on MFC performance cannot be predicted. In addition, the long-term stability of AC cathodes has not previously been investigated, even though the longevity of the cathode is very important for commercial applications of MFCs.

Decreased power production and increased coulombic efficiencies (CEs, i.e. the percent of substrate electrons recovered as current) have been observed over time in a number of studies using Pt catalysts on cathodes. These changes have been attributed to formation of cathode

biofilm which could act as a separator and block proton transfer to the catalysts decreasing power, and could reduce oxygen diffusion to the anode chamber increasing the CE *(12-14)*. When a biofilm was present on a Pt-catalyzed carbon cathode, power production was reduced by 21% (from 24 W m^{-3} to 19 W m^{-3}), and scraping off the cathode biofilm after 40 cycles (42 days) completely restored MFC performance to original levels *(14)*. However, removing the biofilm does not always restore performance. A longer term study was conducted with the same cathodes, with different substrates *(15)*. After one year, power could be increased by 27% in acetate-fed MFCs by cleaning the cathode and removing the cathode biofilm (from 556±48 mW m^{-2} to 704±30 mW m^{-2}). Replacement of the cathodes further increased power, demonstrating that the adverse effect was due to more than just the biofilm. Ethanol-fed MFCs showed the greatest improvement after replacement of old cathodes with new ones (from 375±171 mW m^{-2} to 820±24 mW m^{-2}). The effect of biofilms and long-term operation on cathodes with other types of catalysts, for example metal tetramethoxyphenylporphyrin (TMPP), metal phthalocyanine (Pc) and manganese dioxide, has not been reported *(16-18)*. Thus, the long-term stability of non-Pt catalysts has not been well studied.

The reasons for changes in MFC performance over time can be better understood by using electrochemical impedance spectroscopy (EIS) to identify the contributions of different components to the total internal resistance in MFCs. The use of EIS has shown that solution resistance and membrane resistance were dominant in several studies, accounting for 95% of the total resistance in two-chamber designs *(19)*, and more than 50% of the total resistance in an upflow MFC reactor *(20)* and a tubular graphite-granule membrane-less air cathode MFC *(21)*. This resistance can be minimized by using certain separators and reducing the electrode spacing. Cathode resistance was found to increase in a continuous flow air cathode MFC after 6 months from 1.27 Ω to 15.1 Ω, compared to a decrease in anode resistance of 296 Ω to 1.88 Ω *(22)*. In hydrogen fuel cells cathode performance is usually found to be limited by the charge transfer

processes *(23, 24)*. However, cathode performance can also be adversely affected by diffusion resistance, which arises from diffusion of oxygen through the cathode porous structure, low solubility and diffusivity of oxygen in water, and accumulation of inert gas in the pores *(25, 26)*. In MFC studies, cathode diffusion resistance has been found to be larger than those due to charge transfer processes in several studies *(8, 21)*. EIS spectra of new and used cathodes can provide insight into the reasons for cathode degradation over time.

In this study, AC cathodes were constructed with a less porous diffusion layer (30%) to reduce evaporative water losses and examine the effect of reduced diffusion layer porosity on MFC performance. MFCs with 30% and 70% diffusion layer porosities were then tested for over one year in MFCs to determine their long-term performance and stability. These cathodes were taken from these MFC reactors after one year and electrochemically characterized using EIS and other methods to determine the reasons for the changes in performance over time.

5.2 Materials and methods

5.2.1 Cathodes

AC cathodes having a 70% porous diffusion layer (70% DL) made of a thin layer of polytetrafluoroethylene (PTFE) were manufactured by VITO (Belgium) as previously described *(7, 10)*. Additional cathodes were constructed in the same manner with a reduced porosity layer of 30% (30% DL). These cathodes were compared to Pt-catalyzed carbon cloth cathodes prepared as previously described after one year of operation *(27)*.

5.2.2 MFC construction and operation

MFCs were single-chamber cubic-shaped reactors with an anode chamber 4 cm long and 3 cm in diameter *(28)*. The anodes were ammonia gas treated graphite fiber brushes that were inoculated with a pre-acclimated cell suspension from an existing MFC, and with the MFCs operated in fed-batch mode at 30 °C. A medium containing 1 g/L sodium acetate dissolved in 50 mM phosphorus buffer (Na_2HPO_4, 4.58 g/L; $NaH_2PHO_4 \cdot H_2O$ 2.45 g/L; NH_4Cl 0.31 g/L; KCl 0.13 g/L; trace minerals and vitamins; conductivity of 6.8 mS/cm) was used for the first six months. Thereafter, 2 g/L sodium acetate was used in order to increase the cycle time and reduce the frequency of replenishment of the medium. Previous studies have shown that these two acetate concentrations do not significantly affect power generation *(29)*.

5.2.3 Calculations and measurements

Voltage (E) across the external resistor (1 kΩ, except as noted) in the MFC circuit was measured at 20 min intervals using a data acquisition system (2700, Keithley Instrument, OH) connected to a personal computer. Current ($I = E/R$) and power ($P = IE$) were normalized by the projected surface area of the cathode. The first polarization test was conducted three days after the new cathodes were placed into the reactors. Polarization tests were then conducted once every month with all cells. A single-batch method, based on by varying the external circuit resistances from 1000 to 20 Ω in decreasing order (20 min per resistance), was used to obtain polarization and power density curves. Coulombic efficiencies (CEs) were calculated assuming all COD was removed in one cycle, which slightly underestimated CEs *(2)*.

In order to characterize the changes of cathode permeability over long-term operation, oxygen transfer coefficients were measured for new and used cathodes in the same 4-cm reactor

examined in MFC tests as previously described *(27)*. Dissolved oxygen concentrations were measured using a non-consumptive oxygen probe (NeoFox, Ocean Optics, Inc., Dunedin, FL).

5.2.4 Electrochemical tests

Cathodes were characterized using several electrochemical techniques with a potentiostat (PC4/750, Gamry Instruments): linear sweep voltammetry (LSV), potentiostatic polarization, galvanostatic polarization, and electrochemical impedance spectroscopy (EIS). Cathodes were placed in an electrochemical cell consisting of a working electrode (cathode with 7 cm^2 projected surface area), an Ag/AgCl reference electrode (Bioanalytical Systems, Inc., RE-5B; +0.211 V versus a standard hydrogen electrode, SHE) and a Pt mesh counter electrode *(9)*. This cathode in this electrochemical cell was identical to that in the MFC as the solution was present on one side of the cathode with air on the other side. The only difference was that Pt mesh was used as the counter electrode instead of anode with a biofilm in order to avoid any effect of anode bacteria on the analysis of the cathode. In the LSV tests, the scan rate was 0.1 mV/s, and potential was scanned from +0.5 V to –0.1 V (vs SHE). Potentiostatic and galvanostatic polarization tests were also conducted to assess the performance of the cathodes under more steady-state conditions. Current were normalized by the geometric surface area of the electrode (7 cm^2). In potentiostatic tests the cathodes were held (15 minutes) at successively decreasing potentials from +0.5 V to –0.1 V (vs SHE) in 0.05 V decrements. The steady state current density after each time period was then plotted against the applied potential. For galvanostatic polarization tests a different current was set (0 to –10 mA, in 0.5 mA increments) for 15 minutes and the steady state potential was plotted as a function of current density. The potential was plotted on the x-axis for ease of comparison of results with potentiostatic tests.

Impedance measurements were conducted at polarized conditions close to MFC cathode operating potentials which were 0.2 V, 0.1 V and 0 V (vs SHE) over a frequency range of 100 kHz to 1 mHz with a sinusoidal perturbation of 10 mV amplitude. The spectra for new cathodes were fitted into the equivalent circuit which was a simplified circuit according to the flooded-agglomerate model for porous gas-diffusion electrodes (Figure B-1A) *(30, 31)*. The Faradaic process was represented by a charge transfer element (charge transfer resistance R_{ct} in parallel with double layer capacitance C_{dl}) in series with a diffusion element (diffusion resistance R_d in parallel with pore adsorption capacitance C_{ad}). The charge transfer resistance was obtained from the high frequency part of the EIS spectrum in Nyquist plot where charge transfer processes predominate, and the diffusion resistance was obtained from the low frequency part where diffusion processes predominate. For the used cathodes, a non Faradaic component was added to relate the changes in performance to the pore geometry of cathodes (Fig. S1B). R_f represents ohmic drop resistance of the electrolyte through the microporous film, and C_f the film capacitance. The detailed procedure used to obtain the different resistances is given in the supporting information in Appendix B.

5.3 Results

5.3.1 Long-term performance of MFCs

MFCs were running at fed-batch mode for more than one year to examine their long-term performance with AC cathodes with different DL porosities. Maximum voltages with 70% DL cathodes decreased by 10% from 488±17 mV to 439±7 mV (±S.D. based on duplicates, first and last five cycles, 1 kΩ external resistor) after one year. Cathodes with 30% DL produced higher

voltages than the 70% DL, and showed an 8.6% decrease in voltage from 532±8 mV to 486±14 mV after one year (Figure 5-1B).

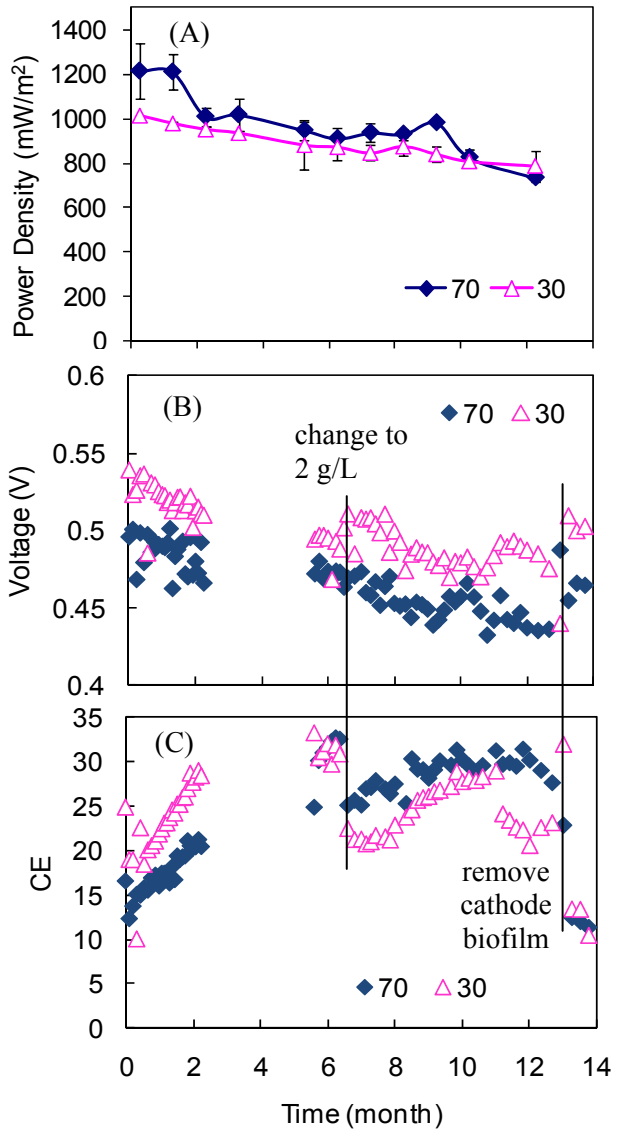

Figure 5-1. (A) Maximum power production (B) Maximum voltage production with 1 kΩ external resistor (C) CE over time using two types of AC cathodes (data for months 2-5 were lost). Concentration of sodium acetate was increased from 1 g/L to 2 g/L after 6 months and cathode biofilm was removed after one year of operation as indicated.

Cathodes with 70% DLs produced higher maximum power densities than the 30% DL cathodes for most of the operation time. The maximum power density of the 70% DL cathode initially was 1214±123 mW m^{-2}, and it decreased by 40% after one year to 734±18 mW m^{-2}. The 30% DL cathode initially produced less power, but it only decreased by 22% after one year (from 1014±2 mW m^{-2} to 789±68 mW m^{-2}) (Figure 5-1A). These power densities are slightly lower than that produced with a new Pt-catalyzed carbon cloth cathode. Using the Pt-catalyzed cathodes in the MFCs after one year resulted in a slightly higher maximum power density of 1456±7 mW m^{-2}, a value which is higher than that previously obtained with a Pt-catalyzed carbon cloth cathode (1060 mW m^{-2}) under similar conditions *(7)*.

Cathodes with 30% DLs initially had slightly higher CEs of 18% than those of the 70% DLs (14%). CEs increased over time for all reactors, likely as a result of the buildup of a biofilm on the cathode which would reduce oxygen intrusion into the anode chamber (Figure 5-1C). The highest CEs of 33% were similar for MFCs with 70% and 30% DLs. When the acetate concentration was doubled after six months, the CEs decreased (especially for the 30% DL cathode). It appeared that the biofilm on the cathode was disrupted (partially removed), although the change in substrate concentration could not be conclusively identified as the reason for this change. It is likely that the disruption of the cathode biofilm allowed more oxygen intruded to the anode chamber, and thus lowered the CE (Figure 5-1C). The 70% DL cathode produced a higher CE after doubling the acetate concentration, perhaps due to a thicker biofilm on this cathode compared to the 30% DL cathode (Figure B-4), which more effectively blocked the oxygen intrusion.

During each polarization test, anode and cathode potentials were also recorded using reference electrodes to track the change of single electrode performance in MFCs. Cathode potentials with a 70% DL shifted to lower potentials over time indicating decreasing performance, while cathode potentials with the 30% DL remained relatively constant (Figure 5-

2A and 2B). For all the reactors, anode potentials were observed to shift to higher potentials over time (Figure 5-2C and 2D).

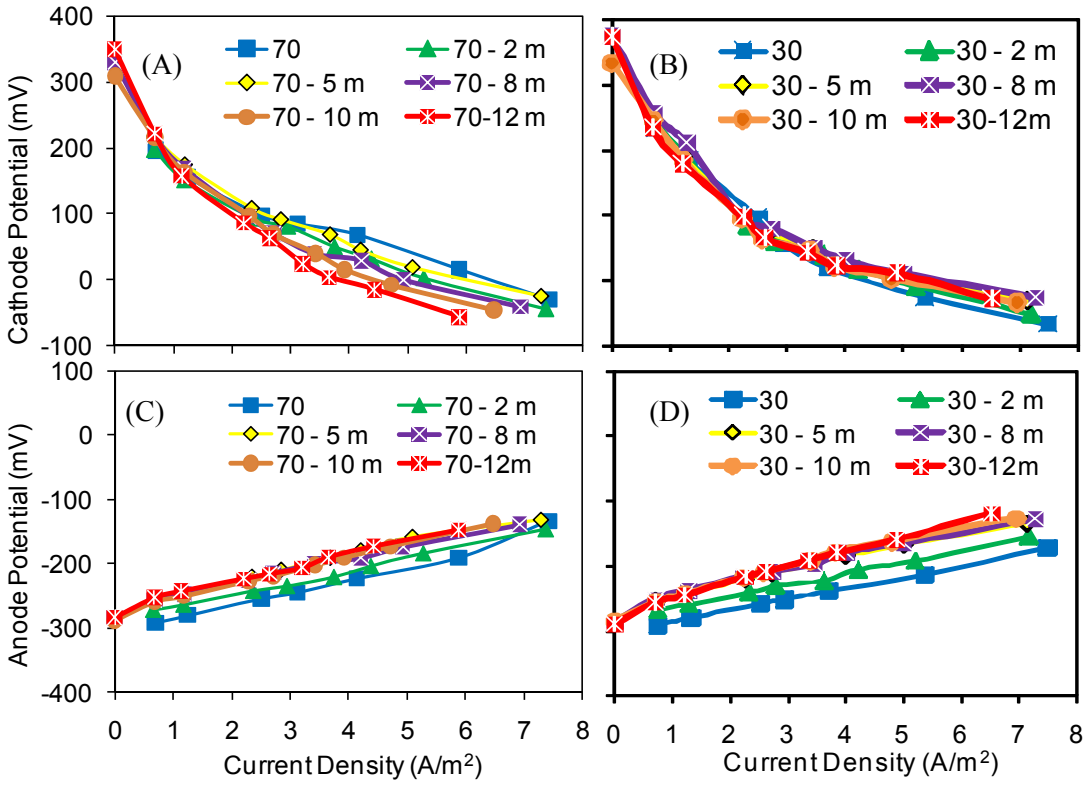

Figure 5-2. Changes of cathode (A, B) and anode potentials (C, D) over time for MFCs using two types of AC cathodes. Polarization tests were conducted after three days of operation (70 for 70% DL and 30 for 30% DL after three days), and every month afterwards (numbers after dash represent the length of operation; selective months for the easy reading of the figure).

To test whether these apparent increased anode potentials were the reason for reduced performance over time, the cathodes were first cleaned and tested, and then replaced with new cathodes. After cleaning the cathode to remove the biofilm, cathodes with different DLs had similar increases in power. Maximum power densities for the 70% DL cathodes increased by 12% to 822±29 mW m^{-2}after removing cathode biofilm, similar to the 11% increase for the 30% DL cathodes to 872±13 mW m^{-2} (Figure 5-3A). The CEs dropped to around 11% for both cathodes (Figure 5-1C). Replacing the used cathodes with new cathodes fully restored the

maximum power production to the same levels obtained one year earlier, with 1148±7 mW m^{-2} with a 70% DL, and 1030±60 mW m^{-2} with a 30% DL (Figure 5-3A). Anode potentials were unchanged by cleaning the cathode surface and using new cathodes (Figure B-5C), indicating that the new cathodes were responsible for the restored performance (Figure B-5B). This shows that anode performance was not changed after one year despite the apparent changes over time based on measurements with the reference electrodes.

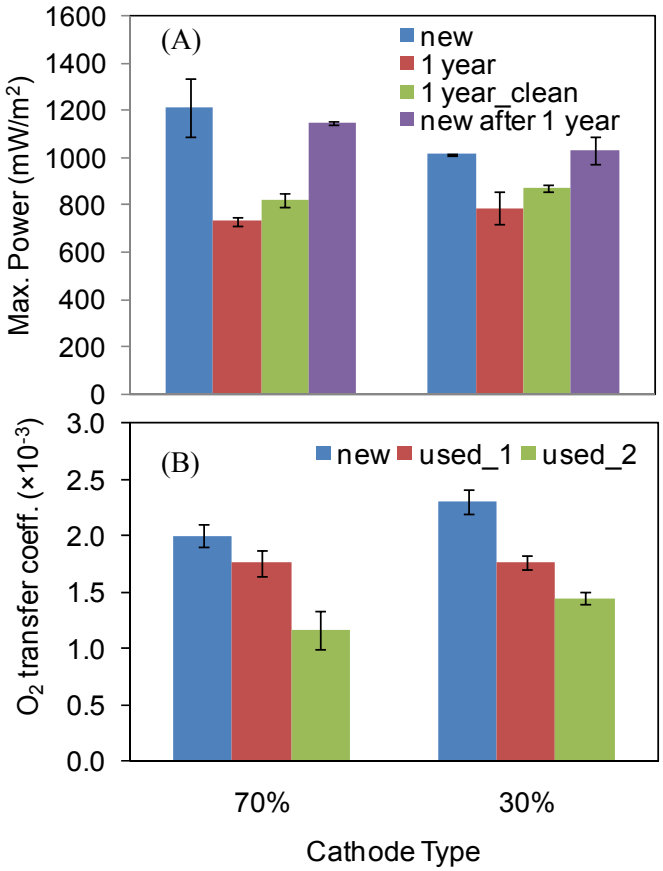

Figure 5-3. (A) Comparison of maximum power production among initial new cathodes (new), used cathodes for one year (1 year), used cathodes for one year with cleaned surface (1 year_clean) and replaced new cathodes after one year (new after 1 year). (B) Oxygen transfer coefficients of two types of cathodes under both new and used conditions (used_1 and used_2 are duplicates in the reactors).

5.3.2 Oxygen permeability of cathodes

Oxygen transfer coefficients of 70% DL cathodes and 30% DL cathodes were similar, with 30% DL slightly higher, despite the different porosities of the DLs (Figure 5-3B). However, the MFCs with 30% DL cathodes did not have a measurable water loss due to the less porous DL. After one year of operation, the oxygen transfer coefficients of both type of cathodes decreased by 30% likely due to the clogging of pores by bacteria or other organic matter. This decrease in oxygen transfer coefficients of the used cathodes was consistent with the increase of diffusion resistances in EIS tests as discussed later.

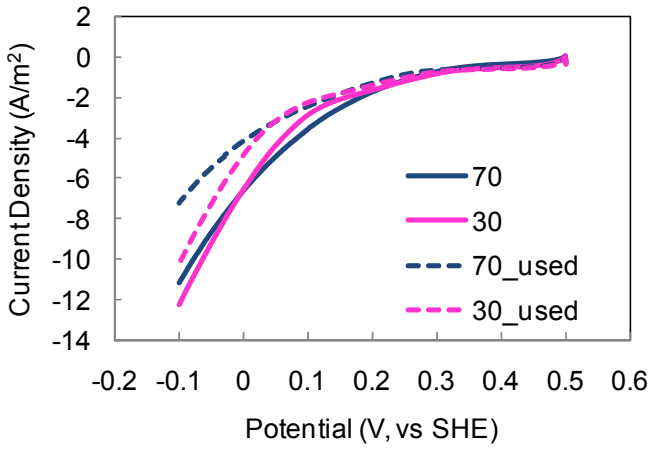

Figure 5-4. LSV of two types of AC cathodes under both new and used conditions.

5.3.3 Electrochemical characterization

Three polarization techniques were performance to evaluate the electrochemical performance of the cathodes in the absence of bacteria. The measurements showed generally consistent results with the different methods, indicating that the 0.1 mV/s was a sufficiently slow scan rate for evaluating the highly porous AC electrodes (Figure 5-4, Figure B-6). At low current densities the 70% DL cathode had better performance than the 30% DL cathode, while the opposite result was

obtained at higher current densities. At current densities (~4 A/m^2) where the MFCs produced the maximum power density with new cathodes, the 70% DL cathode sustained higher current at a given potential (lower overpotential at a given current), showing a better performance than the 30% DL cathode. This result was consistent with the MFC tests where a new 70% DL cathode produced higher maximum power densities. The curves obtained with used cathodes shifted to lower currents (i.e. higher overpotentials), showing an obvious degradation in performance (Figure 5-4). Compared to the new cathodes, the used 70% DL cathode had a larger decrease in current than the 30% DL cathode. This result was also consistent with the MFC tests where the 70% DL cathode exhibited larger decreases in cathode potential over time (Figure 5-2A and B).

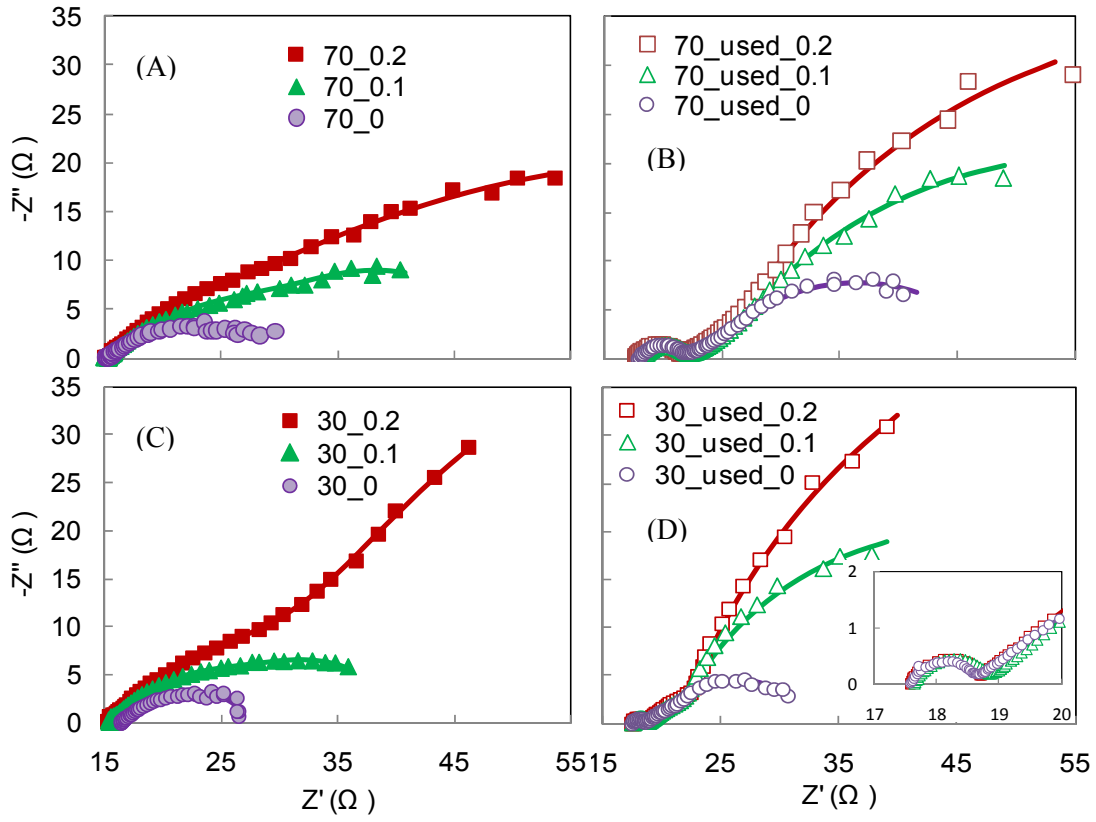

Figure 5-5. Nyquist plots of EIS spectra by two types of AC cathodes under both new and used conditions, at polarized conditions of 0.2 V, 0.1 V and 0 V. (A) new 70%; (B) used 70%; (C) new 30%; (D) used 30%. Symbols represent experimental data, and lines represent the fitting data of equivalent circuit.

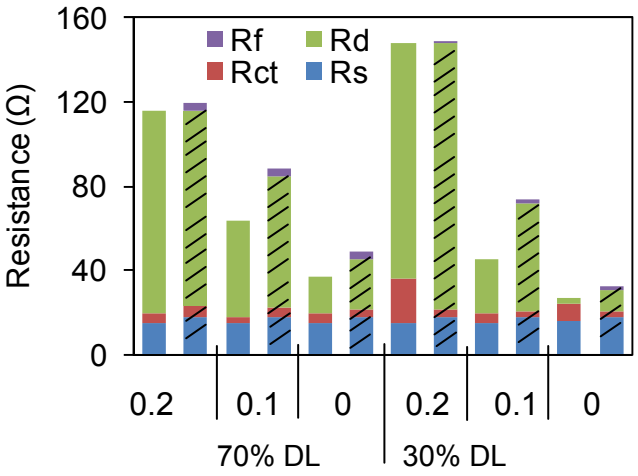

Figure 5-6. Component analysis of internal resistance at different EIS operation conditions (0.2 V, 0.1 V and 0 V) for two types of cathodes under both new (solid) and used (shade) conditions.

EIS was performed on new and used cathodes in an abiotic electrochemical cell. With new cathodes, the internal resistance decreased with increasing overpotential, as shown by the decreasing diameter of the semicircle in Nyquist plot, mainly due to the increasing kinetic driving force by larger overpotentials (Figure 5-5A and C). The Nyquist spectra of used cathodes showed one additional semicircle in the high frequency (HF) range compared to new ones, which was independent of increasing overpotentials (Figure 5-5B and D). As overpotential affects the kinetics of the reaction, it can be concluded that the HF semicircle of used cathodes was not related to the electrode kinetics but a non-Faradaic process.

EIS spectra were fitted to equivalent circuits (Figure B-1A for new cathodes and 1B for used cathodes) to identify the components of the cathode internal resistance. Diffusion resistance (R_d) was found to be dominant in most of conditions for both types of cathodes (Figure 5-6). Charge transfer resistance (R_{ct}) varied over a small range of <10 Ω, except for the new 30% DL at 0.2 V which had an R_{ct} = 21 Ω (Table B-1). At 0.2 V, new 30% DL cathodes had a higher R_d than

70% DL cathodes, while at higher overpotential conditions (0.1 V and 0 V) the R_d of the 30% DL cathodes decreased to values lower than those for the 70% DL. Used cathodes had larger internal resistances than new ones, mainly due the increases of diffusion resistance (Figure 5-6). Both double layer capacitance and adsorption capacitance of the used cathodes decreased compared with new cathodes (Table B-1), suggesting a decrease in active surface area and/or clogging of pores over time.

5.4 Discussion

The 70% DL cathode initially produced maximum power of 1214±123 mW m^{-2} (normalized based on cathode projected surface area; 35 ± 4 W m^{-3} based on liquid volume), but it decreased by 40% after more than one year of operation to 734±18 mW m^{-2}. The 30% DL cathode initially produced less power, but it only decreased by 22% over the same period (from 1014±2 mW m^{-2} to 789±68 mW m^{-2}). The initial power with the 70% DL cathode obtained here (1214 mW m^{-2}) was similar to that reported previously under similar conditions in the same type of MFCs (1220 mW m^{-2}) *(7)*. Changing to new Pt-catalyzed carbon cloth cathodes produced a slightly higher power of 1456±7 mW m^{-2} here, a value which was higher than that previously obtained with that type of cathode (1060 mW m^{-2}) under similar conditions *(7)*. The power density obtained here with the Pt cathodes was higher than that reported by Kiely et al. of 835 mW m^{-2} *(15)*. In their study, the power density with the Pt-catalyzed carbon cloth cathode decreased by 33% to 556 mW m^{-2} after one year. This shows that power densities will decrease with either Pt-catalyzed cathodes or AC cathodes after long-term operation.

Removing the cathode biofilm increased the power production with AC cathodes by 12% (70% DL) and 11% (30% DL). These power densities were still 32% (70% DL) and 14% (30% DL) lower than that obtained using new cathodes after one year (Figure 5-3A). Using new

cathodes completely restored power densities to those originally obtained. These results indicate that while biofilm development impaired power generation, the primary reason for decreased performance was degradation of the AC catalyst performance. These results are different from that obtained by Zhang et al. *(14)* where removing the biofilm restored power production, likely due to much shorter term operation in that study (42 days). The measured decrease in the oxygen transfer coefficient and capacitance (based on EIS spectra) suggest that over time the pores of AC became clogged, reducing the active surface area of the cathode. This led to degraded cathode performance, resulting in an increase in diffusion resistance and a larger overpotential. It was reported in another study with the same AC material that flushing the cell with demineralized improved performance after 100 days of operation in a half cell configuration *(11)*. This shows that better methods to clean the carbon are needed in order to maintain good catalytic activity of the cathode.

An inaccurate trend of increased anode potential over time were observed in this study, likely due to potential shift of a reference electrode, and the uncompensated IR error which is caused by a voltage drop through the electrolyte. The measured anode potential ($E_{a,m}$) was calculated as: $E_{a,m} = U + E_{ref} = E_a - IR$, where U is the measured anode potential versus reference electrode, and E_a is the actual anode potential. The potential shift of a reference electrode can be caused by the contamination of the frit at the electrode tip over time. This suggests that there was drift in the reference electrodes, resulting in a reference electrode having a higher potential causing the lower measured results of anode potentials (more negative U). Reference electrodes were refurbished before use in tests conducted after two months, which should have eliminated this effect. Another reason for the inaccurate trend in anode potentials could be the IR error, which inherently exists due to electrolyte resistance, as it is proportional to the cell current. This IR error would make the measured result more negative than the actual anode potential. The amount of IR error is also a function of the electrode position as current distribution plays a large

role in IR errors *(32)*. In this study, it was not possible to place the reference electrode very close to the brush anode, as is needed to minimize solution resistance. In addition, the brush anode has a large porosity and size, and thus it produces a complex current distribution and potential field. The horizontal position of the reference electrode was fixed by the septum on top of the reactor, but the vertical position of the reference electrode was flexible and could have moved, contributing to a larger portion of the IR error over time.

For EIS data analysis, two different equivalent circuits were used for new and used cathodes due to the changes in shape of the spectra. The circuit for the used cathodes was modified to contain an additional element, resulting in a good fit of the data to the spectra for both cathodes (Figure 5-5). The appearance of the additional semicircle in the HF range of the used cathode could be due to a change in either electrode kinetics or electrode geometry such as pore structure *(33)*. However, it is not possible to identify the meaning of this HF semicircle by a single spectrum, as the model for the charge transfer process and pore geometry are formally indistinguishable (a resistor in parallel with a capacitor). By analyzing the change of spectra according to the varied experimental conditions, the meaning of the semicircle could be better understood. Because varying the cathode overpotential didn't affect this HF semicircle for used cathodes in this study, we conclude that the appearance of this HF semicircle was related to electrode geometry and not kinetics. A similar conclusion was reached with porous Ni electrodes, where the HF semicircle was also independent of overpotential, indicating a non-Faradaic process related to pore structure *(34)*. Therefore, including a non-Faradaic component to the equivalent circuit gave us insight into the reason for the change in performance of the used cathodes.

5.5 Conclusions

These experiments have shown that diffusion layer porosity of AC cathodes can appreciably affect the power production and long-term stability of AC cathodes. A more porous diffusion layer benefited initial power production, but these cathodes exhibited greater degradation in performance over time. Using new cathodes after one year completely restored power densities to those originally obtained, indicating that cathodes and not anodes were responsible for changes in MFC performance. Cathode performance was primarily limited by diffusion processes, and the measured increase in internal resistances over time resulted from increases in diffusion resistance. Thus, the AC in the used cathodes was not as catalytically active as that in new cathodes, likely due to the clogging of micropores. This suggests that AC performance could be restored by developing methods to more effectively clean the AC pores.

5.6 Acknowledgments

The authors thank D. W. Jones for help with the analytical measurements, and Dr. Justin C. Tokash for help with EIS data analysis. This research was supported by Award KUS-I1-003-13 from the King Abdullah University of Science and Technology (KAUST).

5.7 Literature cited

1. Logan, B. E., *Microbial Fuel Cells*. John Wiley & Sons, Inc.: Hoboken, NJ, 2008.
2. Logan, B. E.; Aelterman, P.; Hamelers, B.; Rozendal, R.; Schröder, U.; Keller, J.; Freguiac, S.; Verstraete, W.; Rabaey, K., Microbial fuel cells: methodology and technology. *Environ. Sci. Technol.* **2006,** *40*, (17), 5181-5192.

3. Lovley, D. R., Bug juice: harvesting electricity with microorganisms. *Nat. Rev. Microbiol.* **2006,** *4*, 497-508.

4. Rabaey, K.; Verstraete, W., Microbial fuel cells: novel biotechnology for energy generation. *Trends Biotechnol.* **2005,** *23*, (6), 291-298.

5. Lovley, D. R., The microbe electric: conversion of organic matter to electricity. *Curr. Opin. Biotechnol.* **2008,** *19*, (6), 564-571.

6. Rozendal, R. A.; Hamelers, H. V. M.; Rabaey, K.; Keller, J.; Buisman, C. J. N., Towards practical implementation of bioelectrochemical wastewater treatment. *Trends Biotechnol.* **2008,** *26*, (8), 450-459.

7. Zhang, F.; Cheng, S.; Pant, D.; Bogaert, G. V.; Logan, B. E., Power generation using an activated carbon and metal mesh cathode in a microbial fuel cell. *Electrochem. Commun.* **2009,** *11*, (11), 2177-2179.

8. Zhang, F.; Merrill, M. D.; Tokash, J. C.; Saito, T.; Cheng, S.; Hickner, M. A.; Logan, B. E., Mesh optimization for microbial fuel cell cathodes constructed around stainless steel mesh current collectors. *J. Power Sources* **2011,** *196*, (3), 1097-1102.

9. Zhang, F.; Saito, T.; Cheng, S.; Hickner, M. A.; Logan, B. E., Microbial fuel cell cathodes with poly(dimethylsiloxane) diffusion layers constructed around stainless steel mesh current collectors. *Environ. Sci. Technol.* **2010,** *44*, (4), 1490-1495.

10. Pant, D.; Van Bogaert, G.; De Smet, M.; Diels, L.; Vanbroekhoven, K., Use of novel permeable membrane and air cathodes in acetate microbial fuel cells. *Electrochim. Acta* **2010,** *55*, (26), 7710-7716.

11. Pant, D.; Bogaert, G. V.; Porto-Carrero, C.; Diels, L.; Vanbroekhoven, K., Anode and cathode materials characterization for a microbial fuel cell in half cell configuration. *Water Sci. Technol.* **2011,** *63*, (10), 2457-2461.

12. Yang, S.; Jia, B.; Liu, H., Effects of the Pt loading side and cathode-biofilm on the performance of a membrane-less and single-chamber microbial fuel cell. *Bioresour. Technol.* **2009,** *100*, (3), 1197-1202.

13. Cheng, S.; Liu, H.; Logan, B. E., Power densities using different cathode catalysts (Pt and CoTMPP) and polymer binders (Nafion and PTFE) in single chamber microbial fuel cells. *Environ. Sci. Technol.* **2006,** *40*, 364-369.

14. Zhang, X.; Cheng, S.; Wang, X.; Huang, X.; Logan, B. E., Separator characteristics for increasing performance of microbial fuel cells. *Environ. Sci. Technol.* **2009,** *43*, (21), 8456-8461.

15. Kiely, P. D.; Rader, G.; Regan, J. M.; Logan, B. E., Long-term cathode performance and the microbial communities that develop in microbial fuel cells fed different fermentation endproducts. *Bioresour. Technol.* **2011,** *102*, (1), 361-366.

16. Zhang, L.; Liu, C.; Zhuang, L.; Li, W.; Zhou, S.; Zhang, J., Manganese dioxide as an alternative cathodic catalyst to platinum in microbial fuel cells. *Biosens. Bioelectron.* **2009,** *24*, (9), 2825-2829.

17. Zhao, F.; Harnisch, F.; Schröder, U.; Scholz, F.; Bogdanoff, P.; Herrmann, I., Application of pyrolysed iron (II) phthalocyanine and CoTMPP based oxygen reduction catalysts as cathode materials in microbial fuel cells. *Electrochem. Commun.* **2005,** *7*, 1405-1410.

18. HaoYu, E.; Cheng, S.; Scott, K.; Logan, B., Microbial fuel cell performance with non-Pt cathode catalysts. *J. Power Sources* **2007,** *171*, (2), 275-281.

19. Ramasamy, R. P.; Ren, Z.; Mench, M. M.; Regan, J. M., Impact of initial biofilm growth on the anode impedance of microbial fuel cells. *Biotechnol. Bioeng.* **2008,** *101*, (1), 101-108.

20. He, Z.; Wagner, N.; Minteer, S. D.; Angenent, L. T., The upflow microbial fuel cell with an interior cathode: assessment of the internal resistance by impedance spectroscopy. *Environ. Sci. Technol.* **2006,** *40*, (17), 5212-5217.

21. You, S.; Zhao, Q.; Zhang, J.; Jiang, J.; Wan, C.; Du, M.; Zhao, S., A graphite-granule membrane-less tubular air-cathode microbial fuel cell for power generation under continuously operational conditions. *J. Power Sources* **2007,** *173*, (1), 172-177.

22. Borole, A. P.; Aaron, D.; Hamilton, C. Y.; Tsouris, C., Understanding long-term changes in microbial fuel cell performance using electrochemical impedance spectroscopy. *Environ. Sci. Technol.* **2010,** *44*, (7), 2740-2745.

23. Ciureanu, M.; Roberge, R., Electrochemical impedance study of PEM fuel cells. Experimental diagnostics and modeling of air cathodes. *J. Phys. Chem. B* **2001,** *105*, (17), 3531-3539.

24. Gomadam, P. M.; Weidner, J. W., Analysis of electrochemical impedance spectroscopy in proton exchange membrane fuel cells. *Int. J. Energy Res.* **2005,** *29*, (12), 1133-1151.

25. Adler, S. B., Mechanism and kinetics of oxygen reduction on porous La1-xSrxCoO3-[delta] electrodes. *Solid State Ionics* **1998,** *111*, (1-2), 125-134.

26. Holze, R.; Vielstich, W., The kinetics of oxygen reduction at porous teflon-bonded fuel cell electrodes. *J. Electrochem. Soc.* **1984,** *131*, (10), 2298-2303.

27. Cheng, S.; Liu, H.; Logan, B. E., Increased performance of single-chamber microbial fuel cells using an improved cathode structure. *Electrochem. Commun.* **2006,** *8*, 489-494.

28. Liu, H.; Logan, B. E., Electricity generation using an air-cathode single chamber microbial fuel cell in the presence and absence of a proton exchange membrane. *Environ. Sci. Technol.* **2004,** *38*, (14), 4040-4046.

29. Mehanna, M.; Saito, T.; Yan, J.; Hickner, M.; Cao, X.; Huang, X.; Logan, B. E., Using microbial desalination cells to reduce water salinity prior to reverse osmosis. *Energy Environ. Sci.* **2010,** *3*, (8), 1114-1120.

30. Zhang, J.; Zhang, J., Catalyst Layer/MEA Performance Evaluation. In *PEM Fuel Cell Electrocatalysts and Catalyst Layers*, Zhang, J., Ed. Springer London: 2008; pp 965-1002.

31. Springer, T. E.; Raistrick, I. D., Electrical impedance of a pore wall for the flooded-agglomerate model of porous gas-diffusion electrodes. *J. Electrochem. Soc.* **1989,** *136*, (6), 1594-1603.

32. Scribner, L. L.; Taylor, S. R.; Metals, A. C. G.-o. C. o.; Testing, A. C. G. o. E. M. i.; Symposium on Ohmic Electrolyte Resistance, M.; Compensation, *The Measurement and Correction of Electrolyte Resistance in Electrochemical Tests*. ASTM: Philadelphia, PA, 1990; p vi, 225 p.

33. Keiser, H.; Beccu, K. D.; Gutjahr, M. A., Abschätzung der porenstruktur poröser elektroden aus impedanzmessungen. *Electrochim. Acta* **1976,** *21*, (8), 539-543.

34. Hitz, C.; Lasia, A., Experimental study and modeling of impedance of the her on porous Ni electrodes. *J. Electroanal. Chem.* **2001,** *500*, (1-2), 213-222.

Chapter 6

Improving startup performance with carbon mesh anodes in separator electrode assembly microbial fuel cells [4]

Abstract

In a separator electrode assembly microbial fuel cell (MFC), oxygen crossover from the cathode raises the anode potential and inhibits current generation by exoelectrogenic bacteria, resulting in difficulties in reactor startup. In order to improve startup performance, MFCs with flat carbon mesh anodes were acclimated at set potentials (–0.2 V or +0.2 V versus standard hydrogen electrode), compared with no set potential control. Performance of these reactors inoculated with wastewater was also compared to those inoculated with cell suspensions from existing MFCs under the same conditions. Anodes inoculated with wastewater and acclimated to –0.2 V produced the highest power (1330±60 mW m^{-2}) but they had the longest startup time (20 days). With inoculation using transferred cell suspensions, consistent and reproducible results in terms of faster startup (10 days) and high power production were obtained. Additional electrochemical analyses confirmed that inoculation with a transferred culture consistently improved anode performance, with the best activity obtained for anodes acclimated at –0.2 V. These results imply that rapid startup of larger-scale reactors will require inoculation with pre-acclimated cultures, and that acclimation at –0.2 V could improve power production compared to a more positive potential (+0.2 V) or a lack of set potential.

---

[4] Materials presented in this chapter was summarized in a paper: Zhang, F.; Xia, X.; Luo, Y.; Sun, D.; Call, D. F.; Logan, B. E., Improving startup performance with carbon mesh anodes in separator electrode assembly microbial fuel cells. Submitted to *Journal of Power Sources* **2012**.

6.1 Introduction

Microbial fuel cell (MFC) technologies utilize bacteria to harvest chemical energy as electrical energy *(1-5)*. MFCs are a promising method for wastewater treatment due to removal of contaminants from wastewater while at the same time producing electrical power. Scaling up MFCs requires compact reactor designs and closely spaced electrodes that can minimize solution ohmic losses. To achieve these goals and avoid the direct contact of electrodes that could produce short circuiting, a separator is placed between the anode and cathode forming a separator electrode assembly (SEA) configuration. SEA MFCs have produced high power densities due to the decrease of solution resistance with low impedance to proton transport *(6, 7)*. However, the porous separator which has low impedance to proton transport usually also has low impedance to oxygen transfer *(8)*. Therefore, when the anode is placed very close to the cathode in the SEA configuration, the anode performance is adversely affected by oxygen leakage from the cathode through the separator *(9, 10)*. It has been observed in previous experiments that flat anodes, which are desirable for compact reactors, can result in the most difficulties in startup such as long startup times, unstable anode performance (high anode potentials), and thus low power production *(9, 10)*. In one study, MFCs with inexpensive carbon mesh anodes failed to produce power during startup when inoculated with wastewater and operated in an SEA configuration *(9)*. However, when the anode was first acclimated under conditions where it was kept distant from the cathode (4 cm electrode-spacing), anodes could subsequently be used in SEA MFCs. While this procedure was useful for laboratory experimentation, it would not be practical for startup of larger-scale reactors where electrodes could not be moved around. Brush anodes (1.5 cm in diameter) had better performance than flat anodes (~0.02 cm thickness) in SEA MFCs, likely due to the thickness of the anode which could maintain anoxic zones in the anode *(9)*, but the brush

anode is more expensive and occupies more volume than the carbon mesh. Thus, better strategies are needed for inoculation and startup of SEA MFCs with flat anodes.

Control of anode potentials can be a useful approach for improving startup and power production of MFCs, but there are conflicting reports on optimal set potentials *(11-15)*. In 10 of 14 studies it was reported that more positive potentials (>0 V versus a standard hydrogen electrodes, SHE) reduced startup time and produced higher power densities than more negative potentials (<0 V) *(15)*. However, other studies have shown that reactors with more negative potentials achieved better performance in terms of faster startup, more power output, and more biomass *(13, 14, 16)*. The potentials that normally develop in MFCs at a fixed resistance typically reach very negative values (*ca.* –0.26 V at 1 kΩ external resistance) during optimum performance. This potential is only slightly more positive than $E^{0'}$ (standard reduction potential at pH = 7) of the substrate (*ca.* –0.3 V, 1 g L^{-1} acetate), suggesting that setting more negative potentials worked better because it produced conditions more similar to those in typical MFCs operated with fixed resistances. The more negative potential could also help to provide selective pressures for the evolution of strains more efficient at current generation. For example, a strain of *Geobacter sulfurreducens* acclimated to an anode potential of –0.2 V over a long period of time eventually produced five times higher current densities than that originally produced *(17)*. This strategy of regulating anode potential could be important for starting up larger scale reactors, which can take much longer time to start up than laboratory systems *(18)*. However, the optimal anode potential remains unclear for MFCs, particularly in systems using an SEA setup where oxygen leaking through the cathode can affect the anode potential *(9)*.

The startup of an MFC is affected by many other factors. MFC startup can be improved by using previously acclimated cell suspensions *(19, 20)*. For example, power production with a carbon mesh anode was improved by 28% by inoculating the MFC with a pre-acclimated culture instead of wastewater, but this was only demonstrated in MFCs with anodes sufficiently distant

from the cathode (2 cm) *(20)*. This approach was not examined with the SEA configuration with closely spaced electrodes, or with set potential conditions, during startup with wastewater as a substrate instead of acetate. While well performing MFCs usually contain a high percentage of *Geobacter* species *(13, 14, 21, 22)*, other microbes in the biofilm that can scavenge oxygen can help to improve the startup performance. For example, a co-culture of *G. sulfurreducens* and a nonexoelectrogen, *Escherichia coli*, showed improved startup and performance compared to tests using only *G. sulfurreducens* due to the consumption of oxygen by *E. coli* in the co-culture *(23)*. The initial inoculum source can initially affect startup and performance *(24)*, although in some tests it has been shown that over time (after two months) the communities evolved to be similar in composition and power densities *(22)*. However, long acclimation times before reaching steady conditions may not be desirable for wastewater treatment systems. Other approaches to accelerate the startup time using a wastewater inoculum, such as the addition of different chemicals *(25)*, have not been successful.

In this study, carbon mesh anodes in SEA-type MFCs were acclimated at set potentials of –0.2 V and +0.2 V (versus SHE), where a set anode potential was used to avoid raised anode potentials that could be produced by dissolved oxygen leaking from the cathode to the anode. The performance of these reactors with set anode potentials was compared to that of a control MFC operated at a fixed resistance (no set potential). The use of a wastewater inoculum was also compared to that of an acclimated culture transferred from an operating MFC, in order to identify conditions that might improve the startup performance with flat anodes in the SEA configuration. Electrochemical techniques including cyclic voltammetry (CV), differential pulse voltammertry (DPV) and electrochemical impedance spectroscopy (EIS), were used to compare the activities of the anode biofilms acclimated at different conditions (set anode potentials of –0.2 V or +0.2 V, compared to a control with no set potential), and to characterize the change of anode biofilm activities using the acclimated transferred culture compared to a wastewater inoculum.

6.2 Materials and methods

6.2.1 MFC construction

MFCs were single-chamber, cubic-shaped reactors with an anode chamber 4 cm long and 3 cm in diameter *(26)*. Anodes were carbon mesh (Gaojieshi Graphite Products Co., Ltd., Fujian, China) that were pre-soaked in acetone overnight and then heat treated at 450°C for 30 min *(20)*. Tape was placed around the edges of the mesh before they were cut into circles (projected surface area of 7 cm^2) in order to minimize fraying or unfolding of the loosely woven mesh. Titanium wire was placed across the diameter of the carbon mesh to ensure a good electrical connection. Cathodes were made of activated carbon (AC) (VITO, Mol, Belgium) as previously described *(27, 28)*, in order to avoid the use of precious metals. The porosity of the outer PTFE diffusion layers was 70%. Two layers of wipe cloth (DuPont Sontara, style 8864, with 49% of polyester and 51% of wood pulp, 0.58 mm thick; also known as Amplitude ProZorb Wipers) were used as the separator, with the separator sandwiched between the electrodes as previously described *(7)*. An Ag/AgCl reference electrode (+211 mV versus SHE; RE-5B; BASi) was inserted into the reactor (1 cm from the anode) to measure and allow the regulation of anode potentials. All potentials are reported here versus SHE.

6.2.2 Inoculation and operation

The inoculum source was domestic wastewater from the effluent of the primary clarifier at the Pennsylvania State University wastewater treatment plant. Reactors were inoculated with fresh wastewater for the first cycle. For the next two cycles the reactors were fed a mixture (50:50) of wastewater and a medium containing 1 g L^{-1} sodium acetate dissolved in 50 mM phosphorus buffer (Na_2HPO_4, 4.58 g L^{-1}; $NaH_2PHO_4 \cdot H_2O$ 2.45 g L^{-1}; NH_4Cl 0.31 g L^{-1}; KCl 0.13 g L^{-1}; trace

minerals and vitamins; conductivity of 6.95 mS cm^{-1}). Afterwards, only the acetate medium (1 g L^{-1}) was used. The cell suspensions from these reactors were later used as the pre-acclimated inoculum for new reactors. For the pre-acclimated culture inoculation process, a mixture (50:50) of effluent from the running reactor and acetate medium (1 g L^{-1} sodium acetate dissolved in 50 mM phosphate buffer) was used for inoculation at the first cycle. Afterwards, only acetate medium was used in the rest of the cycles. All reactors were operated in duplicate at 30 °C.

Different anode potentials were set using a potentiostat (VMP3; BioLogic, Claix, France), with data (current, counter electrode potential) recorded at 4 min intervals, and analyzed using EC-Lab V10.02 software. Anode potentials were set to –0.2 V and +0.2 V. A larger range of set potentials (–0.2 V, –0.15 V, –0.1 V, 0 V, +0.2 V) were tested with different wastewater inocula. For the control reactors (no set potential), the external resistance was 1000 Ω during the startup phase (20 days), and it was changed to 100 Ω to produce higher current. The voltages across the resistor were recorded using a data acquisition system (2700; Keithly, Cleveland, OH). After one month when all reactors were fully started up (demonstrated by repeatable cycles of current), the reactors were disconnected from the potentiostat and analyzed in polarization tests. The reactors were left open circuit for one hour after being fed with fresh medium, and then the external resistor was switched from 1000 Ω to 20 Ω in a decreasing order (20 min per resistance) (single cycle method). Power and current were normalized by the electrode projected surface area of 7 cm^2.

6.2.3 Electrochemical tests

Electrochemical techniques including cyclic voltammetry (CV), differential pulse voltammertry (DPV) and electrochemical impedance spectroscopy (EIS) were applied to electrochemically characterize the change of anode biofilm activities using the potentiostat (VMP3; BioLogic,

Claix, France). All tests were conducted using the MFC reactors with the anode as the working electrode and the cathode as the counter electrode. For the CV tests, anode potential was scanned from –0.39 V to +0.31 V at a scan rate of 0.2 mV s^{-1}. DPV was performed from –0.49 V to +0.31 V as previously described *(29)*, with a pulse height of 50 mV, pulse width of 300 ms, step height of 2 mV, and step time of 500 ms (equivalent to scan rate of 4 mV s^{-1}), with current averaged over the last 80% of the step (1 s, 12 points) using an accumulation time of 5 s. EIS was conducted at an anode potential of –0.2 V, which was close to that measured in MFCs without set anode potentials, over a frequency range of 100 kHz to 100 mHz with a sinusoidal perturbation of 10 mV amplitude. Charge transfer resistances were obtained by fitting semi-circles to spectra in Nyquist plots *(30)*.

6.3 Results and discussion

6.3.1 Startup

Startup time was appreciably affected by the inoculum and the set anode potential. For the reactors inoculated with wastewater, startup time was reduced by using the more positive set potential, or from 20 days acclimated at –0.2 V, to 10 days at +0.2 V (Figure 6-1). This decrease in startup time with the more positive potential was probably due to the greater available energy for bacterial growth, which would have enabled faster startup and more biomass production. For the reactors with set anode potentials, the cathode potentials eventually became similar after about 20 days, with values between *ca.* +0.2 and 0 V (Figure C-1). When the reactors are operated with a set anode potential, the cathode potential varies to a value needed to sustain the current generated by the anode. In the case of the reactor operated at a set anode potential of –0.2 V, the resulting cathode potential that was produced was more positive than the anode set

potential, and thus the overall cell voltage was positive. Similarly, the MFCs without a set anode potential (control) also produced positive cell voltages. However, the anode operated at +0.2 V required a cathode potential more negative than this set potential for the generated current (cathode potentials became as low as 0 V), resulting in an overall negative cell voltage and therefore net power consumption. Control reactors (no set potential) had a longer startup time of 12 days, and anode potentials were gradually reduced from +0.45 V at the beginning of startup over the first few days, to a stable potential of –0.26 V after 12 days (Figure C-1). The control reactor had a much longer cycle time (*ca.* 3-4 days) than the reactors with set anode potentials (1 day) (Figure 6-1, C-1), due to the much smaller current (peak at *ca.* 0.65 A m^{-2}) compared to those of the reactors with set anode potentials (peak at *ca.* 6.5 A m^{-2}).

When new MFCs were inoculated with cell suspensions transferred from the operating MFCs, the startup time in the new MFC with set anode potential of –0.2 V was reduced to 10 days, about the same as that obtained with a set potential of +0.2 V (Figure 6-1A and B). The anode acclimated at +0.2 V using the transferred culture inoculum also had a startup time of ~10 days, but its startup current was higher than that produced by MFCs inoculated with wastewater, indicating better startup performance (Figure 6-1B). The control reactor inoculated with the transferred cell suspension had the shortest startup time, producing a stable voltage after only ~3 days (Figure 6-1C). These results show that setting the more positive anode potential of +0.2 V was better than –0.2 V in terms of startup time, and that in all cases the transferred cell suspension from a working MFC was the most reliable method for achieving a short startup time.

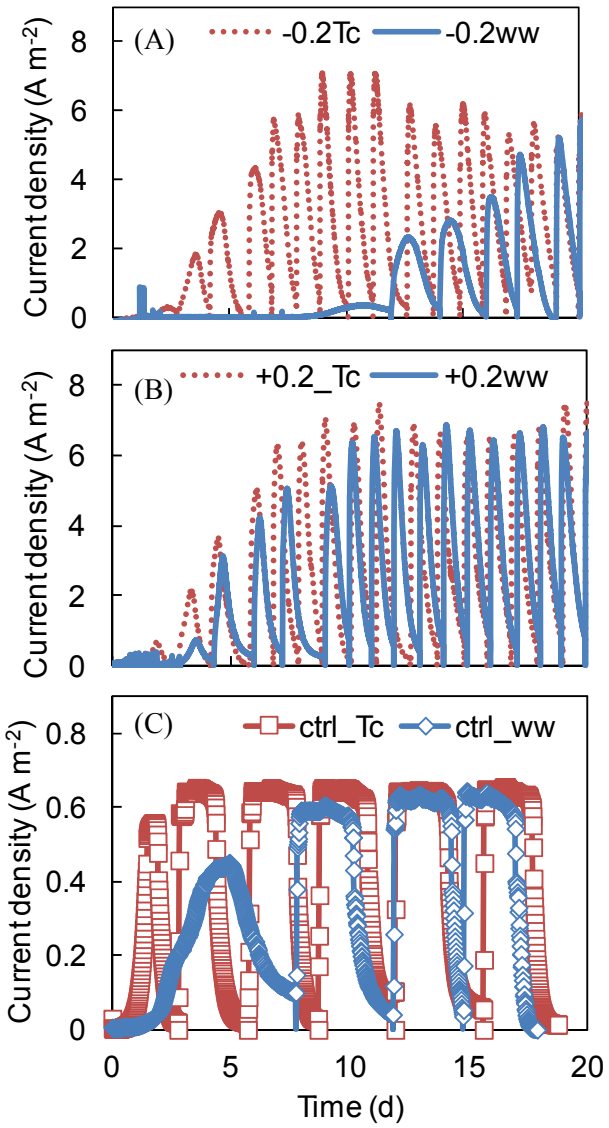

Figure 6-1. Comparison in startup performance with reactors inoculated with wastewater (ww) or acclimated transferred culture (Tc), with set anode potential of (A) –0.2 V, (B) +0.2 V or (C) control (no set potential, ctrl).

6.3.2 Power production

The startup methods that produced the most rapid startup time did not produce conditions that resulted in the highest possible power densities. For the MFCs inoculated with wastewater,

acclimation at a set potential of –0.2 V produced the highest power density of 1330±60 mW m^{-2} in polarization tests, but this MFC did not have the shortest startup time. Much less power was produced by MFCs acclimated to the more positive potential of +0.2 V (910±50 mW m^{-2}) or the control (900±60 mW m^{-2}) (Figure 6-2A). The higher power production by the MFC with the anode acclimated to the more negative potential was probably due to the high selective pressure that was produced by setting the anode potential close to that of the half cell potential for acetate oxidation. This condition would have resulted growth only by bacteria that could adapt to such a low anode potential. This low anode potential is more advantageous for MFC operation as it enables greater power densities to be produced at higher current densities.

There were less differences in maximum power densities among MFCs inoculated with transferred cell suspensions. The maximum power produced for the MFC with a set potential of –0.2 V was 1320±60 mW m^{-2}, similar to that obtained with the wastewater inoculum acclimated to this potential. These power densities were only slightly larger than the maximum power densities with a set potential of +0.2 V (1200±40 mW m^{-2}) or the control (1200±20 mW m^{-2}) with transferred cell suspensions (Figure 6-2A). Therefore, inoculation with transferred culture improved the power production with the reactor acclimated to +0.2 V and the control reactor, but a more negative potential of –0.2 V still produced a higher maximum power.

Cathode potentials were almost identical for reactors acclimated to the different anode conditions in polarization tests, indicating that the anodes were responsible for the differences in power production (Figure 6-2B). Anodes acclimated to –0.2 V had the most negative potentials during the polarization tests, resulting in a larger whole cell voltage and thus higher power production. Anodes acclimated to +0.2 V had anode potentials similar to those of the control reactor, but the potentials were more stable at higher current densities. For the control reactor inoculated with wastewater, power overshoot (a doubling back of the power curve at higher current densities) occurred as a result of a rapid increase in anode potentials, resulting in no

further increase in current densities. Power overshoot was eliminated here when using the transferred cell suspension as the inoculum, as this anode could sustain higher larger current densities (Figure 6-2B). These results from polarization data show that the anode performance was the primary limiting factor in power production.

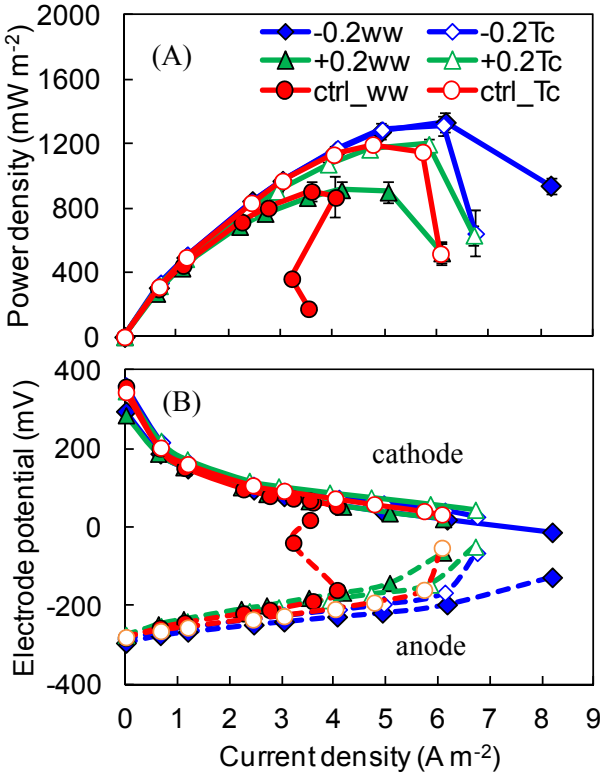

Figure 6-2. (A) Power density curves and (B) electrode potentials with set anode potentials of –0.2 V, +0.2 V and the control (no set potential, ctrl), inoculated with wastewater (ww, solid symbols) or acclimated transferred culture (Tc, open symbols). (In part B, solid lines represent cathode potentials, while dot lines for anode potentials).

6.3.3 Cyclic voltammetry (CV)

CV was used to identify the activities and redox potentials of anode biofilms for the reactors acclimated to different set anode potentials and inoculated with different bacterial suspensions. For the MFCs inoculated with wastewater, anodes acclimated at –0.2 V had the highest peak

current of 8.0 A m^{-2} at potential of –0.105 V, indicating the most active anode biofilm. The reactors acclimated to a higher potential of +0.2 V had a lower peak current of 6.4 A m^{-2}, and the peak potential shifted to a more positive potential of –0.061 V, likely due to the adaption of the biofilm to more positive potentials during the startup. Control reactors produced the smallest peak current (4.6 A m^{-2} at –0.138 V), indicating anodes with lower electrogenic activities (Figure 6-3A).

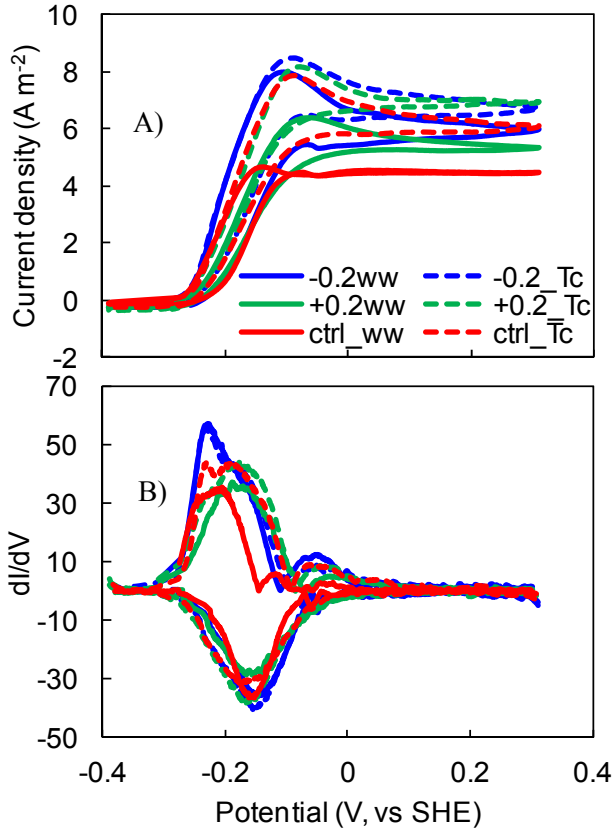

Figure 6-3. (A) CV and (B) DCV with set anode potentials of –0.2 V, +0.2 V and the control (no set potential, ctrl), inoculated with wastewater (ww, solid lines) or pre-acclimated transferred culture (Tc, dot lines).

The use of transferred culture inocula in the MFCs resulted in higher peak currents in all CVs, indicating improved anode performance. Although the peak current (8.5 A m^{-2}) of the anode acclimated to –0.2 V was slightly larger than that of wastewater inoculated MFCs (8.0 A m^{-2}),

this did not result in higher power densities in polarization tests. This lack of a higher power density in MFC tests suggests that the cathode limited power production for the anode acclimated to –0.2 V. The CVs for the control reactor and the MFC acclimated to +0.2 V had large increases in peak current relative to the wastewater inoculated MFCs (Figure 6-3A), in agreement with polarization results showing that these reactors produced higher power densities than those inoculated with wastewater. The peak current in CV and maximum power production generally were positively correlated, as a higher anodic peak current resulted in a higher power production, up until the point where the power production was limited by cathode performance (Figure C-2).

First derivative analysis of the CVs (DCVs) provided additional evidence of the improvement in anode biofilm redox activities by using transferred culture inocula. The anodes acclimated to –0.2 V, when inoculated with either wastewater or a transferred culture, had almost identical DCV plots, with the highest peak at potential of –0.23 V and –0.15 V (inflection point, midpoint potential). For the reactor acclimated to +0.2 V and the control reactor, DCV plots with the transferred culture inocula had higher and broader peaks than those reactors inoculated with wastewater (Figure 6-3B), showing much improved anode ability over a wider potential range. The midpoint potentials did not appreciably change with transferred culture inocula compared to the wastewater, with *ca.* –0.17 V for the reactor acclimated to +0.2 V, and *ca.* –0.19 V for the control. A previous study showed similar midpoint potentials at –0.25 V and –0.19 V for acetate fed *G. sulfurreducens (31).* These potentials can be compared to the midpoint potentials of solubilized multiheme cytochromes implicated in *Geobacter* electron transport, such as $OmcZ_S$ (–0.22 V) *(32)*, OmcB (–0.19 V) *(33)* and periplasmic cytochrome c (PpcA) purified from *G. sulfurreducens* (–0.17 V) *(34)*.

The changes of the CV and DCV curves in the control reactor help to explain why power overshoot was eliminated by using a transferred culture inoculum. With the control reactor inoculated with wastewater, power overshoot occurred because the current could not further

increase beyond 4.1 A m^{-2} in polarization tests. This maximum current was quite similar to the peak current obtained in CV tests (4.6 A m^{-2}) for this reactor, further indicating that limited anode activity caused the power overshoot. Inoculation with an acclimated transferred culture resulted in the anode biofilm exhibiting improved redox activity (higher peak in CV and DCV) over a wider range of anode potentials (broader peak in DCV) for the control reactor, thus the anode was capable of higher current densities at more positive potentials. The anodes acclimated at the set potentials were less likely to exhibit power overshoot in polarization tests (Figure 6-2). This lack of power overshoot probably resulted from the adaption of the biofilm to higher current densities during startup (*ca.* 6.5 A m^{-2}) compared to control reactors (*ca.* 0.65 A m^{-2}), which was consistent with a previous study that adaptation to higher current densities eliminates power overshoot *(35)*.

6.3.4 Differential pulse voltammetry (DPV)

DPV is a technique with improved sensitivity compared to CV that discriminates faradic from capacitive current even at high scan rates. Therefore, DPV can be used to reveal characteristic peaks, while cancelling out capacitive or background current, showing the alteration of redox species within the anode biofilms under different acclimation conditions *(36)*. The height of the peak current in a DPV is directly related to the concentration of the electroactive species in the electrochemical cell, while the peak potential should indicate the half-wave potential ($E_{1/2}$) of the anode, where $E_{1/2} = E_{peak} + \Delta E/2$ *(37)*. DPV analysis showed one broad peak for the wastewater inoculated reactors at the two different set potentials. The reactor acclimated to –0.2 V had a half-wave potential ($E_{1/2}$) of –0.153 V, and the highest peak current among the reactors inoculated with wastewater, indicating the highest electroactive biomass (Figure 6-4). The reactor acclimated to +0.2 V had more positive $E_{1/2}$ of –0.115 V, consistent with CV results which

showed that the peak potential shifted to a more positive direction when acclimated to the more positive potential. The DPV for the control reactor showed a broad peak ($E_{1/2}$ = –0.162 V) and an additional small peak (–0.055 V), indicating multiple active redox couples in the biofilm (Figure 6-4).

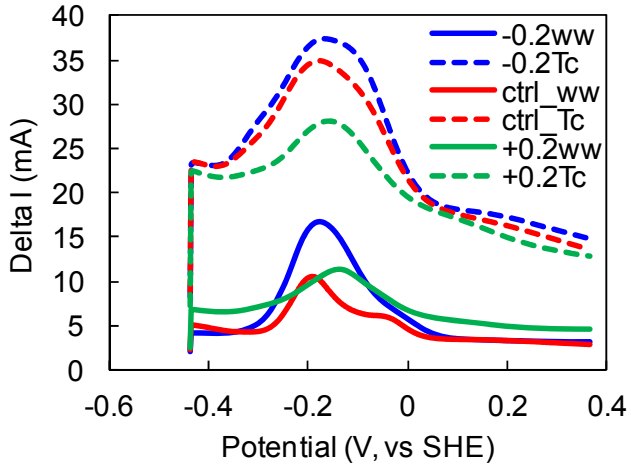

Figure 6-4. DPV with set anode potentials of –0.2 V, +0.2 V and the control (no set potential, ctrl), inoculated with wastewater (ww, solid lines) or transferred culture (Tc, dotted lines).

Reactors that were inoculated with the transferred culture had much higher peak currents in the DPVs, indicating more electroactive biomass in the biofilm. The half-wave potentials for the new reactors did not appreciably change, with values of –0.150 V (–0.2 V), –0.130 V (+0.2 V) and –0.154 V (control) (Figure 6-4), showing that the active redox species did not appreciably change as a result of the transfer process. However, the control reactor only exhibited a single broad peak, indicating reduced redox protein diversity, likely due to the selection of more exoelectrogenic species by the transfer process.

6.3.5 Electrochemical impedance spectroscopy (EIS)

EIS was conducted to identify the anode charge transfer resistances produced by different acclimation conditions and inocula. The anode potential for these EIS tests was set at –0.2 V, which was similar to the anode potentials produced by all MFCs in the absence of a set potential. The reactors inoculated with wastewater and acclimated at the same set potential of –0.2 V had the smallest R_{ct} = 5.3 Ω, consistent with this MFC producing the highest currents in the CV and DPV tests. Anodes acclimated to +0.2 V had much larger R_{ct} = 17.9 Ω, which was also much larger than the control reactor (8.1 Ω) (Figure 6-5). This larger resistance was probably due to the lack of suitable electron transfer pathways for operation at this highly negative anode potential.

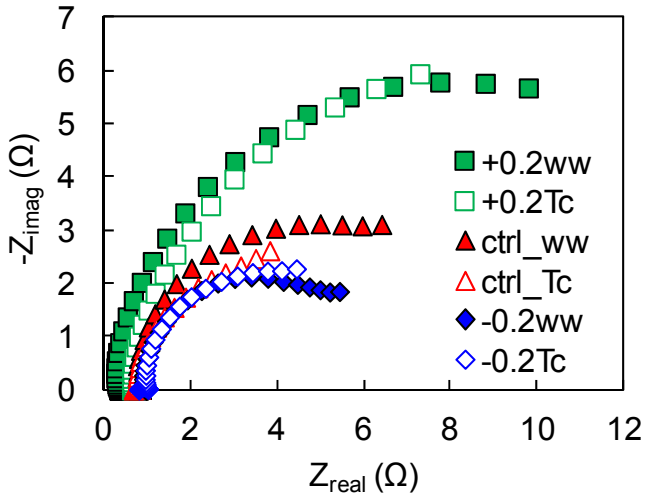

Figure 6-5. Nyquist plot at –0.2 V vs SHE, with MFCs acclimated to set anode potentials of –0.2 V, +0.2 V and the control (no set potential, ctrl), inoculated with wastewater (ww, solid symbols) or acclimated transferred culture (Tc, open symbols).

The reactors inoculated with the transferred culture had lower R_{ct} values, consistent with the improved power production and higher CV or DPV peak currents with these reactors. Anode acclimated to –0.2 V had a slightly lower R_{ct} of 5.1 Ω, while the control reactor had a R_{ct} = 5.9 Ω which was close to that obtained for the reactor acclimated to –0.2 V. Anodes acclimated to more positive potential of +0.2 V still had the largest R_{ct} = 16.5 Ω (Figure 6-5). Therefore, anode

acclimation to the more negative values was more beneficial for power production due to the reduction in charge transfer resistances. Using a pre-acclimated cell suspension for inoculation could decrease the charged transfer resistance and thus improve power production.

6.3.6 Effects of inoculation with different wastewater samples over time

In order to examine the reproducibility of the set anode conditions on the startup of the MFC, the tests were repeated with wastewater taken at different times from the same wastewater treatment plant. Although the source of the wastewater was the same location, wastewater inocula obtained at different times resulted in large variations for the same acclimation condition (set potentials or no set potential). When acclimated at a set potential of –0.2 V the wastewater inoculum obtained at a different time (ww2, Figure 6-6) had a startup time as long as 40 days, with power production of only 875±5 mW m^{-2}. Although this power was higher than those obtained with more positive set potentials of –0.15 V and –0.1 V using the same inoculum (Figure 6-6), it was 34% lower than previously obtained power production of 1330±56 mW m^{-2} (ww1). This variation in startup time and performance was unexpected as previous MFC tests using samples from this wastewater treatment plant have shown more consistent results *(22)*. However, most previous tests were done in MFCs with well spaced electrodes. Thus, it is likely that oxygen intrusion that occurs using closely spaced electrodes can result in much greater variability in MFC startup and performance.

When acclimated to a more positive potential of +0.2 V with another wastewater sample (ww3), the maximum power density of 1130±20 mW m^{-2} was higher than that originally obtained under this condition with the ww1 inoculum (910±50 mW m^{-2}). A similar power density (1060±130 mW m^{-2}) was obtained with acclimation to a set potential of 0 V with the ww3 inoculum (Figure 6-6). The control reactors also had large variation in power production using different wastewater inocula. Originally we obtained 900±60 mW m^{-2} (ww1), compared to

780±60 mW m^{-2} (ww2) and 980±20 mW m^{-2} (ww3). Therefore, different wastewater inocula had large impact on the reactor performance with SEA setup, and acclimation at a set anode potential could not avoid these changes and inconsistent behavior.

When MFCs were inoculated with the transferred cell suspensions from reactors originally inoculated with different wastewater samples taken at different times, reproducible and consistent startup performance and power production were obtained. The pre-acclimated transfer from ww2, with a set potential of –0.2 V, had a reduced startup time to only *ca.* 10 days, compared to 40 days without pre-acclimation, and power production increased to 1280±90 mW m^{-2} (Figure 6-6). Transferred culture inocula resulted in a consistent startup time of 10 days or less, and high power production (>1200 mW m^{-2}) for all acclimation conditions (Figure 6-6). Therefore, inoculation with a pre-acclimated cell suspension was the only method to ensure consistent and reproducible results of both reduced startup time and improved power production.

The inconsistent results produced by the various wastewater inocula were likely due to natural variations of bacteria in the wastewater over time. It was shown that inocula from this treatment plant and other sources showed all converged in maximum power densities and community composition over time (after two months) in MFCs without set potentials with the well spaced electrodes *(22)*. However, for the MFCs examined here without set potentials, but with closely spaced electrodes in the SEA configuration, maximum power densities with the different inocula did not converge to similar values. This different outcome for the SEA MFCs was likely due to the effects of oxygen contamination from the cathode on the anode microbial community due to the SEA setup. This suggests that the use of pre-acclimated inocula is particularly important for reactors with closely spaced electrodes.

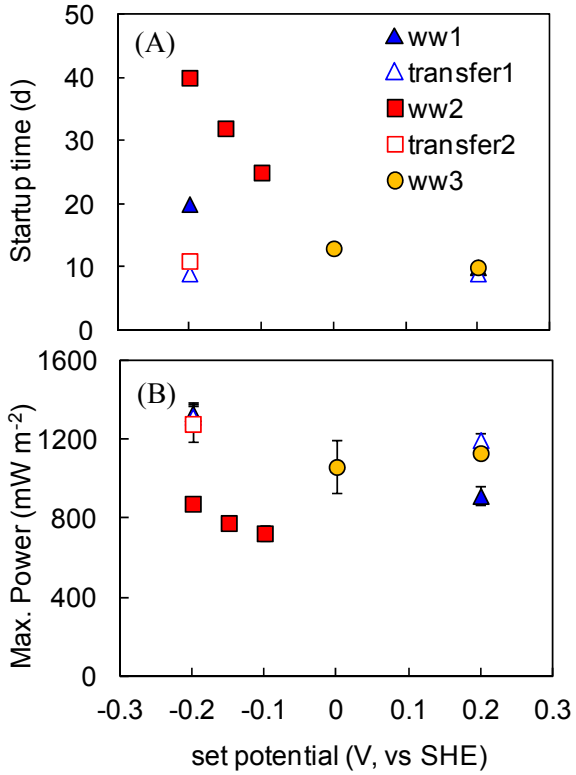

Figure 6-6. Comparison of (A) startup time and (B) maximum power production with different set anode potentials during startup, using different wastewater or acclimated cell suspensions as inocula (ww1 was the wastewater inoculum for the previous figures).

6.3.7 Outlook

The materials used in MFCs with the SEA configuration were very cost-effective relative to those used in many other MFC tests. The carbon mesh anodes cost only $25 per m^2 even for small quantities used here *(20)*. Cathodes were made of activated carbon without precious platinum catalysts, which could cost as little as $50–70 per m^2 *(27)*. The cost of the separator was only $2 per m^2. With the SEA setup and these low-cost materials, power production was 1200 mW m^{-2} (pre-acclimated culture) without set potential, and slightly higher (1330 mW m^{-2}) with a set potential of –0.2 V. These values are higher than that previously obtained with a glass fiber separator in an SEA MFC with the same electrodes used here (960 mW m^{-2}) *(9)*, and the same as

that obtained with a more expensive carbon cloth cathode and a Pt/C cathode (1195 mW m^{-2}) *(7)*. This shows that the separator material used here is a promising alternative to glass fiber separators. The highest power density obtained here (1330 mW m^{-2}) was slightly larger than that obtained with a brush anode and the same activated carbon cathode using a 4-cm electrode spacing (1220 mW m^{-2}) *(27)*, and similar to that obtained with the brush and activated carbon materials in a SEA setup with a glass fiber separator (1300 mW m^{-2}) *(9)*. However, the thinner carbon mesh anode may allow for more compact reactor designs than the larger graphite fiber brush. Thus, carbon mesh anodes in SEA setup are both cost-effective and efficient alternatives to previously used materials in MFCs, particularly when used in SEA arrangements.

6.4 Conclusions

In order to improve the startup performance and power production by SEA MFCs, inoculation using a pre-acclimated cell suspension is needed to provide consistent and reproducible results in terms of reduced startup time and improved power production. Acclimation at a set anode potential of –0.2 V with a pre-acclimated culture inoculum produced slightly improved maximum power densities (~by 10%) compared to the control (no set potential), but this is a relatively small change considering the more complicated three-electrode setup needed. Electrochemical characterization confirmed that anode biofilms were more active with the transferred culture inoculum. For large scale reactor inoculation, it is suggested that pre-acclimated cultures be used as the inoculum to ensure good startup performance.

6.5 Acknowledgments

The authors thank D. W. Jones for help with the analytical measurements, and Dr. Xiuping Zhu and Dr. Justin Tokash for useful discussions. This research was supported by Award KUS-I1-003-13 from the King Abdullah University of Science and Technology (KAUST).

6.6 Literature cited

1. Logan, B. E., *Microbial Fuel Cells*. John Wiley & Sons, Inc.: Hoboken, NJ, 2008.
2. Logan, B. E.; Aelterman, P.; Hamelers, B.; Rozendal, R.; Schröder, U.; Keller, J.; Freguiac, S.; Verstraete, W.; Rabaey, K., Microbial fuel cells: methodology and technology. *Environ. Sci. Technol.* **2006,** *40*, (17), 5181-5192.
3. Logan, B. E.; Regan, J. M., Microbial fuel cells—challenges and applications. *Environ. Sci. Technol.* **2006,** *40*, (17), 5172-5180.
4. Lovley, D. R., Bug juice: harvesting electricity with microorganisms. *Nat. Rev. Microbiol.* **2006,** *4*, 497-508.
5. Lovley, D. R., The microbe electric: conversion of organic matter to electricity. *Curr. Opin. Biotechnol.* **2008,** *19*, (6), 564-571.
6. Fan, Y.; Hu, H.; Liu, H., Enhanced coulombic efficiency and power density of air-cathode microbial fuel cells with an improved cell configuration. *J. Power Sources* **2007,** *171*, (2), 348-354.
7. Zhang, X.; Cheng, S.; Wang, X.; Huang, X.; Logan, B. E., Separator characteristics for increasing performance of microbial fuel cells. *Environ. Sci. Technol.* **2009,** *43*, (21), 8456-8461.

8. Zhang, X.; Cheng, S.; Huang, X.; Logan, B. E., The use of nylon and glass fiber filter separators with different pore sizes in air-cathode single-chamber microbial fuel cells. *Energy Environ. Sci.* **2010,** *3*, (5), 659-664.
9. Hays, S.; Zhang, F.; Logan, B. E., Performance of two different types of anodes in membrane electrode assembly microbial fuel cells for power generation from domestic wastewater. *J. Power Sources* **2011,** *196*, (20), 8293-8300.
10. Cheng, S.; Liu, H.; Logan, B. E., Increased power generation in a continuous flow MFC with advective flow through the porous anode and reduced electrode spacing. *Environ. Sci. Technol.* **2006,** *40*, (7), 2426-2432.
11. Wang, X.; Feng, Y.; Ren, N.; Wang, H.; Lee, H.; Li, N.; Zhao, Q., Accelerated start-up of two-chambered microbial fuel cells: Effect of anodic positive poised potential. *Electrochim. Acta* **2009,** *54*, (3), 1109-1114.
12. Wei, J.; Liang, P.; Cao, X.; Huang, X., A new insight into potential regulation on growth and power generation of *Geobacter sulfurreducens* in microbial fuel cells based on energy viewpoint. *Environ. Sci. Technol.* **2010,** *44*, (8), 3187-3191.
13. Sun, D.; Call, D. F.; Kiely, P. D.; Wang, A.; Logan, B. E., Syntrophic interactions improve power production in formic acid fed MFCs operated with set anode potentials or fixed resistances. *Biotechnol. Bioeng.* **2012,** *109*, (2), 405-414.
14. Torres, C. I.; Krajmalnik-Brown, R.; Parameswaran, P.; Marcus, A. K.; Wanger, G.; Gorby, Y. A.; Rittmann, B. E., Selecting anode-respiring bacteria based on anode potential: phylogenetic, electrochemical, and microscopic characterization. *Environ. Sci. Technol.* **2009,** *43*, (24), 9519-9524.
15. Wagner, R. C.; Call, D. F.; Logan, B. E., Optimal set anode potentials vary in bioelectrochemical systems. *Environ. Sci. Technol.* **2010,** *44*, (16), 6036-6041.

16. Aelterman, P.; Freguia, S.; Keller, J.; Verstraete, W.; Rabaey, K., The anode potential regulates bacterial activity in microbial fuel cells. *Appl. Microbiol. Biotechnol.* **2008,** *78*, (3), 409-418.

17. Yi, H.; Nevin, K. P.; Kim, B.-C.; Franks, A. E.; Klimes, A.; Tender, L. M.; Lovley, D. R., Selection of a variant of *Geobacter sulfurreducens* with enhanced capacity for current production in microbial fuel cells. *Biosens. Bioelectron.* **2009,** *24*, (12), 3498-3503.

18. Cusick, R.; Bryan, B.; Parker, D.; Merrill, M.; Mehanna, M.; Kiely, P.; Liu, G.; Logan, B., Performance of a pilot-scale continuous flow microbial electrolysis cell fed winery wastewater. *Appl. Microbiol. Biotechnol.* **2011,** *89*, (6), 2053-2063.

19. Rabaey, K., Continuous microbial fuel cells convert carbohydrates to electricity. *Water Sci. Technol.* **2005,** *52*, 515.

20. Wang, X.; Cheng, S.; Feng, Y.; Merrill, M. D.; Saito, T.; Logan, B. E., The use of carbon mesh anodes and the effect of different pretreatment methods on power production in microbial fuel cells. *Environ. Sci. Technol.* **2009,** *43*, (17), 6870-6874.

21. Chae, K.-J.; Choi, M.-J.; Lee, J.-W.; Kim, K.-Y.; Kim, I. S., Effect of different substrates on the performance, bacterial diversity, and bacterial viability in microbial fuel cells. *Bioresour. Technol.* **2009,** *100*, (14), 3518-3525.

22. Yates, M. D.; Kiely, P. D.; Call, D. F.; Rismani-Yazdi, H.; Bibby, K.; Peccia, J.; Regan, J. M.; Logan, B. E., Convergent development of anodic bacterial communities in microbial fuel cells. *ISME J* **2012**.

23. Qu, Y.; Feng, Y.; Wang, X.; Logan, B. E., Use of a coculture to enable current production by *Geobacter sulfurreducens*. *Appl. Environ. Microbiol.* **2012,** *78*, (9), 3484-3487.

24. Ieropoulos, I.; Winfield, J.; Greenman, J., Effects of flow-rate, inoculum and time on the internal resistance of microbial fuel cells. *Bioresour. Technol.* **2010,** *101*, (10), 3520-3525.

25. Liu, G.; Yates, M. D.; Cheng, S.; Call, D. F.; Sun, D.; Logan, B. E., Examination of microbial fuel cell start-up times with domestic wastewater and additional amendments. *Bioresour. Technol.* **2011,** *102*, (15), 7301-7306.

26. Liu, H.; Logan, B. E., Electricity generation using an air-cathode single chamber microbial fuel cell in the presence and absence of a proton exchange membrane. *Environ. Sci. Technol.* **2004,** *38*, (14), 4040-4046.

27. Zhang, F.; Cheng, S.; Pant, D.; Bogaert, G. V.; Logan, B. E., Power generation using an activated carbon and metal mesh cathode in a microbial fuel cell. *Electrochem. Commun.* **2009,** *11*, (11), 2177-2179.

28. Zhang, F.; Pant, D.; Logan, B. E., Long-term performance of activated carbon air cathodes with different diffusion layer porosities in microbial fuel cells. *Biosens. Bioelectron.* **2011,** *30*, (1), 49-55.

29. Marsili, E.; Rollefson, J. B.; Baron, D. B.; Hozalski, R. M.; Bond, D. R., Microbial biofilm voltammetry: direct electrochemical characterization of catalytic electrode-attached biofilms. *Appl. Environ. Microbiol.* **2008,** *74*, (23), 7329-7337.

30. Hutchinson, A. J.; Tokash, J. C.; Logan, B. E., Analysis of carbon fiber brush loading in anodes on startup and performance of microbial fuel cells. *J. Power Sources* **2011,** *196*, (22), 9213-9219.

31. Katuri, K. P.; Kavanagh, P.; Rengaraj, S.; Leech, D., *Geobacter sulfurreducens* biofilms developed under different growth conditions on glassy carbon electrodes: insights using cyclic voltammetry. *Chem. Commun.* **2010,** *46*, (26), 4758-4760.

32. Inoue, K.; Qian, X.; Morgado, L.; Kim, B.-C.; Mester, T.; Izallalen, M.; Salgueiro, C. A.; Lovley, D. R., Purification and characterization of OmcZ, an outer-Surface, octaheme c-type cytochrome essential for optimal current production by *Geobacter sulfurreducens*. *Appl. Environ. Microbiol.* **2010,** *76*, (12), 3999-4007.

33. Magnuson, T. S.; Isoyama, N.; Hodges-Myerson, A. L.; Davidson, G.; Maroney, M. J.; Geesey, G. G.; Lovley, D. R., Isolation, characterization and gene sequence analysis of a membrane-associated 89kDa Fe(III) reducing cytochrome c from *Geobacter sulfurreducens*. *Biochem. J.* **2001,** *359*, 147-152.

34. Lloyd, J. R.; Leang, C.; Myerson, A. L. H.; Coppi, M. V.; Cuifo, S.; Methe, B.; Sandler, S. J.; Lovley, D. R., Biochemical and genetic characterization of PpcA, a periplasmic c-type cytochrome in Geobacter sulfurreducens. *Biochem. J.* **2003,** *369*, 153-161.

35. Hong, Y.; Call, D. F.; Werner, C. M.; Logan, B. E., Adaptation to high current using low external resistances eliminates power overshoot in microbial fuel cells. *Biosens. Bioelectron.* **2011,** *28*, (1), 71-76.

36. Marsili, E.; Sun, J.; Bond, D. R., Voltammetry and growth physiology of *Geobacter sulfurreducens* biofilms as a function of growth stage and imposed electrode potential. *Electroanalysis* **2010,** *22*, (7-8), 865-874.

37. Bard, A.; Faulkner, L., *Electrochemical Methods: Fundamentals and Applications*. John Wiley & Sons, Inc: 2001.

Chapter 7

Future Work

In this dissertation, I optimized cathode performance by using coarser mesh as current collectors to improve oxygen transfer, proposed a low-cost PDMS binder with anti-flooding properties to replace Nafion as a binder, and investigated the long-term stability and reasons for degradation in performance of activated carbon (AC) cathodes. I have also investigated the strategies for better startup performance of MFCs with minimized electrode spacing using an SEA configuration for future large scale applications. These studies mostly targeted a specific component of the cathode to address a specific question. However, integration of the optimized components examined here is needed for future tests. Specific issues that need to be addressed for scaling up MFCs are as follows.

1. PDMS binder needs to be examined and optimized for use in AC cathodes. PDMS binder showed comparable power production and improved stability compared to a Nafion binder in cathodes made with a Pt/C catalyst. Future work with a PDMS binder and AC is recommended for the construction of inexpensive air cathodes.
2. Oxygen reduction mechanisms on AC need to be further studied, especially in neutral pH solutions like those used in MFCs. Further optimization of AC cathodes, by using different polymer binders, or through surface modifications of the AC, requires a deeper understanding of oxygen reduction mechanisms on AC.
3. AC used in the cathodes should be optimized by examining different particle sizes, surface areas, pre-treatment methods, types of functional groups that are active for oxygen reduction, and by examining the effects of pore size distribution on performance.

4. MFCs with larger liquid volumes should be tested with the SEA setup using optimized AC cathodes and separators, with domestic wastewater as the fuel. Pre-acclimated cell suspensions should be used as an inoculum to ensure good startup and power production.
5. Cathode anti-fouling methods and catalyst regeneration methods are needed for better long-term stability of cathode performance in MFCs. During my previous long-term test with AC cathodes, pore clogging was concluded to be the reason for performance degradation. Development of an anti-fouling cathode, or a method for *in-situ* regeneration, will increase the stability in performance that is needed for long-term use of these materials in large scale applications of MFCs.

Appendix A

Supporting information for chapter 3

According to the macroporous matrix diffusion model, oxygen transfer coefficient has a linear relationship with porosity of mesh (Figure A-1A). There is generally good agreement between experimental and predicted oxygen transfer coefficients. However, there is not a direct relationship between maximum power production and porosity of mesh cathodes (Figure A-1A), indicating other factors other than oxygen transfer that dominant the cathode performance.

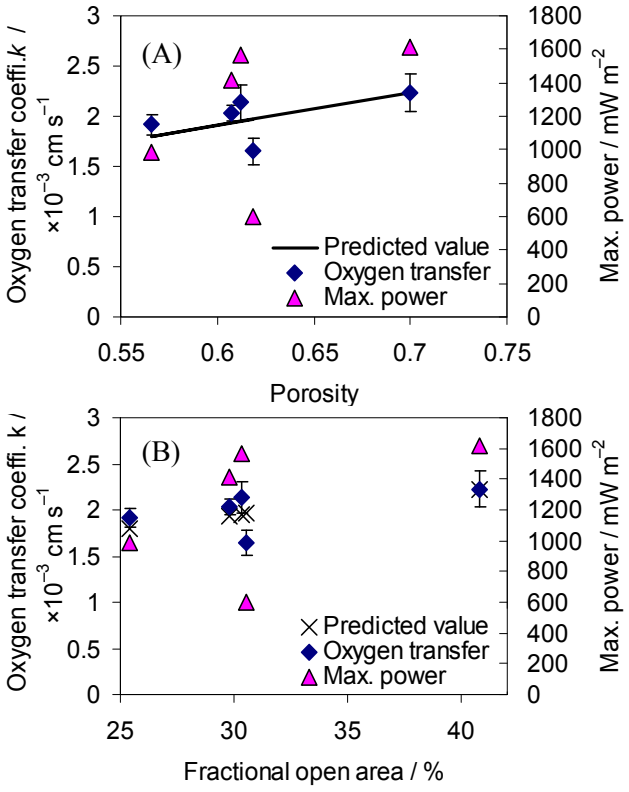

Figure A-1. Experimental and predicted oxygen transfer coefficient (based on the macroporous matrix diffusion model) of SS mesh cathodes with different sized mesh, and maximum power densities achieved by these cathodes, against (A) mesh porosity, (B) mesh fractional open area.

If we consider fractional open area that affects the oxygen transfer to the cathode catalyst layer, we can draw the same conclusion (Figure A-1B). In fact, the size of the mesh openings changes by 440% from fine to coarse, whereas the total open area of the various meshes only changes by 40%. This illustrates the importance of mesh opening size rather than the open area (or similarly the porosity) within each mesh.

Appendix B

Supporting information for chapter 5

Equivalent Circuit Analysis

The equivalent circuit was a simplified circuit according to the flooded-agglomerate model for porous gas-diffusion electrodes (Figure B-1). The charge transfer component and diffusion component in this equivalent circuit are formally indistinguishable in the circuit, but they can be separated through additional analysis of the high and low frequency portions of the EIS results. In our analysis the charge transfer resistance was obtained from the high frequency part of the EIS spectrum in Nyquist plot where charge transfer processes predominate, and the diffusion resistance was obtained from the low frequency part where diffusion processes predominate. According to the Nyquist plots in Figure 5-5, diffusion processes typically showed a larger semicircle. Thus we put in a higher initial value of R_d in the iteration processes to find the final fitting results (Figure B-2). Starting with the spectrum at 0.2 V using the initial values in Figure B-2, the obtained fitting results would be the initial values put into iteration for condition of 0.1 V and so forth. Following this method, R_s, R_{ct}, R_d and capacitance were obtained for all conditions as shown in Table B-1.

The fitting results can be examined by removing either charge transfer component or diffusion component in the equivalent circuit. The fitting with only charge transfer component should give a good fit to the high frequency part of the Nyquist plot, while the fitting with only diffusion component should fit to the low frequency part (Figure B-3).

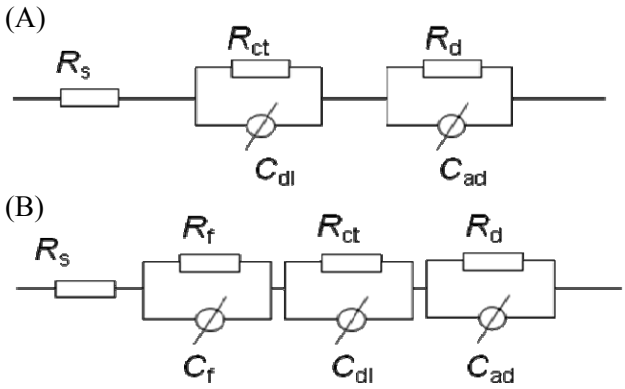

Figure B-1. Equivalent circuit for (A) new cathodes and (B) used cathodes.

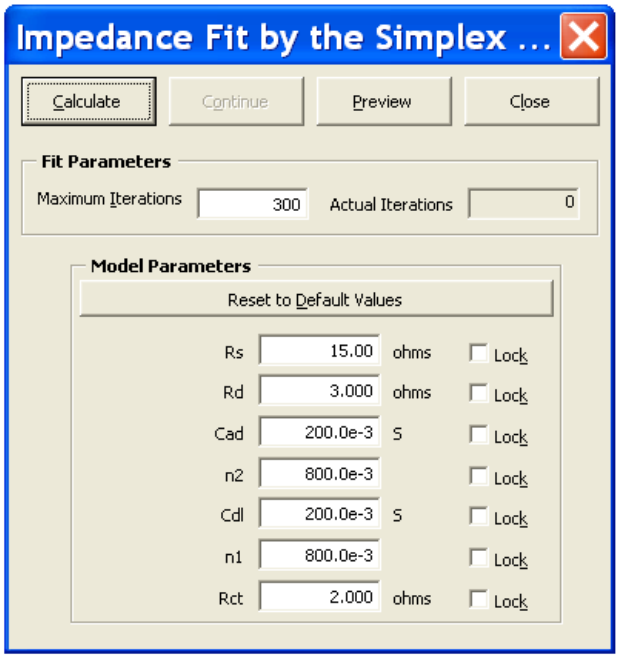

Figure B-2. Initial values for parameters in the equivalent circuit for EIS fitting at condition of 0.2 V. A larger initial value of R_d was used compared to R_{ct} due to the larger semicircles for diffusion processes.

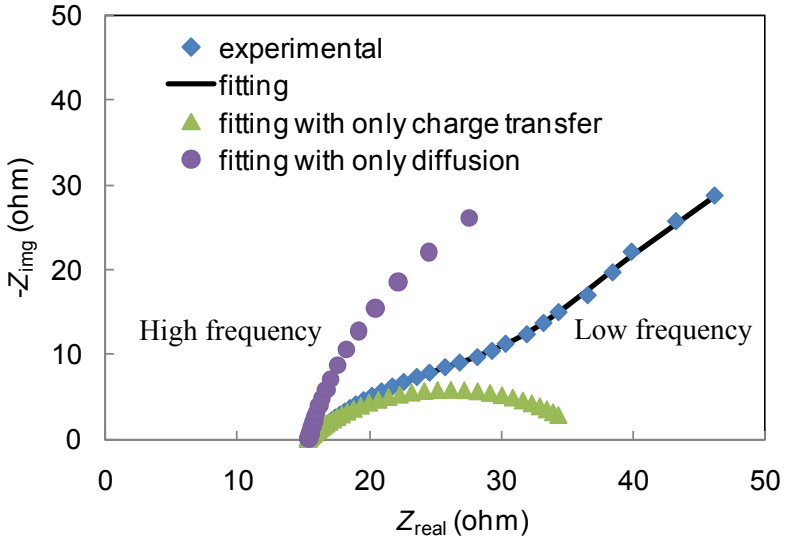

Figure B-3. Resistance identification by fitting into equivalent circuits with only charge transfer component or only diffusion component. 30% DL cathode at 0.2 V was used as the example.

Table B-1. R_{ct}, R_d and capacitance at 0.2 V, 0.1 V and 0 V with two types of AC cathodes under both new and used conditions.

Cathode Type		70	70_used	30	30_used
R_s / Ω	**0.2 V**	15	18	15	18
	0.1 V	15	18	15	18
	0 V	15	18	16	18
R_{ct} / Ω	**0.2 V**	4	6	21	4
	0.1 V	3	5	5	3
	0 V	5	3	8	3
R_d / Ω	**0.2 V**	97	93	112	126
	0.1 V	46	62	25	51
	0 V	17	24	3	10
C_{dl} / mF	**0.2 V**	703	334	568	383
	0.1 V	879	337	896	444
	0 V	614	180	447	537
C_{ad} / mF	**0.2 V**	4694	3579	6007	4684
	0.1 V	3804	4261	2933	5127
	0 V	9312	2851	9958	4405

Cathode analysis

Biofilm development differed on the cathodes. A thicker biofilm developed on the cathodes with the 70% DLs one year of operation compared to those with a 30% DL (Figure B-4).

Figure B-4. Two types of cathode with biofilm developed on the cathode surface after one year of operation in MFCs.

Analysis of power densities and electrode potentials

Power generation by the used cathodes (used for one year) was increased by cleaning the cathode surface and removing the biofilm. However, power densities were only restored to the original levels by using new cathodes (Figure B-5A). Anode potentials were unchanged by these procedures (Figure B-5C).

Potentiostatic polarization and galvanostatic polarization showed the consistent results with LSV (Figure 5-4 and B-6).

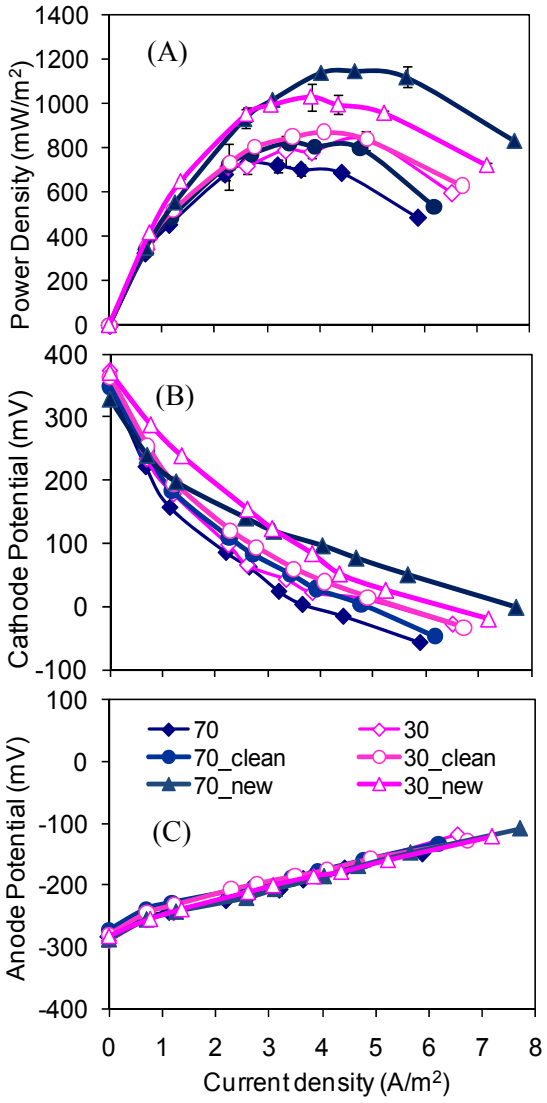

Figure B-5. Comparison of (A) power density curves, (B) cathode potentials, (C) anode potentials of MFCs with used cathodes, used cathodes without biofilm, and changing to new cathodes after one year of operation (for the used cathodes, this is the same data as "70-12 m" and "30-12m" in Figure 5-2).

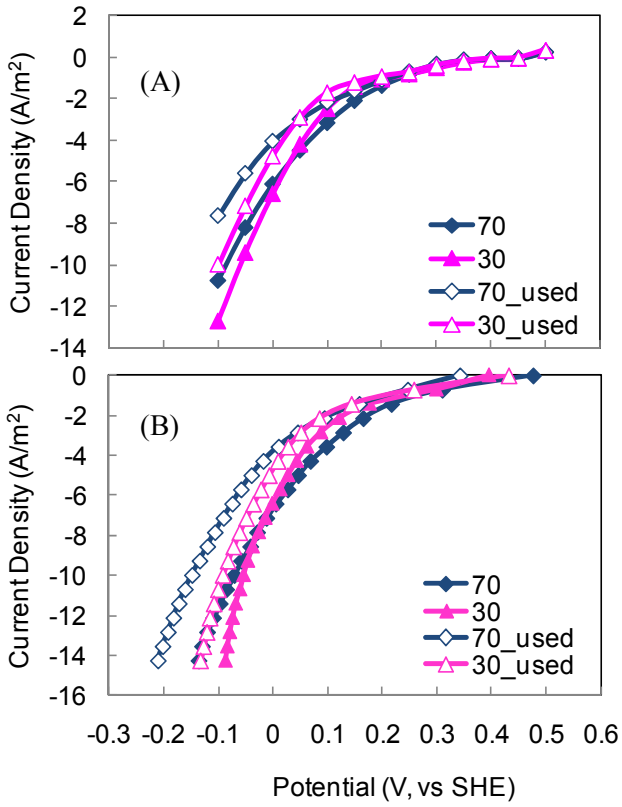

Figure B-6. (A) Potentiostatic polarization and (B) galvanostatic polarization data of two types of AC cathodes under both new and used conditions.

Appendix C

Supporting information for chapter 6

Cathode potentials changed over the course of a cycle to maintain constant anode potential. Cathode potentials had peak stable at *ca.* 0 V at peak current for both set potentials (Figure C-1). Anode potentials of the control reactors gradually reduced from +0.45 V from the beginning of startup to the stable potential of –0.25 V after 12 days (Figure C-1). The control reactor had a much longer cycle time (*ca.* 3-4 days) than the reactors with set anode potentials (1 day) (Figure C-1), due to the much smaller current (peak at *ca.* 0.45 mA) compared to those of the reactors with set anode potentials (peak at *ca.* 4.5 mA).

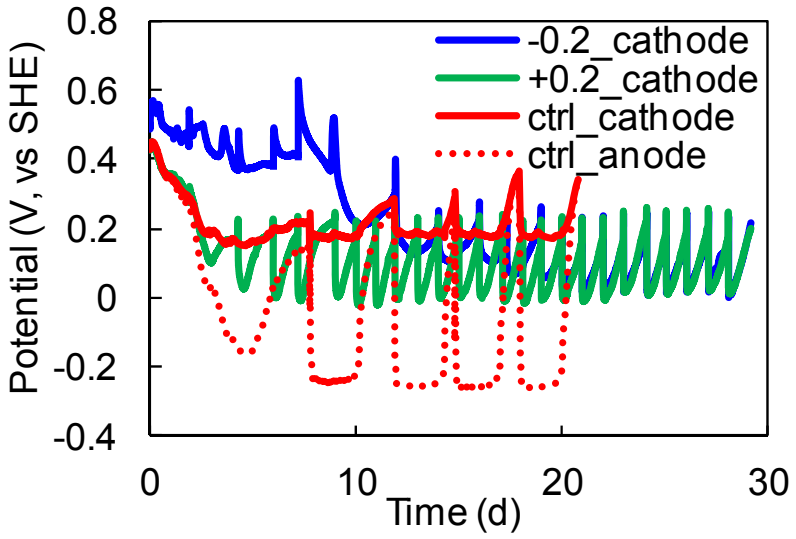

Figure C-1. Change of cathodes potentials over time, and the change of anode potential for the control reactor, all with wastewater inoculum.

The peak current in CV and maximum power production generally were positively correlated, as a higher anodic peak current resulted in a higher power production, up until the point where the power production was limited by cathode performance (Figure C-2).

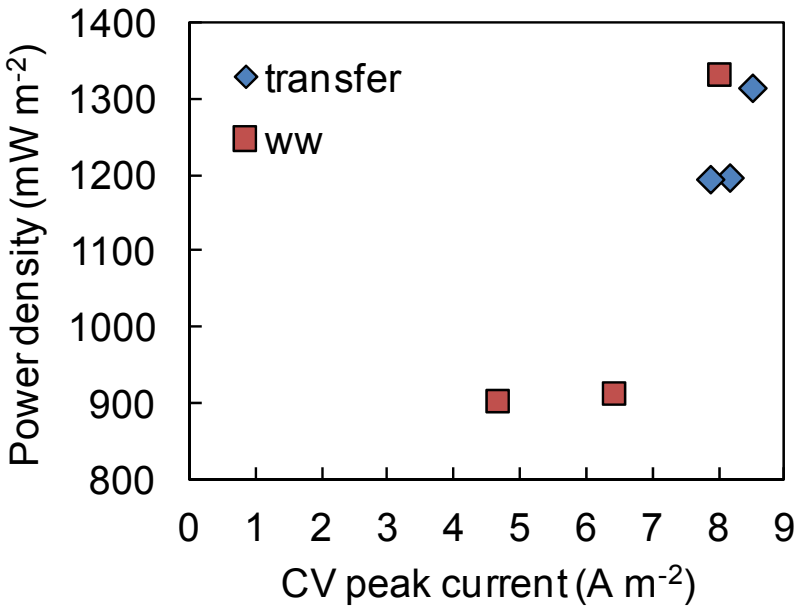

Figure C-2. Positive relationship of maximum power density and CV peak current.

Fang Zhang

EDUCATION

2008-2012 M.S. & Ph.D. in Environmental Engineering, Penn State University,
2004-2008 B.S. in Environmental Engineering & Economics, Tsinghua University

EXPERIENCE

8/2008-Present Research Assistant, Kappe Environmental lab, Penn State University
Advisor: Prof. Bruce E. Logan
6/2007-7/2008 Research Assistant, Lab of Water Environment, Tsinghua University
Advisor: Prof. Xia Huang

HONORS and AWARDS

2012 Penn State University Environmental Chemistry Student Symposium 2012: Best Oral Presentation Award in Environmental Sciences Section (2nd place)
2011 Chinese Government Award for Outstanding Self-financed Students Abroad
2011 Environmental Chemistry Graduate Student Award, Division of Environmental Chemistry, American Chemical Society
2010 Certificate of Merit Award, 239th ACS National Meeting & Exposition, San Francisco, CA
2009 Chevron Scholarship, Penn State University
2008 Outstanding Graduate Award, Tsinghua University
2007 China National Scholarship
2006 HSBC Scholarship, Tsinghua University
2005 Kerry Oils & Grain Scholarship, Tsinghua University

JOURNAL PUBLICATIONS

1. Zhang, F.; Chen, G.; Hickner, M. A.; Logan, B. E., Novel anti-flooding poly(dimethylsiloxane) (PDMS) catalyst binder for microbial fuel cell cathodes. *J. Power Sources* **2012** in press.
2. Zhang, F.; Pant, D.; Logan, B. E., Long-term performance of activated carbon air cathodes with different diffusion layer porosities in microbial fuel cells. *Biosens. Bioelectron.* **2011,** *30*, (1), 49-55.
3. Zhang, F.; Merrill, M. D.; Tokash, J. C.; Saito, T.; Cheng, S.; Hickner, M. A.; Logan, B. E., Mesh optimization for microbial fuel cell cathodes constructed around stainless steel mesh current collectors. *J. Power Sources* **2011,** *196*, (3), 1097-1102.
4. Hays, S.; Zhang, F.; Logan, B. E., Performance of two different types of anodes in membrane electrode assembly microbial fuel cells for power generation from domestic wastewater. *J. Power Sources* **2011,** *196*, (20), 8293-8300.
5. Luo, Y.; Zhang, F.; Wei, B.; Liu, G.; Zhang, R.; Logan, B. E., Power generation using carbon mesh cathodes with different diffusion layers in microbial fuel cells. *J. Power Sources* **2011,** *196*, (22), 9317-9321.
6. Zhang, F.; Saito, T.; Cheng, S.; Hickner, M. A.; Logan, B. E., Microbial fuel cell cathodes with poly(dimethylsiloxane) diffusion layers constructed around stainless steel mesh current collectors. *Environ. Sci. Technol.***2010,** *44*, (4), 1490-1495.
7. Zhang, F.; Cheng, S.; Pant, D.; Bogaert, G. V.; Logan, B. E., Power generation using an activated carbon and metal mesh cathode in a microbial fuel cell. *Electrochem. Commun.* **2009,** *11*, (11), 2177-2179.